

Hamiltonian Complexity in the Thermodynamic Limit

Dorit Aharonov*

Sandy Irani†

April 4, 2022

Abstract

Despite immense progress in quantum Hamiltonian complexity in the past decade, little is known about the computational complexity of quantum physics at the thermodynamic limit. In fact, even defining the problem properly is not straight forward. We study the complexity of estimating the ground energy of a fixed, translationally invariant Hamiltonian in the thermodynamic limit, to within a given precision; this precision (given by n the number of bits of the approximation) is the sole input to the problem. Understanding the complexity of this problem captures how difficult it is for the physicist to measure or compute another digit in the approximation of a physical quantity in the thermodynamic limit. We show that this problem is contained in $\text{FEXP}^{\text{QMA-EXP}}$ and is hard for $\text{FEXP}^{\text{NEXP}}$. This means that the problem is *doubly* exponentially hard in the size of the input. As an ingredient in our construction, we study the problem of computing the ground energy of translationally invariant finite 1D chains. A single Hamiltonian term, which is a fixed parameter of the problem, is applied to every pair of particles in a finite chain. In the finite case, the length of the chain is the sole input to the problem. We show that this problem is contained in $\text{FP}^{\text{QMA-EXP}}$ and is hard for FP^{NEXP} . Our techniques employ a circular clock structure in which the ground energy is calibrated by the length of the cycle. This requires more precise expressions for the ground states of the resulting matrices and even exact analytical bounds for the infinite case which we derive using techniques from spectral graph theory.

*dorit.aharonov@gmail.com

†irani@ics.uci.edu

Contents

1	Introduction	1
1.1	Background: The complexity of condensed matter physics	1
1.2	The complexity of many body quantum physics in the thermodynamic limit	1
1.3	Problem Definition and statement of result	2
1.4	Proof Overview and Techniques	3
1.4.1	Computing Ground Energies of Finite TI Chains	4
1.4.2	Circuit-to-Hamiltonian Construction and the Circular Clock	4
1.4.3	Overview of the Computation Embedded in the Hamiltonian	6
1.4.4	Summary of main new technical contributions in the proof	6
1.5	Related work and Discussion	7
2	Computing Ground Energies for Finite Translationally Invariant Hamiltonians	8
2.1	Containment	8
2.2	Hardness: Overview of the Construction	9
2.2.1	The Track Structure of the Hilbert Space	10
2.2.2	Circuit-to-Hamiltonian construction	10
2.2.3	Overview of the Clock Tracks	11
2.2.4	Structure of the Hamiltonian	12
2.2.5	The description of the two Turing Machines: M_{BC} and M_{TV} .	13
2.2.6	Overview of the Penalty Terms	14
2.3	The Clock Tracks	15
2.3.1	Rules for 1-pointers	16
2.3.2	Rules for 2-pointers	19
2.3.3	Rules for 3-pointers	19
2.3.4	Rules for 4-pointers	21
2.3.5	Rules for i -pointers for $i = 5, \dots, 8$	21
2.3.6	Summary of Track 1 and 2 Clock Configurations	22
2.3.7	Track 3	24
2.4	Turing Machines Used in the Construction	29
2.4.1	Review of Reversible Turing Machines	29
2.4.2	The Binary Counter Turing Machine	30
2.4.3	The Turing Machine M_{TV} used in the Hamiltonian for Finite Chains	33
2.4.4	Adjustments to the Two Turing Machines	34
2.5	The Hamiltonian	36
2.5.1	Local Constraints to Make the Computation Tracks Well-Formed	37
2.5.2	Implementing TM Steps in Propagation Terms	37
2.5.3	Propagation Terms for Each of the 8 Segments	39
2.5.4	Additional Penalty Terms for the Finite Construction	42
2.6	Analysis of the ground energy of the Hamiltonian	43
2.6.1	The evolution of Tracks 1 and 2 is a cycle	43
2.6.2	Analysis of the Ground Energy	44
2.6.3	Bracketed States and the Final Reduction	48
2.6.4	Eigenvalue Bounds	49
3	Computing the Ground Energy Density in the Thermodynamic Limit	53
3.1	Existence of the Limit	53
3.2	Containment	54
3.3	Hardness: Overview of the Reduction	54
3.4	Robinson Tiling	55
3.5	The Final Reduction: Mapping from the GED to $f(x)$	58
3.6	Modifications to the Hamiltonian from the Finite Case	61
3.6.1	Existence of M_{TV-inf} that produces the correct output for most N	65

3.6.2	Additional Penalty Terms for the Infinite Construction	66
3.6.3	Analysis of the ground energy of the modified Hamiltonian	67
4	Acknowledgements	68

1 Introduction

1.1 Background: The complexity of condensed matter physics

The field of Quantum Hamiltonian complexity [13] was born with Kitaev's proof [17] that the local Hamiltonian problem is *QMA*-complete. This fundamental result provides a framework for describing the computational complexity of estimating the ground energy of a given local Hamiltonian. The computational setting of Kitaev's construction, however, is still very far from the problems that naturally arise in condensed matter physics; the local Hamiltonian terms depend strongly on which qubits they act on, and thus the system is far from translationally invariant. Furthermore, the interactions involve more than two particles and are not geometrically local. Subsequent work brought *QMA*-completeness results closer and closer to physical settings. For example, the local Hamiltonian was shown to be still *QMA*-complete even when restricted to qubits on a 2D lattice [19] or when the Hamiltonian is set in 1D with nearest neighbor interactions [1]. Gottesman and Irani [16] showed that 1D systems which are translationally invariant, can exhibit computational hardness - even though the only input is the size of the system.

Despite this important and fundamental progress, it can be argued that such complexity results are still far from capturing the primary challenges in computational many-body physics. Physicists study finite systems by necessity, but the problem which is typically of greatest interest is the estimation of physical quantities (such as the energy density, or two body correlations) in the *Thermodynamic limit*; in this setting, the focus is not the estimation of physical quantities as a *function* of the size of the system, but instead, one is concerned with a *particular* quantity, in the limit of N , the size of the system, going to ∞ .

1.2 The complexity of many body quantum physics in the thermodynamic limit

To the best of our knowledge, there has been relatively little work so far on quantum Hamiltonian complexity in the thermodynamic limit. A particularly important result in this context is the breakthrough work of Cubitt, Perez-Garcia, and Wolf [11], and its follow up [5] in which it was shown that the problem of deciding whether a given translationally invariant 1D Hamiltonian system is gapped or gapless in the thermodynamical limit, is undecidable. This important result provides the first study of *computability* of local Hamiltonian problems in the thermodynamic limit. One could think of this result as a statement that the phase diagram of gappedness in the TL, as a function of the local Hamiltonian term parameters, is uncomputable. In fact this idea is developed more explicitly in [6]. Meanwhile, Bravyi and Gosset prove that in a wide variety of cases, such phase diagrams can be computed [9].

The setting of *computational complexity* in the thermodynamical limit is far less explored. To the best of our knowledge, the only previous paper prior to this one, which studies the computational complexity of the thermodynamical question, is Gottesman and Irani [16]. This study of the infinite case is done as a byproduct of their main result, which is on finite systems ([11] and [5] heavily rely on [16]). More specifically, the problem studied in [16] is parameterized by three polynomials, r , p and q . They show that given an integer N and a Hamiltonian acting on a pair of d -dimensional particles whose entries are integer multiples of $1/r(N)$, determining whether the ground energy density in the thermodynamic limit is below $1/p(N)$ or above $1/p(N) + 1/q(N)$ is *QMA-EXP*-complete. Importantly, in the thermodynamical setting of [16], the Hamiltonian term acting on pairs of particles is given as part of the input.

It is worth asking whether studying the computational complexity of the local Hamiltonian problem, where the Hamiltonian is part of the input, is well justified physically. In physics, it is often the case that studying, say, the AKLT model, is considered to be a different problem than the Ising model. With the computability question, it does seem natural to consider the phase diagram of properties such as gappedness, which justifies varying the Hamiltonian as part of the input. However, this seems much less justifiable in the case of estimating the ground energy density (as is done in the study of the thermodynamical limit result of [16]). We ask: can we study the computational complexity of a *fixed* physical problem, in the thermodynamical limit? In other words, we are concerned with associating a computational complexity view on the problem of the estimation of a single physical quantity for a translationally invariant system described by a *fixed Hamiltonian*. To the best of our knowledge, this problem had not been studied before. Indeed, it is not clear how to even define the problem in computational complexity language. Can we associate computational complexity to a problem whose quantity of interest is merely a single, fixed, number?

This work offers a way to study the computational complexity of thermodynamic limit problems in this fixed-Hamiltonian setting. Our goal is to make the initial step towards the classification of the *computational complexity* of physically motivated local Hamiltonian problems in the thermodynamical limit¹.

To this end, we take here the following approach: we define the problem for a fixed Hamiltonian, by having the input specify only the desired *precision* to which the ground energy density is computed, in terms of number of bits. For a fixed translationally invariant Hamiltonian, this captures the complexity of approximating the expectation value of a physical quantity of interest, as applied to the ground state in the thermodynamic limit. The complexity is measured as a function of the precision of the estimate. The required precision is the only input to the problem.

1.3 Problem Definition and statement of result

We define a problem which to our understanding, captures in the best way the work of a physicist studying a fixed Hamiltonian in the thermodynamical limit. This is the problem of estimating the expectation of value of the ground energy density, in the thermodynamical limit, to some given precision. The given precision is the only input to the problem.

We will formally define the problem for the 2D grid since that is the version of the problem addressed in this paper. There are natural 1D and higher dimensional versions of the problem in which the number of Hamiltonian terms provided scales with the dimension of the underlying grid. The problem in 2D is parameterized by the dimension of each individual particle d , and two $d^2 \times d^2$ Hermetian matrices h^{row} and h^{col} denoting the energy interaction between two neighboring particles in the horizontal and vertical directions on a 2D grid. Then $H_{2D}(N)$ is the Hamiltonian of an $N \times N$ grid of d -dimensional particles in which h^{row} is applied to each neighboring pair in the horizontal direction and h^{col} is applied to each neighboring pair in the vertical direction. $\lambda_0(H_{2D}(N))$ is the ground energy of $H_{2D}(N)$. The ground energy density of the system in the thermodynamical limit is defined as follows:

Definition 1.1. Energy density in the Thermodynamical limit

$$\alpha_0 = \lim_{N \rightarrow \infty} \frac{\lambda_0(H_{2D}(N))}{N^2}$$

This limit always exists (as is shown in Section 3.1). The main problem we consider in this paper is to compute α_0 to within a given precision specified by the input.

Definition 1.2. FUNCTION-GED-2D FOR (h^{row}, h^{col})

Input: An integer n expressed in binary.

Output: A number α such that $|\alpha - \alpha_0| \leq 1/2^n$.

While it would have been possible to devise a decision version of our problem, such as determining the n^{th} bit of the ground energy density, the function version more naturally describes the problem encountered in physics. Moreover, computing the n^{th} bit essentially requires computing bits 1 through $n - 1$, as one can verify that the n^{th} bit of the energy density of a particular state is 0 or 1, but the other bits are required to ensure that the state being measured is a low energy state. A similar observation was made earlier by Ambainis in 2014 [3] who introduced the problem APX-SIM, which is to approximate the value of a local observable applied to a low energy state of a given Hamiltonian. APX-SIM, as well as the function version of local Hamiltonian studied here, are arguably much better physically motivated computational problems than the standard decision version of local Hamiltonian in which the computational task is to determine whether the ground energy is lower or higher than an interval defined by two thresholds provided in the input. The natural complexity of this family of problems are oracle classes, owing to the fact that an inherent challenge of computing a property of a ground state is to verify that the state being measured is in fact the true ground state. The upper bounds all require some form of binary search with queries to a QMA or QMA-EXP oracle. (See Section 1.5 for further discussion).

Our main result is:

Theorem 1.3. *The problem FUNCTION-GED-2D of energy estimation in the TL limit in 2D is $FEXP^{NEXP}$ hard, and is contained in $FEXP^{QMA-EXP}$.*

¹This question was highlighted by I. Cirac in an online discussion in a SIMONS institute quantum workshop, 2017

At first sight, it might seem counter intuitive that this problem is hard; the ground energy density for a fixed Hamiltonian in the thermodynamic limit is just a single number. A hardness result would need to embed a hard computational problem for all instances into a *specific number*. We address this by exploiting the fact that the ground energy density in the thermodynamic limit is an infinite precision number, and we can use different portions of the binary representation of that number to encode the solution to different instances of the problem from which we are reducing. One challenge that arises with this approach is that the solutions to different inputs are encoded as energies of finite systems of varying sizes that are embedded into the infinite plane. These energies are not rational numbers and their binary representations can not be confined to a finite segment of the binary representation of the ground energy density α_0 . In order to recover the solution to a function problem on input x from an estimate of α_0 , it is necessary to subtract off the energy contribution from all $x' < x$. This technique requires tight analytical bounds for the energy contribution for each x . Our approach is described in more detail in the proof overview 1.4.

The solution to the problem of computing the ground energy density in the thermodynamical limit leads naturally to a translationally-invariant problem for finite chains (just as in the proof of [11, 5] who addressed the infinite lattice case by embedding finite chains within it, using Robinson tiles, and then made use of the finite chain TI construction of [16]). We state our results on the finite 1D chain separately below, as we believe that they are of independent interest.

Our results in the finite case pertain to 1D systems, but they can be naturally generalized for higher dimensions. In the 1D case, there is a single $d^2 \times d^2$ hermetian matrix h which parameterizes the problem and $H_{1D}(N)$ is the Hamiltonian resulting from applying h to every pair of neighboring particles in a 1D chain. The function version of the finite translationally-invariant Hamiltonian problem in 1D (FUNCTION-TIH-1D) is defined as follows:

Definition 1.4. FUNCTION-TIH-1D FOR h AND CONSTANT c

Input: An integer N expressed in binary.

Output: A number λ such that $|\lambda - \lambda_0(H_{1D}(N))| \leq 1/N^c$.

The following theorem encapsulates our results for Function-TIH:

Theorem 1.5. *Function-TIH-1D problem is contained in $FP^{QMA-EXP}$ and is hard for FP^{NEXP} .*

A comment is warranted here on the exponential difference between the finite and the infinite case. Roughly, the GED in the thermodynamic limit can be estimated to within $\pm 1/N$ by solving a system of size $poly(N)$. The input is a number n which asks for a precision of $1/2^n$ (and therefore a system of size $poly(2^n)$). Since the input is specified using $\log n$ bits, the complexity is doubly exponential in the size of the input. In the finite case, the size of the system itself (N) is given in binary, so the complexity is only singly exponential. From an expressibility perspective, in the finite case, every value of N can be used to encode the solution to an instance of the problem from which we are reducing. By contrast, in the infinite case, the most efficient reduction we can hope for is where each bit of α_0 encodes an answer to a computational problem. In this case, the system size has to double for each input encoded.

1.4 Proof Overview and Techniques

We use the technique introduced by Cubitt, Perez-Garcia, and Wolf in [11] who incorporate an aperiodic tiling structure into the Hamiltonian term for the infinite plane. They use Robinson tiles [21] which are a finite set of tiling rules that when applied to the infinite plane, force an aperiodic structure with squares of exponentially increasing size, as shown in Figure 13. Each square has size 4^k , for positive integer k , and the density of squares of size 4^k is $1/4^{2k+1}$. A 4×4 square from a Robinson tiling is show in Figure 14. Tiling rules are essentially a classical version of local Hamiltonians, so the tiling rules can be encoded into a layer of the Hilbert space on the infinite plane. As was done in [11], we layer a translationally-invariant 1D Hamiltonian on top of one of the sides of all the squares. The tiling pattern on the lower layer determines where the 1D term is applied. The effect of this structure is that the ground energy density for the infinite plane is the sum of the ground energies for an infinite series of finite 1D systems divided by the density of each square size. Note that the stronger notion of translational invariance is essential here as the same Hamiltonian term is applied to every pair of particles in every finite chain embedded in the infinite plane.

In previous work on computing quantities in the thermodynamic limit, the Hamiltonian term is given as part of the input [16] [11]. In this case, there is an infinite class of Hamiltonians that can be used as the basis of a reduction. If we are reducing from a function problem f , each possible input x can be encoded in a Hamiltonian term such that the energy density of that term in the thermodynamic limit encodes the output of f on x . However, if the Hamiltonian term is a fixed parameter of the problem, then the energy density in the thermodynamic limit is just a single number. A reduction in this case, needs to encode an entire language in one, infinite-precision number α_0 . Different portions of the binary representation of α_0 encode the value of a function f on different inputs. In our construction, bits $4x^2$ through $4(x+1)^2$ encode the value of $f(x)$. As noted earlier, bits $4x^2$ through $4(x+1)^2$ will also include the "overflow" from the energy contributions of $f(x')$ for every $x' < x$. These values need to be calculated to the required precision and subtracted off from α_0 in order to recover the bits required to reconstruct the value of $f(x)$.

The top segment of each square of size $4x^2$ in the Robinson tiling is layered with a translationally-invariant 1D Hamiltonian whose ground energy encodes the value $f(x)$, where the function problem f is from the oracle complexity class $\text{FEXP}^{\text{NEXP}}$. We use a technique pioneered by Krentel [18] (see also [20]) who proved that the optimization version of certain NP-hard problems are complete for FP^{NP} . This idea was also used for the finite quantum constructions in [3, 14, 15, 22]. The idea is to use an accounting scheme that applies a cost to every string y representing guesses for the sequence of responses to all the oracle queries made. The verifier is used to check *yes* instances so that incorrect *yes* guesses incur a very high cost and every *no* guess incurs a more modest cost. The accounting scheme ensures that the minimum cost y corresponds to the correct sequence of oracle responses. These costs must necessarily decrease exponentially because the oracle queries are adaptive. An incorrect oracle response could potentially change the oracle queries made in the future and it is important that the penalty for an incorrect guess on the i^{th} query results in a higher penalty that could potentially be saved on all of the future queries. Note that the costs must depend on the input because they decrease exponentially with each oracle query and therefore have to range from a constant to exponential in m , where m is the number of oracle queries made. Encoding the costs directly into the Hamiltonian then is not an option in the translationally-invariant setting in which the Hamiltonian term is a fixed constant, independent of the input to the problem. We address this challenge by using the length of an encoded computation as a means of calibrating the ground energy. The correct length is computed by a Turing Machine with a finite set of rules that is embedded into the Hamiltonian term.

1.4.1 Computing Ground Energies of Finite TI Chains

We explain now how we prove Theorem 1.5. The output of a TM computation with access to an oracle is embedded into an optimization problem so that the minimum cost/energy solution corresponds to a correct computation of the Turing Machine. The cost mechanism ensures that the lowest energy state corresponds to the string y with the correct responses to the oracle queries. This cost mechanism must necessarily depend on the size of the input but also must be implemented with a fixed, constant-sized, Hamiltonian term. This is achieved by embedding the computation of the desired cost using the (constant-sized) set of rules of a Turing Machine and then translating that cost into the energy by varying the length of the computation. The clock used in the circuit-to-Hamiltonian construction is circular. Every computation (even correct ones) incur a cost once in the cycle. We obtain tight analytical bounds on the lowest eigenvalue of the resulting matrix. We then use the fact that longer cycles correspond to smaller ground energies to ensure that the ground energy will encode the correct string y of oracle responses.

1.4.2 Circuit-to-Hamiltonian Construction and the Circular Clock

As is typical in hardness results for finding ground state energies, we use Kitaev's circuit-to-Hamiltonian construction in which the ground state corresponds to the history state of a computation [17]. If the Hamiltonian is represented in a basis where each state is the configuration of the computation at different points in time, then the resulting matrix is the Laplacian of a path graph. The first node in the path corresponds to the initial configuration and the last node corresponds to the final configuration. The process of transitioning from one state to another is regulated by a clock encoded in a different part of the Hilbert space than the computation. In the absence of any additional penalty terms, the ground energy is 0 and is achieved by the state that is a uniform

superposition of all states in the computation, entangled with the clock state for that point in time:

$$\sum_{t=0}^L |t\rangle |\phi_t(v\text{-init})\rangle.$$

$|t\rangle$ denotes the state of the clock and $|\phi_t(v\text{-init})\rangle$ denotes the state of the computation after starting in state $|v\text{-init}\rangle$ and progressing for t clock steps. There are additional penalty terms that penalize any state in which the initial state is not the correct initial state. There is also an additional penalty term that penalizes a computation that finishes in a rejecting state. The difference between an accepting or rejecting computation is therefore reflected in the ground energy. A rejecting computation will correspond to Hamiltonian that is the Laplacian of a path with an additional penalty term for the rejecting state. In the case of a deterministic computation, this will result in a $+1$ term along the diagonal. In the case of a quantum computation which has an inherently probabilistic measurement as the outcome, the penalty term will still be close to diagonal. The ground energy in this case can be shown to be $\Omega(1/L^3)$. On the other hand, if the computation is accepting with high probability, the ground energy will be exponentially small.

Our construction makes use of a circular clock so that the propagation matrix corresponds to the Laplacian of a cycle. If the size of the 1D chain is N , the computation encoded in the Hamiltonian consists of running a reversible Turing Machine for $O(N)$ steps in the forward direction and then the same number of steps in the reverse direction, so that the state of the computation space returns to its initial state. The entire process takes a polynomial number of clock steps $p(N)$ and is then repeated a variable number of times. The length of a timer is encoded in the Hilbert space for the clock. If the timer length is T , the process is repeated $2T + 1$ times. Thus the total length of the clock cycle is $(2T + 1) \cdot p(N)$. In our construction, every computation, regardless of the outcome of the computation, will incur two consecutive penalties of $+1/2$ at a particular point in the cycle. The resulting matrix is the propagation matrix for a cycle of length $L = (2T + 1) \cdot p(N)$ with an additional $+1/2$ at two consecutive locations on the diagonal. We show that the lowest eigenvalue for this matrix is exactly

$$\left(1 - \cos\left(\frac{\pi}{L + 1}\right)\right) = \Theta\left(\frac{1}{L^2}\right). \quad (1)$$

Thus varying the length of the cycle allows us to calibrate the ground energy. If the ground energy can be computed to a $1/\text{poly}$ precision for a sufficiently high degree polynomial, then the value of L can be recovered, from which T can be recovered. We encode the answer to the function f from which we are reducing in the value of T .

In addition to varying the length of the cycle, we can also penalize some incorrect computations more directly. Certain conditions are checked every iteration of the computational process that is repeated $2T + 1$ times. If one of those conditions is violated, that will trigger a penalty that occurs every $p(N)$ clock steps for a total of $2T + 1$ times during one full iteration of the cycle of length $(2T + 1) \cdot p(N)$. This will result in a matrix corresponding to a cycle of length $L = (2T + 1) \cdot p(N)$ with an additional $+1$ every $p(N)$ locations along the cycle. We show that the lowest energy eigenvalue of this matrix is at least

$$\frac{1}{8} \left(1 - \cos\left(\frac{\pi}{2p(N) + 1}\right)\right) = \Theta\left(\frac{1}{(p(N))^2}\right).$$

We use this mechanism to create the large costs that penalize an incorrect *yes* guess. Then we calibrate the length of the clock T so that guesses y that have more *no* guesses will take shorter time, resulting in a larger ground energy in (1). T will have the required exponentially decreasing costs to account for the adaptive nature of the queries. T will also encode the value to the function $f(x, y)$ which is the outcome of the computation of f on input x , when the string y is used for the oracle responses made by the Turing Machine computing f . If \tilde{y} is the set of correct oracle responses, then $f(x) = f(x, \tilde{y})$. These features are all encapsulated in the following function $T(x, y)$:

$$T(x, y) = f(x, y) + 2^m \left[4^{m+1} + \sum_{j=1}^m y_j \cdot 4^{m-j+1} \right] \quad (2)$$

One of the functions performed by the repeated computation is to compute $T(x, y)$ and to verify that timer mechanism that regulates the number of iterations is in fact equal to the correct $T(x, y)$. We can then prove

that the ground energy of the Hamiltonian is the expression in 1 with $L = (2T(x, \tilde{y}) + 1) \cdot p(N)$, where \tilde{y} is the correct string of oracle responses. Note that this construction requires a much sharper analysis of lowest eigenvalues of matrices than was used in previous constructions of this kind, which is given in Section 2.6.4.

1.4.3 Overview of the Computation Embedded in the Hamiltonian

Now we give an overview of the computation used in the construction. First, a Turing Machine that increments a binary counter is run for $(N - 2)$ TM steps, where N is the length of the chain. The number of TM steps is controlled by a unary counter that advances from one end of the chain to the other. If the starting configuration has the string "1" on the work tape, after $(N - 2)$ TM steps, there will be some string x on the work tape representing the number of increment operations performed. x is then used as the input to the next stage of the computation. This idea of using a binary counter TM to translate the size of the chain into an input string x was used in [16] as well. Define $N(x)$ to be the number such that after $(N(x) - 2)$ TM steps, the binary counter TM completes an increment operation with x on the work tape. The function mapping x to $N(x)$ is the reduction. The complete specification of the binary counter Turing Machine as well as an explicit formula for $N(x)$ is given in Section 2.4.2.

There is also a read-only witness track on which a binary string is stored. The first m bits are used as the guess y for the oracle responses and the remaining bits are used as witnesses for the verifier as needed. If $f \in \text{FP}^{\text{NEXP}}$, then f is computed by a polynomial time Turing Machine M with access to an oracle for language $L \in \text{NEXP}$. The exponential time verifier for L is called V . First M is simulated on input x using the oracle responses given by y . This completely determines the oracle inputs x_1, \dots, x_m . If y guesses that an oracle response is *yes* ($y_i = 1$) then V is simulated on input x_i using a witness w_i from the witness track. If any of the computations are rejecting, a character is placed on the work tape that will trigger a penalty term at the end of the computation. Next the function $T(x, y)$ is computed and written in unary so that it can be checked against the time T used to regulate the number of iterations of the clock. We argue in the analysis that the second stage of this computation can also be computed in at most $(N - 2)$ TM steps. Then the entire process is reversed, so that the configuration returns to its initial state with the string 1 on the work tape. The pseudo-code for the computational process executed in the second $N - 2$ TM steps is given in Figure 2.

Note that since we are reducing from a function $f \in \text{FP}^{\text{NEXP}}$, the verifier V and hence all of the computations described above are classical. We still need a quantum construction to execute the clock and create a ground state that is a superposition of the states of the computation at each clock step. The Section 1.5 includes a discussion about which parts of the construction can be made quantum and where the obstacles lie in reducing from a language in $\text{FP}^{\text{QMA-EXP}}$.

1.4.4 Summary of main new technical contributions in the proof

While the results in the paper make use of many previously known techniques from Hamiltonian complexity, there are several novel technical contributions introduced here which we hope will be useful elsewhere. Typically, circuit-to-Hamiltonian constructions distinguish between accepting and rejecting computations with an additional additive term applied along the diagonal of the propagation matrix for a path. In the case of an accepting computation, the additive cost is exponentially small, and in the rejecting case, the additive cost is close to 1. Our construction must distinguish between many different values for the cost function, which requires a more precise handle on the lowest eigenvalue of the resulting matrix. The circular clock structure which we introduce here gives rise to a propagation matrix for a cycle. Every computation has a fixed cost (two consecutive $1/2$ terms) along the diagonal, so the lowest eigenvalue is strictly decreasing with the length of the cycle. We give exact analytical bounds for the lowest eigenvalue of the resulting matrix which allows us to apply a carefully calibrated cost function for different strings corresponding to oracle responses to queries.

The precise formulation of the lowest eigenvalue is also essential in simultaneously encoding an infinite sequence of numbers (values $f(x)$ for an infinite sequence of x 's) into a single, infinite-precision number. Although the lowest eigenvalue for each finite segment length is a trigonometric function (of the form $1 - \cos(\pi/L)$), given enough high-order bits for $1 - \cos(\pi/L)$, the integer L can be determined, which allows us then to compute $1 - \cos(\pi/L)$ to an arbitrary precision. Thus, given an estimate for α_0 of high enough precision, we can inductively subtract off the energy contributions of $f(x')$ for each $x' < x$, which then leaves enough information to determine $f(x)$.

The use of the circular clock also requires some additional care, as it is important that the computation part of the state also returns to its initial state at the end of the cycle. By contrast, if the computation is a path, the ending state of the computation can be arbitrary. We handle this by embedding a computation which executes a process in the forward direction for a certain number of steps. Since the action on the computation tracks is reversible, the computation can be undone by executing the same number of reverse steps. This forward/backward loop is repeated a fixed number of times (depending on the desired length of the cycle) which ensures that the computation always returns to its original state.

1.5 Related work and Discussion

To the best of our knowledge, this is the first time the complexity of calculating physical quantities in the thermodynamic limit for a fixed Hamiltonian is characterized from a computational perspective. Technically, our proofs required relying on many known ideas from previous works, many of them mentioned above, but we also needed to come up with some novel techniques which we hope will be useful in further Quantum Hamiltonian complexity research. Those are highlighted above in Subsection 1.4.4.

We note that the importance of the fact that the Hamiltonian is independent of the input, was very much the focus of the main result in [16], regarding finite systems, where much effort is devoted to making sure the Hamiltonian is fixed. Bausch, Cubitt, and Ozols give a follow-up construction in which the dimension of the particle is 40 (in contrast to the very large constant from [16]). However, the local Hamiltonian term is a weighted sum of fixed terms, where the weights depend on the input. To the best of our knowledge, the current work is the first to address the computational complexity of a local problem in the thermodynamical limit, in the translational invariant setting, with a fixed Hamiltonian which is a parameter of the problem and does not depend on the input.

The results are not tight; We believe that in fact, the problem is hard for $\text{FP}^{\text{QMA-EXP}}$. The complexity classes QMA-EXP and NEXP differ in several ways. The first is that in QMA-EXP, the verifier is a quantum exponential time algorithm and the witness provided to the verifier is a quantum state on an exponential number of qubits. This contrasts with NEXP where the verifier and witness are both classical. The second important difference is that QMA-EXP is a class of promise problems in which the instances can be classified as *valid* or *invalid*. Valid instances are further partitioned into *yes* and *no* instances. On a valid *no* instance, the verifier will reject with high probability regardless of the witness that is provided. On a valid *yes* instance, there is a witness that will cause the verifier to accept with high probability. If an instance is invalid, there are no guarantees whatsoever on the behavior of the verifier. By contrast, NEXP is a class of languages, in which every instances is a *yes* or *no* instance which has a corresponding guaranty on the behavior of the verifier. One can imagine an intermediate class (QMA-EXP-L) which is a language version of QMA-EXP in which the verifier and witness are quantum but the languages contained in the class do not have invalid instances. The results in this paper can be extended to show that the problems we study are complete for $\text{FP}^{\text{QMA-EXP-L}}$. However, since QMA-EXP-L is not a class of particular interest, we chose to simplify the exposition and show hardness for FP^{NEXP} with a classical verifier and witness. Quantumness is still required in the construction in order to create the computation state which is the superposition of each clock step of an encoded computation.

Interestingly, the fact that QMA is a class of promise problems instead of languages was originally overlooked by Ambainis [4] and later clarified by Gharibian and Yirka [15]. If the oracle is for a promise problem, there are no guarantees on the responses for invalid queries. This means that there could be more than one string of correct oracle queries, since we only require that responses be correct on valid instances. Gharibian and Yirka show that for the problems they study, namely decision problems related to local measurements on the ground state of a Hamiltonian, the ground state of their construction must correspond to one of the correct oracle response strings. This idea works fine if the quantity being measured is not the actual energy itself: the ground state corresponds to correct oracle responses and then this string y of oracle responses determines the outcome of the measurement. However, if the problem is to compute the ground energy, a hardness result requires encoding the answer to a computational problem into the ground energy itself. In the presence of invalid queries, the ground energy is an unknown and uncontrolled quantity. This appears to be an obstacle, even when the Hamiltonian terms are position-dependent as in the constructions of [15, 14], as well as in the translationally-invariant constructions given here and in [22]. It remains an open question to determine tight complexity bounds for computing the ground energy to within a given level of precision, even in the finite non-translationally-invariant

case.

It should also be noted that problems studied by Watson, Bausch, and Gharibian [22] are similar to the results presented here for finite systems. They examine the complexity of general local measurements, in contrast to our problem of computing the energy. However, the underlying problem of encoding the cost scheme for oracle guesses in a translationally-invariant way is similar. They use a different scheme to encode the costs in the Hamiltonian term than ours. As written, their Hamiltonian term includes parameters that depend on the input, so their paper does not apply to the fixed Hamiltonian setting. However following the first announcement of these results, we have discussed this with them [7], and based on our reading of their paper and the discussion with the authors, it is likely that their techniques can be adapted to eliminate this dependence. It's still not clear whether their scheme could be adapted for the infinite case since we require a very tight analysis of the resulting eigenvalues in order to recover the solution to a function problem from which we are reducing using a sufficiently tight approximation of the ground energy density.

We note that in this paper we use the notion of translationally invariant Hamiltonians in the strong sense, namely, the terms acting on different adjacent pairs of particles are the same. This is in contrast to quite a few previous works on translationally invariant systems, in which the notion of translationally-invariance was relaxed, to allow more expressiveness of the input. In particular, [10] studied the classification of families of Hamiltonian terms in which the Hamiltonian is sum of local terms, each is some weight times some Hamiltonian term taken from some fixed set. This notion was coined *semi-translational invariance* [2] and is a considerably weaker notion.

2 Computing Ground Energies for Finite Translationally Invariant Hamiltonians

2.1 Containment

Using binary search with queries to a QMA-EXP oracle, it is possible in polynomial time to determine $\lambda_0(H_N)$ to within $\pm 1/q(N)$, for any polynomial $q(N)$. There is a little subtlety regarding the fact that the queries are made to a promise problem instead of a language. The algorithm below shows how an oracle to a language in QMA-EXP can be used to compute the ground energy of H_N . The oracle computes a decision version of the translationally-invariant Hamiltonian problem:

DECISION-TIH FOR h AND CONSTANT c

Input: A number N specified with n bits, and λ , specified with cn bits.

Output: Accept if $\lambda_0(H_N) \leq \lambda$ and Reject if $\lambda_0 \geq \lambda + 1/2^{cn}$.

Here is an algorithm to compute the Function-TIH in $\text{FEXP}^{\text{QMA-EXP}}$ with access to an oracle for Decision-TIH which is in QMA-EXP. The algorithm maintains two variables u and l , which are an upper and lower bound on $\lambda_0(H_N)$. If the number of rounds is r then the precision is $O(1/2^r)$.

Lemma 2.1. *After the final iteration, $\lambda_0 \in [l, u]$ and $u - l = 1/2^r$.*

Proof. Let u_j and l_j be the values of u and l after iteration j . We prove by induction on j , that $\lambda_0 \in [l_j, u_j]$ and $u_j - l_j = 1/2^j$.

If the result of the first query is Accept, then $\lambda_0 \leq \lambda_1 + 1/2^{j+1} = l_{j-1} + 1/2^j = u_j$. By the inductive hypothesis, $\lambda_0 \geq l_{j-1} = l_j$. $u_j - l_j = (l_{j-1} + 1/2^j) - l_{j-1} = 1/2^j$.

If the result of the second query is Reject, then $\lambda_0 \geq \lambda_2 = l_{j-1} + 2/2^{j+1} = l_j$. By the inductive hypothesis, $\lambda_0 \leq u_{j-1} = u_j$. Also, by the inductive hypothesis, $u_{j-1} - l_{j-1} = 1/2^{j-1}$. $u_j - l_j = u_{j-1} - (l_{j-1} + 2/2^{j+1}) = 1/2^{j-1} - 1/2^j = 1/2^j$.

If the result of the first query is Reject, then $\lambda_0 \geq \lambda_1 = l_{j-1} + 1/2^{j+1} = l_j$. If the result of the second query is Accept then, $\lambda_0 \leq \lambda_2 + 1/2^{j+1} = l_{j-1} + 3/2^{j+1} = u_j$. $u_j - l_j = (l_{j-1} + 3/2^{j+1}) - (l_{j-1} + 1/2^{j+1}) = 1/2^j$. \square

Corollary 2.2. *Function-TIH $\in \text{FP}^{\text{QMA-EXP}}$.*

<p>ALGORITHM FOR FUNCTION-TIH</p> <p>(1) Initialize $u \leftarrow 1$ and $l \leftarrow 0$.</p> <p>(2) for $j = 1, \dots, r$</p> <p>(3) Send two queries to Decision-TIH with the following two input λ's (padded with 0's to have length $j + 1$):</p> <p>(4) $\lambda_1 = l + 1/2^{j+1}$</p> <p>(5) $\lambda_2 = l + 2/2^{j+1}$</p> <p>(6) if the result of query 1 is Accept:</p> <p>(7) $u \leftarrow l + 1/2^j$</p> <p>(8) if the results of queries 1 and 2 are both Reject:</p> <p>(9) $l \leftarrow l + 1/2^j$</p> <p>(10) if the result of query 1 is Reject and the result of query 2 is Accept:</p> <p>(11) $u \leftarrow l + 3/2^{j+1}$</p> <p>(12) $l \leftarrow l + 1/2^{j+1}$</p> <p>end</p>
--

Figure 1: Pseudo-code for the Function-GED.

Proof. Use the binary search algorithm in Figure 1. Choose r to be cn , where the constant c can be chosen so that after cn iterations, the desired precision $1/q(N)$ is at most $1/2^{cn}$. \square

2.2 Hardness: Overview of the Construction

We start with an arbitrary $f \in \text{FP}^{\text{NEXP}}$ and construct a Hamiltonian term h that operates on two d -dimensional particles. Let H_N denote the Hamiltonian on a chain of N d -dimensional particles resulting from applying h to each neighboring pair in the chain. The reduction will map an input string x of length n to a positive integer $N = N(x)$ such that $N(x)$ can be computed in time polynomial in n . We will show that there is a polynomial q such that there is a polynomial time algorithm, which can compute $f(x)$ given a $1/q(n)$ -approximation of $\lambda_0(H_N)$, namely a value E , where $|E - \lambda_0(H_N)| \leq 1/q(n)$.

We will also assume without loss of generality that if the last bit of x is 0, then $f(x) = 0$. If f does not have this property, then we can define a new function f' such that $f'(x0) = 0$ and $f'(x1) = f(x)$. Any polynomial time algorithm to compute f' can be used to compute f .

Since $f \in \text{FP}^{\text{NEXP}}$, f can be computed by a polynomial-time Turing Machine M with access to an oracle for language $L \in \text{NEXP}$. The verifier for L is a Turing Machine V which runs in time exponential in the size of the query input and uses a witness whose length is also exponential in the size of the query input. We will assume that there are constants c_1 and c_2 such that on input x of length n , the number of queries made by M is at most $c_1 n$ and if M makes a query \bar{x} to the oracle, the size of the witness w required is at most $2^{c_2 n}$ and the running time of V on input (\bar{x}, w) is at most $2^{c_2 n}$. This assumption which follows from a standard padding argument, is given in Section 2.4.3.

As is typical in hardness results for finding ground state energies, we use Kitaev's circuit-to-Hamiltonian construction in which the ground state will correspond to the history state of a computation [17]. Note that since we are reducing from $\text{FEXP}^{\text{NEXP}}$, the computation encoded in the ground state is classical. A quantum state is still needed in the construction in order to create the history state which is a quantum superpositions of the state of the computation at each point in time. The ground state of the Hamiltonian will correspond to a uniform superposition of the state of the computation at each point in time. The process of transitioning from one state to another is regulated by a clock encoded in a different part of the Hilbert space than the computation. The next subsection outlines how the Hilbert space of each particle is divided to encode the clock and the computation.

2.2.1 The Track Structure of the Hilbert Space

The Hilbert space of each particle is a tensor product of 6 different spaces which will be used to form 6 tracks. There are also two additional states $\langle \ominus \rangle$ and $\langle \otimes \rangle$. So the Hilbert space for particle i is

$$\mathcal{H}_i = \{\langle \ominus \rangle, \langle \otimes \rangle\} \oplus (\mathcal{H}_{i,1} \otimes \mathcal{H}_{i,2} \otimes \mathcal{H}_{i,3} \otimes \mathcal{H}_{i,4} \otimes \mathcal{H}_{i,5} \otimes \mathcal{H}_{i,6}).$$

Later, we will introduce constraints that enforce the condition that for a low energy state, the leftmost particle must be in state $\langle \ominus \rangle$, the right particle must be in state $\langle \otimes \rangle$ and the particles in between are not in states $\langle \ominus \rangle$ or $\langle \otimes \rangle$. We will call all such standard bases states *bracketed*. The space spanned by all bracketed states is \mathcal{H}_{br} and the final Hamiltonian is invariant on \mathcal{H}_{br} . For any bracketed state, Track k of the system of N particles consists of the tensor of $\mathcal{H}_{i,k}$ as i runs from 2 to $N - 1$. Thus, the state of the system can be pictured as:

$\langle \otimes \rangle$	$\langle \ominus \rangle$...	Track 1: Clock second hand	...	$\langle \ominus \rangle$	$\langle \ominus \rangle$
$\langle \ominus \rangle$	$\langle \ominus \rangle$...	Track 2: Clock minute hand	...	$\langle \ominus \rangle$	$\langle \ominus \rangle$
$\langle \ominus \rangle$	$\langle \oplus \rangle$...	Track 3: Clock hour hand	...	$\langle \otimes \rangle$	$\langle \otimes \rangle$
$\langle \ominus \rangle$	q_0	...	Track 4: Tape head and state for TM V	...	$\langle \ominus \rangle$	$\langle \otimes \rangle$
1	#	...	Track 5: Turing Machine Work Tape	...	#	#
0/1/0/1	...	Track 6: Quantum witness for V	...	0/1/0/1		

Tracks 1 through 3 are called *Clock Tracks*. Tracks 4 through 6 are called *Computation Tracks*. The symbols in the figure above represent standard basis states for each portion of the Hilbert space of the particle $\mathcal{H}_{i,j}$ whose meaning will be described later. The states for the computation tracks will depend on the Turing Machine being simulated. We will use Γ to denote the tape alphabet for the TM and Q to denote the set of states. The standard basis for each $\mathcal{H}_{i,j}$ are:

$$\begin{aligned} \mathcal{H}_{i,1}: & \{ \langle \ominus \rangle, \langle \otimes \rangle \} \cup \{ \langle \leftarrow \rangle, \langle \rightarrow \rangle \mid i = 1, \dots, 8 \} \\ \mathcal{H}_{i,2}: & \{ \langle \ominus \rangle, \langle \oplus \rangle, \langle \otimes \rangle, \langle \leftarrow \rangle \} \\ \mathcal{H}_{i,3}: & \{ \langle \oplus \rangle, \langle \otimes \rangle, \langle \leftarrow \rangle, \langle \rightarrow \rangle \} \\ \mathcal{H}_{i,4}: & \{ \langle \ominus \rangle, \langle \otimes \rangle \} \cup Q \\ \mathcal{H}_{i,5}: & \Gamma \quad (\text{which includes } 0, 1, \text{ and } \#) \\ \mathcal{H}_{i,6}: & \{0, 1\} \end{aligned}$$

An overview of the structure of the clock is given in Subsection 2.2.3. The details of the terms governing the clock are given in Section 2.3. The computation tracks will represent the configuration of a Turing Machine. A typical configuration for the computation tracks will look like:

$\langle \ominus \rangle$	$\langle \ominus \rangle$	$\langle \ominus \rangle$	$\langle \ominus \rangle$	q_1	$\langle \ominus \rangle$	$\langle \ominus \rangle$	$\langle \ominus \rangle$	$\langle \ominus \rangle$	$\langle \otimes \rangle$
$\langle \ominus \rangle$	γ	σ	σ	γ	σ	$\#$	$\#$	$\#$	$\#$
$\langle \ominus \rangle$	1	0	1	0	0	1	0	1	1

The symbols $\sigma, \gamma \in \Gamma$ are elements in the tape alphabet of the TM, and $q_1 \in Q$ is a state of the TM. Track 6 contains a read-only binary string which stores the guesses for the oracle responses and witnesses used in verifier computations. An overview of the computations performed on the computation tracks is given in Subsection 2.2.5. The details regarding how the steps of the Turing Machine are encoded in the Hamiltonian are given in Section 2.5.2.

2.2.2 Circuit-to-Hamiltonian construction

The Hamiltonian is a sum of two body terms, and there are two types of terms. Type I terms will have the form $|ab\rangle\langle ab|$ where a and b are possible states. This has the effect of adding an energy penalty to any state which has a particle in state a to the immediate left of a particle in state b . In this case, we will refer to ab as an *illegal pair*. We will sometimes consider the restriction of an illegal pair to a set of tracks. In this case we implicitly mean that the Hamiltonian term acts as the identity on the remaining (unspecified tracks). For example the term $|\langle \leftarrow \rangle \langle \leftarrow \rangle\rangle\langle \leftarrow \rangle \langle \leftarrow \rangle|$ applied to Track 2 means that any pair of neighboring particles in which $\mathcal{H}_{i,2} \otimes \mathcal{H}_{i+1,2}$ is in state $|\langle \leftarrow \rangle \langle \leftarrow \rangle\rangle$ will contribute +1 to the energy of the state. The restriction of an illegal pair to a set of tracks will

sometimes be referred to as an *illegal pattern*. We will refer to standard basis states of the whole chain or a subset of the tracks as *configurations*. Any configuration which has an illegal pattern or illegal pair is said to be illegal.

We will sometimes use a regular expression to define a subset of standard basis states. Throughout the construction, we will make use of the following lemma (Lemma 5.2 from [16])

Lemma 2.3. *For any regular expression over the set of particle states in which each state appears at most once, we can define a set of illegal pairs such that for any standard basis state x for the system, x is a substring of a string in the regular set if and only if x does not contain an illegal pair.*

We will refine this a bit further for bracketed states:

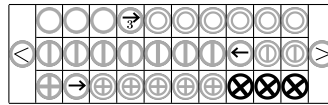
Lemma 2.4. [Regular Expressions for Standard Basis States] *Consider any regular expression over the set of particle states in which each state appears at most once. If the corresponding regular set only contains bracketed strings, then we can use illegal pairs to ensure that for any bracketed standard basis state x for the system, x is in the regular set if and only if x does not contain any illegal pairs.*

Proof. If x is a substring of y and x and y are both bracketed, then $x = y$. □

Type II terms will have the form: $\frac{1}{2}(|ab\rangle\langle ab| + |cd\rangle\langle cd| - |ab\rangle\langle cd| - |cd\rangle\langle ab|)$. These terms enforce that for any eigenstate with zero energy, if there is a configuration A with two neighboring particles in states a and b , there must be a configuration B with equal amplitude that is the same as A except that a and b are replaced by c and d . Even though a Type II term is symmetric, we break this symmetry and associate with each such term a direction by choosing an order on the pair of pairs. If we decide that ab precedes cd , then we denote the term as: $ab \rightarrow cd$. Type II terms are also referred to as *transition rules*. We will say that configuration A transitions into configuration B by rule $ab \rightarrow cd$ if B can be obtained from A by replacing an occurrence of ab with an occurrence of cd . We say that the transition rule applies to A in the forward direction and applies to B in the backwards direction. The sum of all the Type II terms is called h_{prop} or the *propagation Hamiltonian*. Again, we may specify that a transition rule acts on a particular subset of the tracks: $ab_{\mathcal{T}} \rightarrow cd_{\mathcal{T}}$, where \mathcal{T} is a subset of the tracks. This implicitly means that the Hamiltonian term acts as the identity on the remaining tracks. It will also sometimes be convenient to say that a transition rule applies to every state except a particular standard particle basis state. In this case, we will denote the rule by: $a(-b) \rightarrow cd$ to indicate that the rule applies to every ax pair, where $x \neq b$.

2.2.3 Overview of the Clock Tracks

A typical configuration of the clock tracks looks like:



Track 1 will have exactly one pointer that shuttles back and forth between the left and right ends of the chain according to the transition rules. The \rightarrow pointer moves to the right and the \leftarrow pointer moves to the left. Constraints are added to ensure that any Track 1 configuration with no pointers or more than two pointers incurs an energy penalty. The Track 1 pointers come in 8 different varieties and are labeled with tags in the range from 1 through 8. A Track 1 pointer labeled i is called an i -pointer. There are two i -pointers for each i : $\leftarrow i$ and $i \rightarrow$. The different types of Track 1 pointers act as a means of program control as they trigger different operations on the three computation tracks (Tracks 4, 5, and 6). A right-to-left sweep of an i pointer, for $i = 1, 2, 3$, advances the Turing Machine configuration on the computation tracks by exactly one TM step. The 1-pointer and 2-pointer execute a step of a different Turing Machine than the 3-pointer. A left-to-right sweep of an i -pointer for $i = 5, 6, 7$, applies the reverse steps of the Turing Machines. The 4-pointers and 8-pointers act as the identity on the computation tracks and are used to trigger Type I penalty terms which enforce that the computation in a low energy state has the correct input and output.

The odd numbered i -pointers make a single round trip, beginning and ending at the same end of the chain. The even numbered pointers make multiple round trips, where the number of iterations is regulated by a pointer

on Track 2. The Track 1 pointer is like the second hand of a clock while the Track 2 pointer is like the minute hand. In each iteration of an even numbered i -pointer, the Track 2 pointer is advanced by one location. When the Track 2 pointer reaches the end of the chain, the i -pointer transitions to an $(i + 1)$ -pointer. The 8-pointer transitions to a 1-pointer, forming a cycle of clock configurations for Tracks 1 and 2. A maximal sequence of consecutive clock steps in which the Track 1 pointer (left or right) is labeled with i is called an i -segment. Figure 6 shows the number of clock steps in each segment. A more graphical representation is given in Figure 12. A segment that consists of a single round trip of the Track 1 pointer lasts for $2(N - 2)$ clock steps. A segment that consists of multiple round trips of the Track 1 pointer last for $(N - 2)(2N - 5)$ clock steps.

We classify configurations for Tracks 1 and 2 as either *correct* or *incorrect* and show that the incorrect clock configurations will never be in the support of the ground state. There are exactly $p(N) = 4(N - 2)(2N - 3)$ correct clock configurations for Tracks 1 and 2. Starting with any of these, if we apply the transition rules $p(N)$ times, we will cycle through all the correct clock configurations for Tracks 1 and 2 and return to the initial configuration.

The third clock track acts like an hour hand in that the pointer on Track 3 moves by one location each time Tracks 1 and 2 iterate through a cycle (every $p(N)$ clock steps). Each correct configuration for Track 3 has a *timer length* which regulates the number of clock steps in a full cycle of the clock. If the length of the timer is T , then Track 3 cycles through $2T + 1$ configurations before repeating. The transition rules never alter the length of the Track 3 pointer. For each Track 3 configuration, Tracks 1 and 2 will complete a cycle lasting $p(N)$ clock steps. Thus the total number of clock steps in a cycle for Tracks 1, 2, and 3 is $(2T + 1) \cdot p(N)$.

We add constraints to ensure that the Track 3 configurations in the support of the ground state must be of the form

$$\langle \leftarrow \oplus^* (\rightarrow + \leftarrow) \oplus^* \otimes^* \rangle.$$

The number of \oplus or \otimes particles is the length of the timer for Track 3. The Track 3 pointer shuttles back and forth between the left end of the chain and the left-most \otimes particle. In the sample configuration shown above, the Track 3 timer has length 6 which will result in 13 iterations of the cycle for Tracks 1 and 2 for every cycle of the entire clock.

In the construction, every computation (even correct computations) will have a small cost at least once in a cycle of $(2T + 1) \cdot p(N)$ clock steps. The smallest eigenvalue will be $\Theta(1/L^2)$, where $L = (2T + 1) \cdot p(N)$ is the length of the cycle. Thus we can regulate the smallest eigenvalue by controlling the length of a cycle.

2.2.4 Structure of the Hamiltonian

The clock propagation terms naturally creates a structure on the underlying Hilbert space. We refer to a standard basis state for Tracks 1, 2, and 3 as a *clock configuration*. We first define a set of clock configurations that are *well formed*. The condition of being well-formed can be checked by local conditions by Lemma 2.4, so any configuration that is not well-formed will have high energy. We will also show that the Hamiltonian is closed on the span of well-formed configurations, so we can consider the space spanned by well-formed configurations separately from the perpendicular space. We can define a graph structure on the set of well-formed clock configurations, where edges represent transitions:

Definition 2.5. [Configuration Graph] *The vertices of the configuration graph correspond to the well-formed clock configuration for Tracks 1, 2, and 3. There is a directed edge from configuration c_1 to configuration c_2 , if c_2 can be reached from c_1 by the application of one transition rule in the forward direction.*

We show that every well-formed clock configuration has at most one in-coming and at most one out-going edge in the configuration graph. We also show that the well-formed clock configurations can be further divided into *correct* and *incorrect* configurations and that incorrect clock configurations will never be in the support of the ground state. For each $T \in \{0, \dots, N - 3\}$, there is a cycle of length $(2T + 1)p(N)$ consisting of all the correct clock configurations in which the Track 3 timer has length T . For a particular T , we will denote these clock configurations by $|c_{T,s,t}\rangle$. The value of s is in the range $0, \dots, 2T$ and denotes the configuration of the Track 3 timer. The value of t is in the range $0, \dots, p(N) - 1$, and denotes the configurations for Tracks 1 and 2.

The Track 1 pointer triggers steps of a Turing Machine whose configuration is stored on on the computation tracks. The computation consists of $N - 2$ steps of two Turing Machines (M_{BC} and M_{TV} described below) in the forward direction and then $N - 2$ steps of each Turing Machine (M_{TV} and then M_{BC}) in the reverse direction.

Each clock step produces a unitary operation on the computation tracks, so that if the computation begins a cycle for Tracks 1 and 2 in state $|\phi\rangle$, then after $p(N)$ clock steps of the transition function, Tracks 1 and 2 will be back to their original configuration and the computation tracks will have returned to state $|\phi\rangle$. Thus, each cycle (for all three tracks) consists of the same computation repeated $2T + 1$ times, where T is the length of the timer on Track 3.

Tracks 4 and 5 will denote the contents of the work tape of the Turing Machine along with the state and head location. Let $\{|v\rangle\}$ be the standard basis for Tracks 4 and 5. Let $\{|w\rangle\}$ be a basis for the read-only witness on Track 6. If we fix the computation state to be some $|v\rangle|w\rangle$ at time $(0, 0)$, then the state of the computation tracks at some time (s, t) , depends only on t and not on s or T . We will call this state $|\phi(v, w, t)\rangle$. For each T and $|v\rangle|w\rangle$, We can then define the ortho-normal set:

$$S_{T,v,w} = \{|c_{T,s,t}\rangle|\phi(v, w, t)\rangle : \text{for } s \in \{0, \dots, 2T\}, t \in \{0, \dots, p(N) - 1\}\}.$$

The sum of all the transition terms in the Hamiltonian applied to a chain of length N (which we call $H_{N,prop}$) is closed on the span of each $S_{T,v,w}$ and is $1/2$ times the Laplacian of a cycle graph with $(2T + 1)p(N)$ vertices. All of the other terms of the Hamiltonian will be diagonal in this basis. Thus, the Hamiltonian is closed on the span of each block, so we can consider each block separately. Note that the $|c_{T,s,t}\rangle$ are by definition correct clock states.

Some of the blocks will have a *periodic cost* which consists of at least one $+1$ every $p(N)$ locations along the diagonal. These costs come from an illegal configuration that appears in each of the repeated computations. We will show that the smallest eigenvalue for each such block is at least $1/2(p(N))^2$ and will therefore not contain the ground state. Meanwhile in every block, there will be two consecutive $+1/2$ costs for clock configuration $|c_{T,0,0}\rangle$ and $|c_{T,0,1}\rangle$. The matrix for a block with timer length T that does not have a periodic cost is $H_{N,prop}$ for a cycle of length $(2T + 1)p(N)$ with two consecutive additional $+1/2$ terms on the diagonal. We prove in Lemma 2.54 that the smallest eigenvalue of this matrix is exactly

$$\left(1 - \cos \frac{\pi}{(2T + 1)p(N) + 1}\right) = \Theta\left(\frac{1}{[(2T + 1)p(N)]^2}\right).$$

Therefore the ground state for the Hamiltonian will belong to the block with the largest T that does not have a periodic cost.

2.2.5 The description of the two Turing Machines: M_{BC} and M_{TV} .

The constructions will make use of three different Turing Machines, M_{BC} , M_T and M_V . We will assume that all three are reversible. This is a valid assumption since it is known that any Turing Machine can be transformed into a reversible TM. There may be some additional overhead, but it is not significant.

As explained in Subsubsection 2.3, Track 3 is responsible for the FOR loop which counts the cycles; in each cycle, 8 segments are executed, with the help of the clocks advanced in track 1 and 2. These 8 segments consist, essentially, of 4 main segments: running two Turing machines, M_{BC} and M_{TV} , each for $N - 2$ steps, and then running them backwards. These are interspersed with shorter segments that are required to ensure that the number of TM steps is exactly $N - 2$ for M_{BC} and M_{TV} . This cycle is repeated $2T + 1$ times, where the value of T is written on track 3 initially.

Binary Counter Turing Machine: The initial configuration of M_{BC} will have the head in state q_0 pointing to a 1 followed by all blank symbols to the right. The head of M_{BC} will never move to the left of the original starting location. M_{BC} will repeatedly execute an increment operation. Each increment operation starts with the head in state q_0 at the left end of a binary string whose right-most bit is 1. After the increment operation, the head is back to the original location in state q_f and the binary string (interpreted as a the reverse of a binary number) has been incremented. M_{BC} then transitions to q_0 for the next increment operation. The Turing Machine M_{BC} is described in detail in Section 2.4.2.

The reduction will map x to an integer N such that after $N - 2$ steps of M_{BC} , the contents of the the work tape is x , and the head is in state q_f in its original location. The function $N(x)$, mapping x to N , is the actual reduction. The function $N(x)$ is calculated explicitly in Section 2.4.2

The Turing Machine M_T assumes that the string x is written on the work tape and a witness string is written on another auxiliary track (which will be Track 6 in our construction). The Turing Machine M_T will start in an initial state p_0 with the head located at the leftmost input symbol. Then M_T will compute $m = c_1|x|$, where c_1 is a constant that is determined by M . Let y denote the first m bits of the witness string and y_i the i^{th} bit of y . Then M_T will simulate Turing Machine M on input x using oracle responses denoted by y to obtain the output string $f(x, y)$. Note that by assumption $|f(x, y)| = m$. Then M_T will compute the following quantity and write that value in unary on the worktape:

$$T(x, y) = f(x, y) + 2^m \left[4^{m+1} + \sum_{j=1}^m y_j \cdot 4^{m-j+1} \right]$$

The function $T(x, y)$ is used to implement a cost scheme which introduces an exponentially decreasing penalty for every *no* guess in the string y . The exponentially decreasing penalties is needed because of the adaptive nature of the oracle queries. It ensures that the cost due to an incorrect *no* guess for query i outweighs any advantage that could be gained in future requests.

The Turing Machine M_V simulates M with input x and oracle queries y from the witness tape. If the oracle responses are fixed, then the input to each oracle query is also fixed. Let x_i denote the input to the i^{th} oracle query. The next $m \cdot 2^{c_2|x|}$ bits of the witness after y are divided into m segments of length $2^{c_2|x|}$, where c_2 is a constant determined by M and V . Let w_i denote the string formed by the bits in the i^{th} segment. For each i such that $y_i = 1$, M_V runs the verifier V on input (x_i, w_i) . Recall that V is the verifier for language L , which is the oracle language for the function $f \in \text{FP}^{\text{NEXP}}$.

We will dovetail M_T and M_V together to form a single computation executed by Turing Machine M_{TV} .

Timer and Verification Turing Machine: The computation of M_{TV} starts with x written in binary on the worktape and finishes in the following configuration: The first symbol is σ_A if all of the verifier computations were accepting and σ_R if any of the verifier computations were rejecting. Then $T(x, y)$ is written in unary on the worktape using the character σ_X . The remainder of the work tape is arbitrary but can not contain the symbols σ_A , σ_R , or σ_X . The head never moves to the left of the starting location and M_{TV} will end in state p_f with the head back in the original start location. The pseudo-code for M_{TV} is given in Figure 2.

The following definition allows us to refer to the correct output of M_{TV} whose behavior depends on the input pair (x, w) as well as Turing Machines M and V :

Definition 2.6. [Correct Output of M_{TV}] Define $\text{OUT}(x, w, M, V)$ as the correct output of M_{TV} on input (x, w) using Turing Machines M and V , as described in Figure 2.

2.2.6 Overview of the Penalty Terms

The 8-pointer for Track 1 makes a single round trip, starting and ending at the left end of the chain. This is the last iteration of a Track 1 pointer in a cycle for Tracks 1 and 2, so we use this pointer to check that the configuration of the Turing Machine tracks is in the correct initial configuration to begin the computation again in the next cycle for Tracks 1 and 2. Thus, as the 8-pointer sweeps from right to left, it will trigger an energy penalty if the the configuration of Tracks 4 and 5 do not correspond to the correct starting configuration. The correct starting configuration has the head in the left-most location in state q_0 , with tape contents: $1\#\#\#\#\dots$. We will refer to the correct starting configuration for Tracks 4 and 5 as $|v\text{-init}\rangle$. Thus any block corresponding to $S_{T,v,w}$ in which $v \neq v\text{-init}$ will incur a periodic cost and will not contain the ground state.

Any computation which does start in the correct initial state will have the correct x written in binary after $N - 2$ steps of M_{BC} . Then M_{TV} will then be run $N - 2$ steps. At the end of the 3-segment, there will be an σ_A or σ_R in the first location of the work tape followed by the quantity $T(x, y)$ written in unary, where y is the string corresponding to the first m bits of the witness track. The 4-pointer then makes a single round trip and adds a penalty if the timer on Track 3 is not exactly equal to the correct $T(x, y)$ computed by M_{TV} . This will result in a periodic cost for any block whose Track 3 timer length T is not the correct $T(x, y)$ for input x and the y from its witness track.

```

INPUT:  $(x, w)$ 
(1) Compute  $N = N(x)$ 
(2)  $m$  is the number of oracle queries made by  $M$  on input  $x$ 
(3)  $r$  is the size of the witness used by  $V$  on any oracle query generated by  $M$  on input  $x$ 
(4)  $m$  and  $r$  are hard-coded functions of  $|x|$  determined by  $M$  and  $V$ .
(5) Simulate Turing Machine  $M$  on input  $x$ 
(6) Use  $y$  for the responses to the oracle queries, where  $y$  denotes the first  $m$  bits of  $w$ 
(7) Simulation generates  $x_1, \dots, x_m$ , inputs to oracle queries
(8) REJECT = FALSE
(9) for  $i = 1 \dots m$ 
(10) if  $y_i = 1$ 
(11) Simulate  $V$  on input  $(x_i, w_i)$ 
(12)  $w_i$  is the string formed by bits  $m + (i - 1)r + 1$  through  $m + ri$  of the witness track
(13) If  $V$  rejects on input  $(x_i, w_i)$ 
(14) REJECT = TRUE
(15) if (REJECT)
(16) Write  $\sigma_R$  in the left-most position of the work tape
(17) else
(18) Write  $\sigma_A$  in the left-most position of the work tape
(19) Compute  $T(x, y)$ 
(20) Write the value of  $T(x, y)$  in unary with  $\sigma_X$  symbols starting in the second position of the work tape
OUTPUT:  $(\{\sigma_A, \sigma_R\}(\sigma_X)^{T(x,y)}; x, w)$ 

```

Figure 2: Pseudo-code for the Turing Machine M_{TV} .

The 4-pointer also causes a penalty if the leftmost symbol on the work tape after M_{TV} 's computations is σ_R instead of σ_A . This will cause a periodic cost for any block with oracle guesses y such that y guesses that the i^{th} oracle response should be *yes* ($y_i = 1$) but the input x_i to the i^{th} oracle query is actually a *no* instance. This introduces a periodic cost for every y that has an incorrect *yes* guess. The incorrect *no* guesses are penalized by making the timer $T(x, y)$ shorter which will result in a larger ground energy for that block even without a periodic cost.

Note that the value of $T(x, y)$ effectively introduces a penalty for every $y_i = 0$ by making the timer length $T(x, y)$ shorter. Moreover these penalties are decreasing exponentially with i . This is important because the queries are adaptive. An incorrect oracle response could potentially change the oracle queries made in the future and it is important that the penalty for an incorrect guess on the i^{th} query results in a higher penalty that could be potentially gained on any of the future queries $i + 1$ through m . The proof then shows that the smallest eigenvalue must come from a block corresponding to \tilde{y} , the correct oracle responses. The final step of the reduction is to show that if the correct ground energy

$$\left(1 - \cos \frac{\pi}{L + 1}\right),$$

for $L = (2T(x, \tilde{y}) + 1)p(N)$, can be estimated to within $1/poly(N)$, then the integer $(2T(x, \tilde{y}) + 1)p(N)$ can be determined. The value of $f(x) = f(x, \tilde{y})$ can then be easily extracted from $T(x, \tilde{y})$.

2.3 The Clock Tracks

We start by defining the set of well-formed clock configurations. Penalty terms will be added so that we can assume that the ground state will be in the span of all well-formed clock configurations.

Definition 2.7. [Well-formed Clock Configurations] Any standard basis state of Tracks 1 through 3 is called a clock configuration. A clock configuration is said to be well formed if the configuration has the following form for each track:

1. Track 1: $\langle \circ \circ^* (\uparrow + \downarrow) \circ^* \rangle$
2. Track 2: $\langle \circ \circ^* (\rightarrow + \leftarrow) \circ^* \rangle$
3. Track 3: $\langle \circ \oplus^* (\rightarrow + \leftarrow) \oplus^* \otimes^* \rangle$

By Lemma 2.4, we can use Type I constraints to give an energy penalty to any clock state that is bracketed but not well-formed.

Definition 2.8. [Hamiltonian Terms to Enforce Well-formed Clock Configurations] Let h_{wf-cl} denote the Hamiltonian terms with the constraints that give an energy penalty for any clock state that is bracketed but not well-formed.

We will prove (Lemma 2.16) that the set of transition rules is closed on the set of well-formed clock configurations. Since every clock configuration that is not well-formed has an energy of at least 1, we can restrict our attention to the subspace spanned by well-formed clock configurations. We will also show that the in-degree and out-degree of every vertex in the configuration graph is bounded by 1 and therefore the graph consists of a set of disjoint paths and cycles.

We will further partition the set of well-formed clock configurations into *correct* and *incorrect* configurations. Lemma 2.19 shows that the configuration graph has additional structure as each connected component contains only correct or only incorrect configurations. Moreover, every incorrect configuration is in a path of length at most $p(N)$ which ends in a illegal configuration. Since all other terms are diagonal in the standard basis, the overall Hamiltonian will be closed on the span of states with an incorrect clock configuration and those states will have energy at least $\Omega(1/p(N)^2)$. In addition, there are exactly $(2T + 1)p(N)$ correct clock configurations whose timer length is T and those configurations form a cycle of length $(2T + 1)p(N)$ in the configuration graph.

Since correct configurations will form cycles under the transition rules, it will be convenient to define a Time 0 in the cycle:

Definition 2.9. [Time 0]

1. A clock configuration is at Time 0 for Track 2 if it's Track 2 state is $\langle \circ \rightarrow \circ^* \rangle$
2. A clock configuration is at Time 0 for Tracks 1 and 2 if it's Track 1 state is $\langle \circ \rightarrow \circ^* \rangle$ and its Track 2 state is $\langle \circ \rightarrow \circ^* \rangle$.
3. A clock configuration is at Time 0 for Tracks 1, 2, and 3 if it's Track 1 state is $\langle \circ \rightarrow \circ^* \rangle$, it's Track 2 state is $\langle \circ \rightarrow \circ^* \rangle$, and its Track 3 state is $\langle \circ \rightarrow \oplus^* \rangle$.

For each correct Track 3 configuration, Tracks 1 and 2 cycle through all possible correct configurations, starting with the Time 0 configuration for Tracks 1 and 2. This sequence is called a *cycle for Tracks 1 and 2*. Each cycle for Tracks 1 and 2 consists of 8 segments, starting with a 1-segment and ending with a 8-segment. Figure 6 shows a summary of all of the segments in a single cycle for Tracks 1 and 2. A more graphical representation is given in Figure 12.

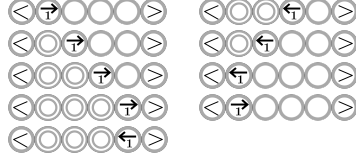
In the remainder of this section, we will describe the propagation terms for the clock as well as some Type I constraints that enforce additional constraints on the clock configuration. These sum of the additional Type I terms will be denoted h_{cl} .

2.3.1 Rules for 1-pointers

The 1-pointers make many iterations between the left and the right ends of the chain. This is accomplished by the following four generic transition terms:

$$\begin{array}{ccccccc} \uparrow \circ & \rightarrow & \circ \uparrow & \quad & \uparrow \circ & \rightarrow & \circ \uparrow & \quad & \circ \uparrow & \rightarrow & \uparrow \circ & \quad & \circ \uparrow & \rightarrow & \uparrow \circ \end{array}$$

Note that these rules will be enhanced to trigger certain actions on the other tracks. The following sequence shows one round trip:

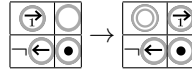


In general, one iteration of a Track 1 pointer will take $2(N - 2)$ clock steps.

As the \rightarrow sweeps from right to left, it advances the counter on Track 2. Thus, we replace the rule $\rightarrow \leftarrow \rightarrow$ with the following two rules for the left-moving pointer:



We will enforce constraints that a left-moving 1-pointer should never be vertically aligned with a right pointer on Track 2, so the first rule above applies only if \bullet is not \rightarrow . We will add a constraint to enforce that during a 1-segment, the arrow on Track 2 points right, so a right-moving 1-pointer advances to the right as long as the state underneath it on Track 2 is not \leftarrow :

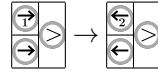


This rule replaces the generic rule $\rightarrow \leftarrow \rightarrow$ shown above.

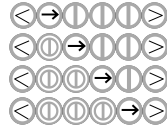
The 1-pointers continue to shuttle back and forth until the \rightarrow on Track 2 reaches the right end of the chain, so we have the transitions:



Where $\bullet \neq \rightarrow$ or \leftarrow . The 1-pointer transitions to a left-moving 2 pointer only when the \rightarrow has reached the right end of the chain:



The change on Track 2 from \rightarrow to \leftarrow indicates that the Track 2 counter will now be moving from right to left. For each iteration of the 1-pointer, the state on Track 2 changes as follows:



During all of the iterations with the 1-pointer, Track 2 should be in a state $\leftarrow \uparrow^* \rightarrow \uparrow^* \rightarrow$, so we make illegal any configuration in which \rightarrow is on top of \leftarrow on Track 2. Also, when the right-moving pointer on Track 2 is advanced by the left-moving 1-pointer on Track 1, the two pointers pass each other. Therefore it will be illegal to have a left-moving 1-pointer on top of a right-moving pointer on Track 2. The following local patterns are illegal and there are no out-going transitions from these configurations:



The two illegal patterns in (3) are added as Type I constraints to h_{cl} .

Figure 3 shows a summary of the transition rules for the 1-pointers. Note that some of these will be further refined when we describe how the right-moving Track 1 pointers trigger changes on the computation tracks. The transition rules are labeled TR- i so that we can refer to them later.

A 1-segment begins with the \rightarrow pointer at the left end of the chain and ends with \rightarrow at the right end of the chain before it transitions to \leftarrow . Thus, the 1-segment lasts for $N - 3$ full iterations plus on additional half-iteration. Figure 4 shows the first and last full iterations of a 1-segment as well as the last half iteration.

There are a total of $N - 3$ full iterations as the \rightarrow on Track 2 moves from the left end of the chain to the right end of the chain. Since each full iteration takes $2(N - 2)$ clock steps, this accounts for a total of $2(N - 2)(N - 3)$ clock steps. Then in the last half iteration the \rightarrow on Track 1 sweeps from the left end of the chain to the right

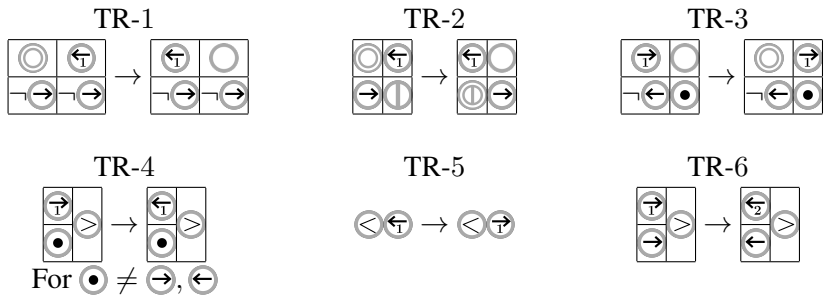


Figure 3: Transition rules involving 1-pointers.

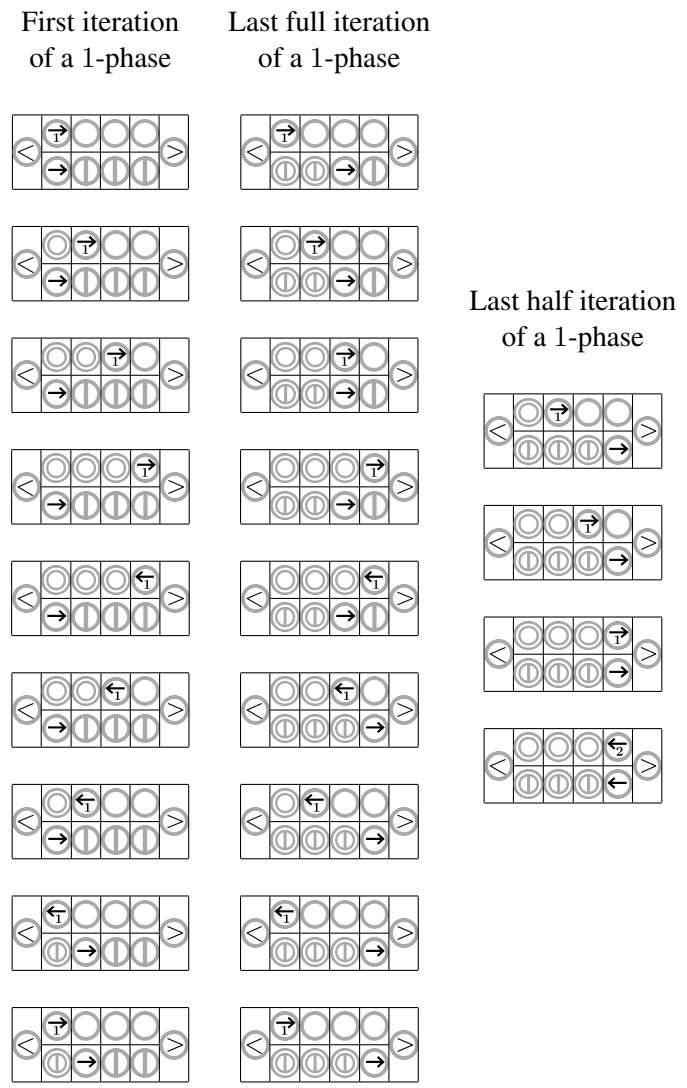


Figure 4: The first iteration, the last full iteration, and the last half iteration of a 1-phase. The very last transition illustrates the transition to the next 2-phase.

end of the chain ($N - 3$ clock steps) and then the \rightarrow transitions to \leftarrow (one final clock step). The total number of clock steps in a 1-segment is:

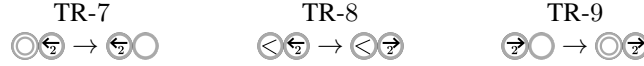
$$2(N - 2)(N - 3) + (N - 3) + 1 = (N - 2)(2N - 5).$$

Claim 2.10. *Starting from Time 0 for Tracks 1 and 2, every combination of clock configurations for Tracks 1 and 2 is reached except those in which Track 2 has a left pointer \leftarrow and those that contain a \rightarrow on Track 1 vertically aligned with the \rightarrow on Track 2.*

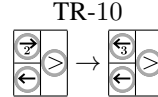
Proof. Number the non-bracket particles 1 through $N - 2$. The \rightarrow pointer on Track 2 can be in any of the $N - 2$ locations. Suppose the \rightarrow pointer on Track 2 is on location i . The Track 1 pointer can be right-moving \rightarrow in any of the $N - 2$ locations or left-moving \leftarrow in any of the locations besides i . So there should be a total of $(N - 2)[(N - 2) + (N - 3)] = (N - 2)(2N - 5)$ configurations. Starting at Time 0 for Tracks 1 and 2, the Track 1 pointer is \rightarrow in location 1 and the Track 2 pointer is \rightarrow in location 1. The Track 1 pointer sweeps to the right in every possible location (by TR-3). When it hits the right end in location $N - 2$ it changes to \leftarrow (by TR-4), and then sweeps left to location 2 (by TR-1). Every allowable configuration with the Track 2 pointer in location 1 is reached. In the next clock step, the Track 1 pointer and the Track 2 pointer swap locations (by TR-2). In a general iteration, the Track 2 pointer is in location i and the Track 1 pointer starts as \leftarrow in location $i - 1$. The Track 1 pointer sweeps left to location 1, transitions to \rightarrow , sweeps right to location $N - 2$, transitions back to \leftarrow and then sweeps left to location $i + 1$. Every allowable configuration with the Track 2 pointer in location i is reached. In the next clock step, the Track 1 pointer and the Track 2 pointer swap locations (by TR-2) and a new iteration begins. In each iteration, all $2N - 5$ configurations with the Track 2 pointer location i are reached. In the last configuration, the Track 1 pointer \rightarrow and Track 2 pointer \rightarrow are in location $N - 2$. The Track 1 pointer transitions to \leftarrow and the Track 2 pointer transitions to \leftarrow (by TR-6). \square

2.3.2 Rules for 2-pointers

The 2-pointers just make a single round trip starting and ending at the right end of the chain:



When the right-moving 2-pointer reaches the right end of the chain, it transitions to a left-moving three pointer. At this point the Track 2 state should be $\leftarrow \circ \circ^* \leftarrow \circ$, so this transition only happens if the Track 2 symbol is \rightarrow :

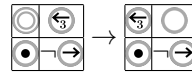


Moreover the following patterns is illegal and the Type I constraint that adds the energy penalty for this patterns is added to h_{cl} :



2.3.3 Rules for 3-pointers

The 3-pointers also make many iterations between the left and the right ends of the chain. We will add a constraint to enforce that during a 3-segment the arrow on Track 2 points left, so a left-moving 3-pointer advances to the left as long as the state underneath it on Track 2 is not \rightarrow :



As the \rightarrow sweeps from left to right, it advances the counter on Track 2. Thus, we have the following two rules for the left-moving pointer:



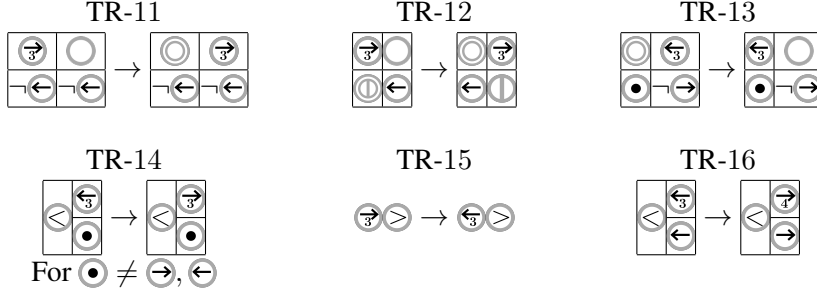


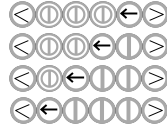
Figure 5: Transition rules involving 1-pointers.

We will enforce constraints that a right-moving 3-pointer should never be vertically aligned with a left-moving pointer on Track 2, so the first rule above applies only if \bullet is not \leftarrow .

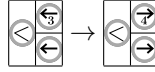
The 3-pointers continue to shuttle back and forth until the \leftarrow on Track 2 reaches the left end of the chain, so we have the transitions:



where \bullet is any state other than \leftarrow or \rightarrow . For each iteration of the 3-pointer, the state on Track 2 changes as follows:



The 3-pointer transitions to a right-moving 4 pointer only when the \leftarrow has reached the left end of the chain:



During all of the iterations with the 3-pointer, Track 2 should be in a state $\langle \bullet \bullet \bullet \bullet \rangle$. Therefore, we make illegal any configuration in which \leftarrow on Track 1 is on top of \rightarrow on Track 2. Also, when the left-moving pointer on Track 2 is advanced by the right-moving 3-pointer on Track 1, the two pointers pass each other. Therefore it will be illegal to have a right-moving 3-pointer on top of a right-moving pointer on Track 2. The following local patterns are illegal and there are no out-going transitions from these configurations:

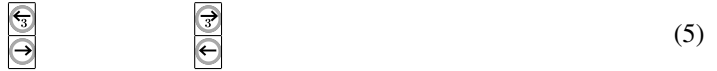
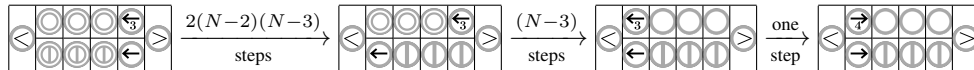


Figure 5 shows a summary of the transition rules for the 3-pointers. Note that some of these will be further refined when we describe how the right-moving Track 1 pointers trigger changes on the computation tracks.

A 3-segment begins with the 3-pointer on Track 1 at the right end of the chain, does $N - 3$ full iterations, ending with the 3-pointer at the right end of the chain. Then it does a half iteration in which the 3-pointer moves to the left end of the chain and then one final clock step in which the \leftarrow on Track 1 transitions to \rightarrow .



Therefore, a 3-segment lasts for $(N - 2)(2N - 5)$ clock steps.

Claim 2.11. Starting from a configuration in which \leftarrow is on the left end of the chain on Track 1 and \leftarrow is on the right end of the chain on Track 2, every combination of clock configurations for Tracks 1 and 2 is reached by applications of the transition rules, except those in which Track 2 has a right pointer \rightarrow and those that contain a \rightarrow on Track 1 vertically aligned with the \leftarrow on Track 2.

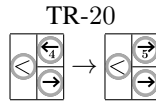
Proof. Number the non-bracket particles 1 through $N - 2$. The \leftarrow pointer on Track 2 can be in any of the $N - 2$ locations. Suppose the \leftarrow pointer on Track 2 is on location i . The Track 1 pointer can be a left-moving \leftarrow in any of the $N - 2$ locations or a right-moving \rightarrow in any of the locations besides i . So there should be a total of $(N - 2)[(N - 2) + (N - 3)] = (N - 2)(2N - 5)$ configurations. Starting at time $N - 2$ for Tracks 1 and 2, the Track 1 pointer is \leftarrow in location $N - 2$ and the Track 2 pointer \leftarrow is in location $N - 2$. The Track 1 pointer sweeps to the left in every possible location (by TR-13). When it hits the left end in location 1 it changes to \rightarrow (by TR-14), and then sweeps right to location $N - 3$ (by TR-11). Every allowable configuration with the Track 2 pointer in location $N - 2$ is reached. In the next clock step, the Track 1 pointer and the Track 2 pointer swap locations (by TR-12). In a general iteration, the Track 2 pointer is in location i and the Track 1 pointer starts as \rightarrow in location $i + 1$. The Track 1 pointer sweeps right to location $N - 2$, transitions to \leftarrow , sweeps left to location 1, transitions back to \rightarrow and then sweeps right to location $i - 1$. Every allowable configuration with the Track 2 pointer in location i is reached. In the next clock step, the Track 1 pointer and the Track 2 pointer swap locations (by TR-12) and a new iteration begins. In each iteration, all $2N - 5$ allowable configurations with the Track 2 pointer location i are reached. In the last configuration, the Track 1 pointer \leftarrow and Track 2 pointer \leftarrow are in location 1. The Track 1 pointer transitions to \rightarrow and the Track 2 pointer transitions to \rightarrow (by TR-16). \square

2.3.4 Rules for 4-pointers

The 4-pointers just make a single round trip starting and ending at the left end of the chain:



When the right-moving 4-pointer reaches the left end of the chain, it transitions to a right-moving five pointer. At this point the Track 2 state should be $\leftarrow \rightarrow \circ^* \rightarrow$, so this transition only happens if the Track 2 symbol is \rightarrow :

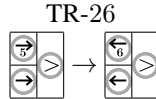


Moreover the following pattern is illegal and the Type I constraint that adds the energy penalty for this pattern is added to h_{cl} :



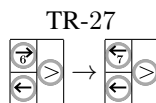
2.3.5 Rules for i -pointers for $i = 5, \dots, 8$

The 5-pointers make $N - 3$ full iterations plus an additional half iteration, starting at the left end of the chain and ending at the right end of the chain. Their rules are identical to the rules for the 1-pointers, except that they eventually transition to a 6-pointer when the Track 2 pointer reaches the right end of the chain. TR-1 through TR-5 are duplicated with \rightarrow and \leftarrow replaced with \rightarrow and \leftarrow and named TR-21 through TR-25.



The Type I terms from (3) are duplicated with \rightarrow and \leftarrow replaced with \rightarrow and \leftarrow and added to h_{cl} .

The 6-pointers make a single round trip, starting and ending at the right end of the chain. The rules for these pointers are identical to the 2-pointers given above, except that they transition to 7-pointers when they reach the right end of the chain. TR-7 through TR-9 are duplicated with \rightarrow and \leftarrow replaced with \rightarrow and \leftarrow and named TR-21 through TR-26.



The Type I terms from (4) are duplicated with \rightarrow and \leftarrow replaced with \rightarrow and \leftarrow and added to h_{cl} .

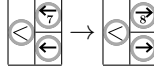
The 7-pointers make $N - 3$ full iterations plus an additional half iteration, starting at the right end of the chain and ending at the left end of the chain. Their rules are identical to the rules for the 3-pointers, except that

Segment	Start	End	Track 1 State	Track 2 State	Number of Steps
1	Left	Right	$\langle \circ \circ^* (\overrightarrow{7} + \overleftarrow{7}) \circ^* \circ \rangle$	$\langle \circ \circ^* \rightarrow \circ \circ^* \rangle$	$(N-2)(2N-5)$
2	Right	Right	$\langle \circ \circ^* (\overrightarrow{2} + \overleftarrow{2}) \circ^* \circ \rangle$	$\langle \circ \circ^* \leftarrow \circ \rangle$	$2(N-2)$
3	Right	Left	$\langle \circ \circ^* (\overrightarrow{3} + \overleftarrow{3}) \circ^* \circ \rangle$	$\langle \circ \circ^* \leftarrow \circ \circ^* \rangle$	$(N-2)(2N-5)$
4	Left	Left	$\langle \circ \circ^* (\overrightarrow{4} + \overleftarrow{4}) \circ^* \circ \rangle$	$\langle \circ \rightarrow \circ \circ^* \rangle$	$2(N-2)$
5	Left	Right	$\langle \circ \circ^* (\overrightarrow{5} + \overleftarrow{5}) \circ^* \circ \rangle$	$\langle \circ \circ^* \rightarrow \circ \circ^* \rangle$	$(N-2)(2N-5)$
6	Right	Right	$\langle \circ \circ^* (\overrightarrow{6} + \overleftarrow{6}) \circ^* \circ \rangle$	$\langle \circ \circ^* \leftarrow \circ \rangle$	$2(N-2)$
7	Right	Left	$\langle \circ \circ^* (\overrightarrow{7} + \overleftarrow{7}) \circ^* \circ \rangle$	$\langle \circ \circ^* \leftarrow \circ \circ^* \rangle$	$(N-2)(2N-5)$
8	Left	Left	$\langle \circ \circ^* (\overrightarrow{8} + \overleftarrow{8}) \circ^* \circ \rangle$	$\langle \circ \rightarrow \circ \circ^* \rangle$	$2(N-2)$

Figure 6: A summary of the i -segments for $i = 0, \dots, g$.

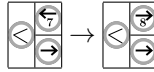
they eventually transition to an 8-pointer when the Track 2 pointer reaches the right end of the chain. TR-11 through TR-15 are duplicated with $\overrightarrow{3}$ and $\overleftarrow{3}$ replaced with $\overrightarrow{7}$ and $\overleftarrow{7}$ and named TR-31 through TR-35.

TR-36



The Type I terms from (5) are duplicated with $\overrightarrow{3}$ and $\overleftarrow{3}$ replaced with $\overrightarrow{7}$ and $\overleftarrow{7}$ and added to h_{cl} .

The 8-pointers make a single round trip, starting and ending at the left end of the chain. The rules for these pointers are identical to the 4-pointers given above, except that they transition to a 1-pointer at the end of the iteration.



We will wait to re-number these transition rules because the 8-pointers also cause the Track 3 pointer to advance one location. These rules will be replaced in the next section with rules that involve Track 3 as well.

Figure 6 summarizes the segments. In general, the the different i -pointers will trigger one application of a transition function of a Turing Machine on the computational tracks as it sweeps from left to right. The labels on the pointers provide a way of controlling which Turing Machine transition function is executed at which time. The 4-segments and 8-segments will be used to check conditions on the lower tracks, triggering an energy penalty if any of the conditions are violated.

2.3.6 Summary of Track 1 and 2 Clock Configurations

Throughout the construction, we will need to maintain that the transition rules are well defined for well-formed clock configurations. For now, we prove this fact for the transition rules that apply to Tracks 1 and 2.

Lemma 2.12. [Bound on Reachable Configurations in One Clock Step] *For every well formed clock configuration for Tracks 1 and 2, A , there is at most one configuration that can be reached from A by a transition rule applied in the forward direction and at most one configuration that can be reached from A by a transition rule applied in the reverse direction*

Proof. Every transition rule TR-1 through Tr-40 applies in the forward direction to a two-particle configuration in which the Track 1 state is one of the following four cases:



If the clock configuration is well-formed then the Track 1 state has the form $\langle \circ \circ^* (\overrightarrow{i} + \overleftarrow{i}) \circ^* \circ \rangle$. In any clock configuration of that form, there is exactly one occurrence of any of the four patterns shown above. The additional constraints on the other tracks can only decrease the number of rules that apply in the forward direction to a given Track 1 configuration. Therefore, there is at most one location and at most one rule that can be applied in the forward direction to get a new clock configuration.

Every transition rule TR-1 through TR-40 applies in the backward direction to a two-particle configuration in which the Track 1 state is one of the following four cases:



In any well-formed clock configuration, there is exactly one occurrence of these four patterns on Track 1. The additional constraints on the other tracks can only decrease the number of rules that apply in the reverse direction to a given Track 1 configuration. Therefore, there is at most one location and at most one rule that can be applied in the reverse direction to get a new clock configuration. \square

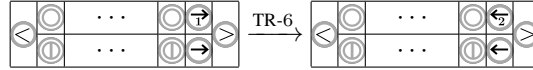
Eventually, we will define correct and incorrect clock configurations for all three tracks. However, it will be useful to first define properties required of the configurations for Tracks 1 and 2 and establish some properties about how they are connected by the transition rules.

Definition 2.13. [Correct and Incorrect Clock Configurations for Tracks 1 and 2] A well formed clock configuration for Tracks 1 and 2 is called correct if the following conditions hold and is called incorrect otherwise:

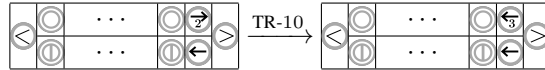
1. If the pointer on Track 1 is an i -pointer for $i \in \{4, 8\}$, then Track 2 is at Time 0.
2. If the pointer on Track 1 is an i -pointer for $i \in \{2, 6\}$, then Track 2 is in configuration $\langle \textcircled{1}^* \textcircled{4} \rangle$.
3. If the pointer on Track 1 is an i -pointer for $i \in \{1, 5\}$, then the pointer on Track 2 is $\textcircled{4}$.
4. If the pointer on Track 1 is an i -pointer for $i \in \{3, 7\}$, then the pointer on Track 2 is $\textcircled{4}$.
5. If the pointer on Track 1 is an i -pointer for $i = 1, 3, 5, 7$, then it is not vertically aligned with the pointer on Track 2 and pointing on the opposite direction.

Lemma 2.14. [Correct Configurations Form Cycles] Starting from the Time 0 configuration for Tracks 1 and 2, the transition rules will reach every correct configuration for Tracks 1 and 2 exactly once before returning to the Time 0 configuration after $p(N) = 4(N - 2)(2N - 3)$ clock steps.

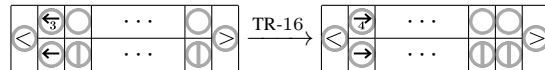
Proof. Claim 2.10 shows that starting from Time 0 and applying the transition rules $(N - 2)(2N - 5)$ times, every correct clock configuration with a 1-pointer is reached, ending in the configuration:



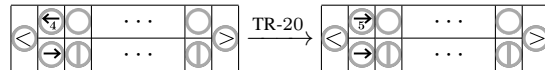
The rules for the 2-pointers do not alter Track 2. The 2-pointer moves to the left and then to the right, reaching every location with $\textcircled{4}$ and then every location with $\textcircled{2}$ until it reaches configuration:



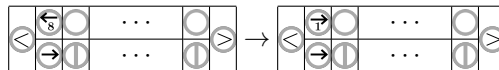
Then by Claim 2.11, every correct configuration with a 3-pointer is reached, ending in configuration:



The rules for the 4-pointers do not alter Track 2. The 4-pointer moves to the right and then to the left, reaching every location with $\textcircled{2}$ and then every location with $\textcircled{4}$ until it reaches configuration:



Since the rules for the 5, 6, 7, and 8-pointers are the same as the 1, 2, 3, and 4-pointers, the same argument holds for those segments. In the final clock step, the 8-pointer transitions back to the 1-pointer which puts the clock configuration back at time 0:



The 1, 3, 5, and 7-segments each take $(N - 2)(2N - 5)$ clock steps. The 2, 4, 6, and 8-segments each take $2(N - 2)$ clock steps. The total number of clock steps (and therefore the number of correct clock configurations for Tracks 1 and 2) is:

$$p(N) = 4[(N - 2)(2N - 5)] + 4[2(N - 2)] = 4(N - 2)(2N - 3).$$

□

Lemma 2.15. [Incorrect Configurations form Short Paths] *Any clock incorrect configuration for Tracks 1 and 2 will reach an illegal configuration from h_{cl} in at most $2(N - 2)$ clock steps from which there is no out-going transition.*

Proof. If the Track 1 pointer is a 1-pointer or a 5-pointer, and the clock configuration is incorrect, then either the Track 2 pointer is \rightarrow and is vertically aligned with \leftarrow or \leftarrow or the Track 2 pointer is \leftarrow (in any location). In the former case, the current configuration is illegal and there is no outgoing transition, since TR-1 (TR-21) applies only if the Track 2 symbol under the \leftarrow (\leftarrow) is not \rightarrow . In the latter case, the 1-pointer (or 5-pointer) will keep moving until it is in a state \rightarrow (or \rightarrow) directly over the \leftarrow on Track 2. This is an illegal configuration and there are no outgoing transitions since TR-3 and TR-4 (TR-23 and TR-24) do not apply if the Track 2 pointer is in state \leftarrow . The number of clock steps until the illegal configuration is reached is at most $2(N - 2)$, the time for a round trip for the Track 1 pointer.

The symmetric argument holds if the Track 1 pointer is a 3 or 7-pointer, with the role of left and right reversed.

The 4-pointers and 8-pointers make a single round trip starting and ending at the left end of the chain and do not cause any changes on Track 2. Eventually, the left end of the chain will be reached. If Track 2 does not have \rightarrow in the left end of the chain, the following illegal configuration will be reached within $2(N - 2)$ clock steps, from which there is no outgoing transition:



The 2-pointers and 6-pointers make a single round trip starting and ending at the right end of the chain and do not cause any changes on Track 2. Eventually, the right end of the chain will be reached. If Track 2 does not have \leftarrow in the left end of the chain, the following illegal configuration will be reached within $2(N - 2)$ clock steps, from which there is no outgoing transition:



□

2.3.7 Track 3

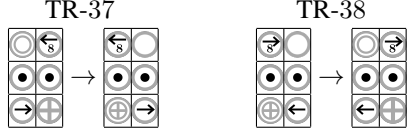
In the absence of any transition rules involving Track 3, a sequence of clock configurations in which Tracks 1 and 2 begin and end at Time 0 form a cycle of length $4(N - 2)(2N - 3)$ in the configuration graph. We now add transition rules which cause Track 3 to change every such cycle. This will result in the clock configurations for Tracks 1 through 3 forming a larger cycle in the configuration graph. We will refer to a sequence of clock steps in which the configurations on Tracks 1 and 2 begin and end at the same state a *Track 1-2 Cycle*.

In a well-formed clock configuration, the configuration of Track 3 has the form:

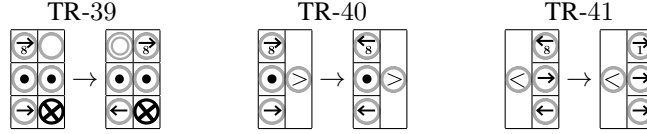
$$\leftarrow \oplus^* (\rightarrow + \leftarrow) \oplus^* \otimes^* \rightarrow.$$

The transition rules will never change the number of \otimes particles at the right end of the chain on Track 3. The \rightarrow and \leftarrow pointers will move back and forth between the locations with \oplus or \oplus . The *length* of the clock on Track 3 is the total number of \oplus or \oplus symbols and the transition rules will leave the length fixed. The only pointers from Track 1 that interact with Track 3 are the 8-pointers. Each sweep of the 8-pointer will update the state of the Track 3 clock by moving the pointer over by one location or reversing the direction of the Track 3 pointer.

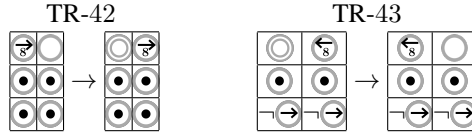
If the Track 3 pointer is facing right, it will advance as the 8-pointer on Track 1 moves left. If the Track 3 pointer is facing left, it will advance as the 8-pointer on Track 1 moves right.



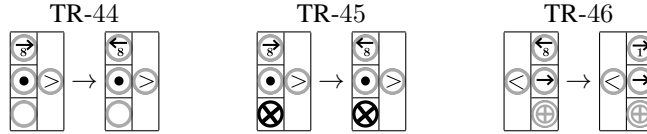
The arrow on Track 3 changes direction when it reaches the end of the chain on the left end or the \otimes particles on the right end. The 8-pointer that points in the same direction as the Track 3 pointer will trigger the change in direction. Recall that the 8-pointer also checks that the Track 2 state is at Time 0, meaning that the pointer on Track 2 is \rightarrow and at the left end of the chain. Therefore, TR-41 applies only if the Track 2 state is \rightarrow .



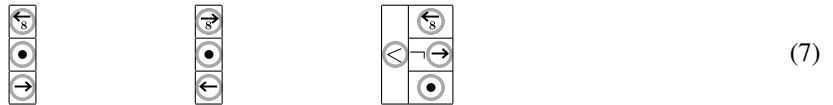
Other than the configurations described in the four rules above, the 8-pointers do not trigger any other change on Track 3. So in the absence of a pointer on Track 3, the 8-pointer just moves along:



TR-42 applies when the bottom row $\bullet\bullet$ is in $\{\oplus\otimes, \oplus\oplus, \oplus\oplus, \rightarrow\oplus, \oplus\rightarrow, \otimes\otimes\}$



It should never happen that the Track 1 pointer is an 8-pointer and is vertically aligned with the Track 3 pointer, pointing in the opposite direction. It should also never happen that the 8-pointer reaches the left end of the chain and Track 2 is not at Time 0. So the following three patterns are illegal:



There should be no outgoing transitions from a configuration that contains one of those patterns. Also, there is no out-going transition from the pattern below, so it is also added to h_{cl} as an illegal pattern:



Now that all the transition rules that pertain to the clock tracks are complete, we are ready to analyze the structure of the configuration graph. The first lemma establishes that the configuration graph is well-defined since the set of transition rules is closed on the set of well-formed configuration. The second part of the lemma establishes a degree bound which implies that the configuration graph consists of a disjoint set of paths and cycles.

Lemma 2.16. [Degree Bound for the Configuration Graph] *The transition rules are closed on the set of well-formed clock configurations. Furthermore, for every well-formed clock configuration, there is at most one transition rule that applies in the forward direction and at most one transition rule that applies in the reverse direction.*

Proof. The transition rules all preserve the number of pointers on each Track. They also preserve the property that on Track 1 \odot particles are to the left of the pointer and \circ particles are to the right of the pointer. Similarly,

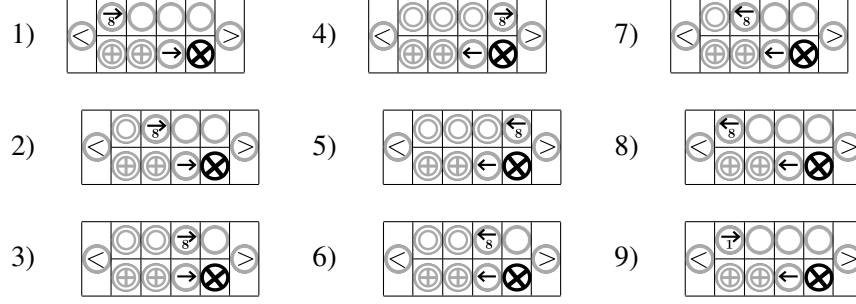


Figure 7: The middle 8-segment of a complete cycle in which the Track 3 pointer changes from right-moving to left-moving.

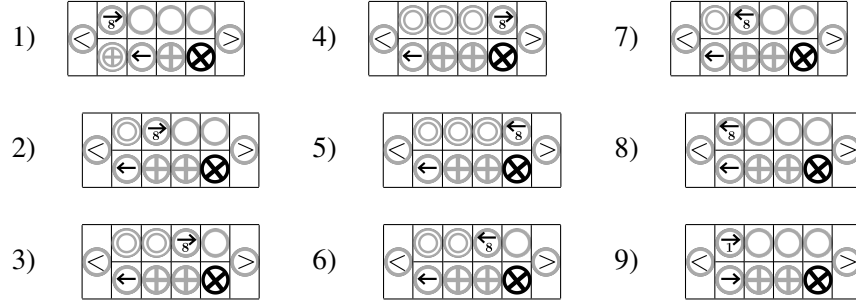


Figure 8: The last 8-segment of a complete cycle in which the Track 3 pointer advances by one location and changes direction. Tracks 1 and 3 are shown.

the transition rules maintain the property that on Track 2, $\textcircled{\oplus}$ particles are to the left of the pointer and $\textcircled{\ominus}$ particles are to the right of the pointer. On Track 3, the transition rules maintain the property that $\textcircled{\oplus}$ particles are to the left of the pointer and $\textcircled{\ominus}$ particles are to the right of the pointer as well as the fact that $\textcircled{\oplus}$ particles are to the left of $\textcircled{\otimes}$ particles. Therefore when a transition rule is applied to a well-formed clock configuration, the result is another well-formed clock configuration.

Lemma 2.12 shows that at most one configuration for Tracks 1 and 2 can be reached in the forward direction or the reverse direction from a well-formed clock configuration for Tracks 1 and 2. The additional constraints introduced by Track 3 can only further limit the applicable transition rules. \square

We are ready now to describe the cycle of configurations reached by starting in the Time 0 configuration for Tracks 1, 2, and 3 and repeatedly applying the transition rules. If T is the length of the timer on Track 3, then the Track 3 state at Time 0 is $\langle \ominus \ominus \ominus \ominus \textcircled{\otimes}^* \ominus \rangle$. There is one iteration of the 8-pointers for every Track 1-2 cycle. After T iterations of the 8-pointer, the arrow on Track 3 has advanced to the right end of the non- $\textcircled{\otimes}$ states (as shown below). In the $T + 1^{\text{st}}$ iteration of the 8-pointer, the pointer on Track 3 reverses directions but stays in the same place. After $T - 1$ more iterations, the pointer on Track 3 is one place away from the left end of the chain. Finally, in the next iteration, the Track 3 pointer moves one position to the left and changes directions. The number above each arrow below shows the number of 8-segments (which happen every $p(N)$ clock steps) to get from one Track 3 configuration to the next.

$$\langle \ominus \ominus \ominus \ominus \textcircled{\otimes}^* \ominus \rangle \xrightarrow{T} \langle \ominus \ominus \ominus \ominus \textcircled{\otimes}^* \ominus \rangle \xrightarrow{1} \langle \ominus \ominus \ominus \ominus \textcircled{\otimes}^* \ominus \rangle \xrightarrow{T-1} \langle \ominus \ominus \ominus \ominus \textcircled{\otimes}^* \ominus \rangle \xrightarrow{1} \langle \ominus \ominus \ominus \ominus \textcircled{\otimes}^* \ominus \rangle$$

Figure 7 shows the middle 8-segment in which the Track 3 pointer stays in the same location and changes direction. Figure 8 shows the last 8-segment in which the Track 3 pointer advances by one location and changes direction. The number of 8-segments until the clock configuration is again at Time 0 for Tracks 1, 2, and 3 is $2T + 1$. Each Track 1-2 Cycle takes $p(N) = 4(N - 2)(2N - 3)$ clock steps, so starting at Time 0, the total number of clock steps for the clock configuration to return to Time 0 for Tracks 1, 2, and 3 is $(2T + 1)p(N)$.

The definition below partitions the set of well-formed clock configurations into a *correct* set and an *incorrect* set. We will show that the set of $(2T + 1)p(N)$ clock configurations with timer length T that are reached in a cycle starting and ending at Time 0 will be exactly the set of correct configurations with timer length T . The definition provides a characterization of the incorrect configurations which will allow us to ensure that each of the incorrect configurations are contained in a short path ending in an illegal configuration which incurs a penalty from h_{cl} . Since H will be closed on each connected component of configurations, we can analyze each component separately and lower bound the energy of the states with incorrect clock configurations.

Definition 2.17. [Correct Clock Configurations (for Tracks 1, 2, and 3)] *A well formed clock configuration for Tracks 1, 2 and 3 is called correct if the following conditions hold and is called incorrect otherwise:*

1. *The configuration for Tracks 1 and 2 is correct.*
2. *If the pointer on Track 1 is an 8-pointer, then it is not vertically aligned with the pointer on Track 3 pointing on the opposite direction.*
3. *If the pointer on Track 3 is \leftarrow and in the leftmost location, then the Track 1 pointer is an 8-pointer.*
4. *If the pointer on Track 3 is pointing right and next to a dead state ($\rightarrow \otimes$) and the Track 1 pointer is an 8-pointer, then the 8-pointer is not vertically aligned with a \otimes state on Track 3.*

The first step is to count the number of correct configurations whose time length is T .

Lemma 2.18. [Number of Correct Clock Configurations] *The number of correct clock configurations with timer length T is $(2T + 1)p(N)$.*

Proof. By Lemma 2.14, there are $p(N)$ correct clock configurations for Tracks 1 and 2. There are $2(T + 1)$ possible Track 3 configurations in a well-formed clock state:

$$\left\langle \oplus^j \rightarrow \oplus^{T-j} \otimes^* \right\rangle \qquad \left\langle \oplus^{T-j} \leftarrow \oplus^j \otimes^* \right\rangle,$$

where j can range from 0 to T . We will start with $2(T + 1)p(N)$ candidate correct configurations and subtract off the configurations that violate one of conditions 2, 3, or 4 in Definition 2.17. Note that the set of configurations that violate each one of those conditions is disjoint, so we can consider them separately.

Condition 2 says that the 8-pointer can not be vertically aligned with the 3-pointer and pointing in the opposite direction. There are $T + 1$ possible locations for the 3-pointer and two directions. Each of these $2(T + 1)$ configurations for the 3-pointer eliminates one possible configuration for the 8-pointer. (Subtract $2(T + 1)$)

For condition 3, there are $p(N) - 2(N - 2)$ correct configurations for Tracks 1 and 2 in which the Track 1 pointer is not an 8-pointer. None of these are allowed when the Track 3 pointer is all the way to the left of the chain and pointing to the left. (Subtract $p(N) - 2(N - 2)$)

If the non-bracket particles are numbered from 1 to $N - 2$, then the Track 3 pointer is in position $T + 1$ if it is immediately to the left of a \otimes particle. Condition 4 says that the 8-pointer can not be to the right of this location. So there are $(N - 2) - (T + 1)$ locations for the 8-pointer that are not allowed and two directions for each location. (Subtract $2[(N - 2) - (T + 1)]$)

The total number of correct states is

$$2(T + 1)p(N) - 2(T + 1) - [p(N) - 2(N - 2)] - 2[(N - 2) - (T + 1)] = (2T + 1)p(N).$$

□

Lemma 2.19. [Structure of the Configuration Graph] *In the configuration graph, the correct clock configurations with timer length T form a cycle of length $(2T + 1)p(N)$. Every correct clock configuration for Tracks 1 and 2 occurs exactly $2T + 1$ times in the cycle at intervals of exactly $p(N)$. All other well-formed clock configurations are in paths of length at most $p(N)$ that end in an illegal configuration.*

Proof. If the length of the timer on Track 3 is T , then there are $2(T + 1)$ possible Track 3 configurations in a well-formed clock state:

$$\left\langle \oplus^j \rightarrow \oplus^{T-j} \otimes^* \right\rangle \qquad \left\langle \oplus^{T-j} \leftarrow \oplus^j \otimes^* \right\rangle,$$

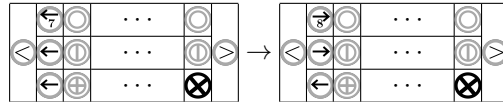
where j can range from 0 to T . We can order the configurations from 0 to $2T + 1$ so that the configurations on the left come first and each set is ordered by increasing j . At Time 0 for Tracks 1, 2, and 3, Track 3 is in configuration 0. Tracks 1 and 2 cycle through all correct configurations every $p(N)$ clock steps. At each point that Time 0 for Tracks 1 and 2 is reached, Track 3 has advanced to the next configuration, except in the last Track 1-2 cycle in which the configuration on Track 3 goes from $2T$ to $2T + 1$ and then to 0 in a single 8-segment(see Figure 8). Because the configuration graph is a cycle, $(2T + 1)p(N)$ unique configurations have been reached.

We will argue that any configuration reached by applying transition rules to the clock configuration at Time 0 will be correct. By Lemma 2.18, these must be exactly the set of correct clock configurations. We consider each condition in Definition 2.17 in turn.

1. **Condition 1:** Lemma 2.14 establishes that any configuration reached from Time 0 for Tracks 1 and 2 is correct for Tracks 1 and 2.
2. **Condition 2:** Note that Time 0 for Tracks 1, 2, and 3 is a correct configuration and none of the transition rules can result in an 8-pointer on Track 1 vertically aligned with the Track 3 pointer pointing in the opposite direction.
3. **Condition 3:** If Track 3 is in configuration $2T + 1$ (with an \ominus in the leftmost location), it must have entered that configuration in an 8-segment since only the 8-pointer can alter Track 3. In the last clock step of the 8-segment, when the Track 1 pointer transitions from an 8-pointer to a 1-pointer, TR-41 is applied which also flips the direction of the Track 3 pointer. Track 3 remains unchanged until the next 8-phase.
4. **Condition 4:** When Track 3 first enters configuration T (which is $\langle \ominus \oplus^T \ominus \otimes^* \ominus \rangle$) the 8-pointer on Track 3 is sweeping left, so afterwards it will be to the left of the \ominus on Track 3. The next time, the Track 3 configuration changes, the 8-pointer is sweeping right. TR-39 will cause the pointer on Track 3 to change directions as it passes the Track 3 pointer. Therefore, when the 8-pointer is over the \otimes states on Track 3, the Track 3 pointer will be \ominus .

Now we need to argue that if a well-formed clock configuration is incorrect, it will reach an illegal configuration within $p(N)$ steps from which there will be no outgoing transition. Again, we consider each condition from Definition 2.17 in turn.

1. **Condition 1:** If the configuration is incorrect for Tracks 1 and 2, Lemma 2.15 shows that an illegal configuration will be reached within $2(N - 2) \leq p(N)$ steps from which there is no outgoing transition.
2. **Condition 2:** If the pointer on Track 1 is an 8-pointer that is vertically aligned with the pointer on Track 3 pointing on the opposite direction, the current configuration is illegal due to term (7) and there are no out-going transition rules that apply.
3. **Condition 3:** Now suppose the pointer on Track 3 is \ominus , in the leftmost location and the Track 1 pointer is not an 8-pointer. The transition rules will advance Tracks 1 and 2 until the configuration below is reached.



This will transition to an illegal configuration due to term (7) from which there is no out-going transition rule. Since a cycle for Tracks 1 and 2 take $p(N)$ clock steps, an illegal configuration will be reached in at most $p(N)$ clock steps.

4. **Condition 4:** Finally suppose that the Track 3 configuration is $\langle \ominus \oplus^T \ominus \otimes^* \ominus \rangle$ and the Track 1 pointer is an 8-pointer to the left of the \ominus on Track 3. The 8-pointer on Track 1 will sweep right, turn around, and then sweep left. In at most $2(N - 2)$ clock steps, the following configuration is reached which is illegal due to the term (8) and there is no outgoing transition:



□

2.4 Turing Machines Used in the Construction

Tracks 4 through 6 are the computational tracks. Track 4 will store the state and head location for the Turing Machine, Track 5 will store the work tape, and Track 6 will be a read-only track storing the guess for the oracle queries and the witnesses for the verification computations. The clock pointer on Track 1 will trigger certain actions on the computation tracks, depending on the label of the pointer and the state of the computation tracks.

Section 2.2.5 gives an overview of the two deterministic, reversible Turing Machines M_{BC} and M_{TV} used in the construction. In this section, we provide more specific descriptions. Section 2.4.1 reviews basic concepts of deterministic reversible TMs from [8] and [11]. Section 2.4.2 gives a detailed description of the binary counter TM, M_{BC} , including a closed formula for the reduction $N(x)$ that maps a string x to the number of steps required by M_{BC} to produce x . Section 2.4.3 outlines the properties required of M_{TV} and argues that a reversible TM exists with those properties. Finally, Section 2.4.4 describes several transformations that we need to apply to M_{TV} for the construction. Note that when we translate the two Turing Machines into the transition rules of the Hamiltonian, they will both operate on the same Hilbert space for Tracks 4, 5, and 6, so we need to expand the state set and tape alphabet for the two Turing Machines to make them equal. The computation encoded in the Hamiltonian will execute M_{BC} for $N - 2$ steps and then (a transformed) M_{TV} for $N - 2$ steps. In order to dovetail one TM with the next, we formally define a combined Turing Machine (which we call $M_{BC} + M_{TV}$). The Turing Machine $M_{BC} + M_{TV}$ will pick up the computation after $N - 2$ steps of M_{BC} , finish the current increment operation of M_{BC} , and then transition to M_{TV} . Finally, we need to address the fact that M_{TV} may finish its computation before the end of the $N - 2$ steps. Since M_{TV} is reversible, it will continue to execute some unknown operations until the clock runs out, which could potentially alter the contents of the work tape. In order to guarantee that the tape contents contain the correct output after exactly $N - 2$ steps of M_{TV} , we introduce a time-wasting process which ensures that the operation of the Turing Machine is reversible and maintains the contents of the tape for at least an additional $N - 2$ steps after the final state is reached. Lemma 2.37 establishes that the transformed $M_{BC} + M_{TV}$ has the required properties for the construction.

2.4.1 Review of Reversible Turing Machines

Bernstein and Vazirani [8] define several properties of Turing Machines and Quantum Turing Machines which we summarize here. We will consider *generalized* Turing Machines, also considered in [11], in which the head can move left, right, or stay in the same place at a particular step. These options are denoted by $\{L, R, N\}$. A Turing Machine is defined by a 5-tuple: $(Q, \Gamma, I, \delta, q_f, q_0)$. Q is the finite set of states, Γ the tape alphabet, and $I \subset \Gamma$ is the input alphabet. There is a special blank symbol $\# \in \Gamma - I$. The tape consists of an infinite sequence of cells or locations, each of which stores a symbol from Γ . The *head* of the Turing Machine points to a particular location of the tape. The *current symbol* is the symbol written in the location where the head is pointing. A *configuration* of the Turing Machine consists of the contents of the tape, the location of the head and the current state. For any $x \in I^*$, the initial configuration consists of the string x written on the tape with blank symbols everywhere else, and the head pointing to the leftmost symbol in x in the state q_0 . The transition function δ maps pairs from $Q - \{q_f\} \times \Gamma$ to $Q \times \Gamma \times \{L, R, N\}$. In a single step of the Turing Machine, if the current symbol is a , the state is q , and $\delta(q, a) = (p, b, D)$, then the symbol a will be overwritten by b , the new state will be p and the head will move one step in the direction D . We say that a Turing Machine *halts* when it reaches the state q_f . Since we will be interested in Turing Machines that act as a permutation on a finite set of configurations, we will have transition functions that are also defined on pairs of the form (q_f, a) .

Definition 2.20. [Reversible Turing Machines] A (classical) Turing Machine is said to be reversible if each configuration has at most one predecessor.

Definition 2.21. [Unidirectional Turing Machines] A TM is said to be unidirectional if each state can be entered from only one direction. This means that if $\delta(p, a) = (b, q, D)$ and $\delta(p', a') = (b', q, D')$, then $D = D'$.

Each state q of a unidirectional TM has a unique direction $D_q \in \{L, R, N\}$ that determines the direction from which q is entered. Once these directions are defined for each state, the direction component in any transition rule triple (p, b, D) is completely determined by the state q . The *reduced transition rule* $\delta_r : Q \times \Gamma \rightarrow Q \times \Gamma$ is well defined since the direction can be recovered from the output state alone. It will be helpful to refer

collectively to the set of states that are reached from the same direction:

$$\begin{aligned} Q_L &= \{q \mid D_q = L\} \\ Q_R &= \{q \mid D_q = R\} \\ Q_N &= \{q \mid D_q = N\} \end{aligned}$$

Bernstein and Vazirani show local conditions that characterize whether a TM is reversible.

Theorem 2.22. [Theorem B.1 and Cor B.3 in [8]] *A TM M is reversible if and only if M satisfies the following two conditions:*

1. M is unidirectional.
2. The reduced transition function is one-to-one.

We will make use of several other properties of Turing Machines given below. The first two are standard from [8]. The third is introduced here for the purposes of our construction.

Definition 2.23. [Normal Form TM] *A reversible TM is in normal form if*

$$\forall a \in \Gamma \quad \delta(q_f, a) = (a, q_0, N).$$

We will refer to the tape cell where the head is located in the initial configuration as the *start cell*. Occasionally, it will be convenient to refer to a numbering of the tape cells. The start cell will be numbered 1 and rest of the cells to the left and right are numbered accordingly.

Definition 2.24. [Proper TM Behavior on a Particular Input] *A TM behaves properly on input x , if on input x , the TM halts in the start cell and the head never moves to the left of the start cell.*

Definition 2.25. [Compact TMs] *For positive integer c , a TM is c -compact, if for every $t \geq 1$, it reaches at most t locations of the tape after $t + c$ steps.*

We will generally assume that a reversible Turing Machine has a transition function that is well-defined for every pair in $Q \times \Gamma$. This is a reasonable assumption as the transition function can always be expanded if it is only defined on a subset of $Q \times \Gamma$.

Fact 2.26. *Let M be a reversible Turing Machine whose transition function δ is defined on a subset of $Q \times \Gamma$. δ can be expanded so that it is well-defined on all of $Q \times \Gamma$ and the resulting Turing Machine is also reversible.*

2.4.2 The Binary Counter Turing Machine

The Turing Machine tape in our construction will be composed of two tracks. The *work track* will be stored in Track 5 and will hold the contents of the work tape, each symbol of which comes from a set Σ . The *witness track* will be stored in Track 6 in the construction and contains a read-only binary witness. Therefore the set of tape symbols Γ is actually $\Sigma \times \{0, 1\}$. It will be convenient to separate the two tracks in describing a Turing Machine configuration. Thus if x and w are two binary strings, the input (x, w) has w on the witness track and input x followed by blank ($\#$) symbols on the work track. The left-most bits of x and w are vertically aligned. The initial configuration on input (x, w) has the head pointing to the leftmost bit of x and y in the start state q_0 . The Binary Counter Turing Machine M_{BC} is unaffected by the contents of the witness track (Track 6), so we will only describe its behavior in terms of the contents of Track 5.

We assume that M_{BC} begins each iteration in state q_0 at the left end of a binary string whose right-most bit is 1. The binary string can be interpreted as a binary number in reverse. If x is a binary string, then we interpret the string as representing the number x^R in binary. The Turing Machine executes an increment loop, and finishes in state q_f , back in the starting location, with a string x' written on the tape. The value of $(x')^R$ is the value of x^R plus 1. Note that the condition that the binary string x' ends in 1 will be maintained. In the construction, the starting configuration will have the string 1 on the tape, followed by $\#$ symbols, with the head in state q_0 , pointing to the 1. The transition rules for M_{BC} are given in Figure 9. The pseudo-code for M_{BC} is given in Figure 10.

	0	1	#
q_0	$(q_f, 1, N)$	$(q_1, \#, R)$	-
q_1	$(q_2, \#, R)$	$(q_1, 0, R)$	$(q_3, \#, R)$
q_2	$(q_4, 0, L)$	$(q_4, 1, L)$	-
q_3	-	-	$(q_4, \#, L)$
q_4	-	-	$(q_5, 1, L)$
q_5	$(q_5, 0, L)$	-	$(q_f, 0, N)$

Figure 9: A summary of the transition rules for M_{BC} . The transition rules are well-defined as long the Turing Machine begins with the head pointing to the left end of a binary string whose rightmost bit is 1, followed by # symbols. M_{BC} reaches a final state in the position in which it began, with the binary string incremented (in reverse notation) and # symbols to the right of the new string. The rules can be extended so that they are well defined on every $Q \times \{0, 1, \#\}$ pair, so that the reduced transition function remains one-to-one and the Turing Machine remains unidirectional. The rule $\delta(a, q_f) = (q_0, a, N)$ is included for every $a \in \{0, 1, \#\}$ so that the resulting Turing Machine is in normal-form.

Lemma 2.27. [Number of Steps for One Iteration of M_{BC}] M_{BC} is a normal-form reversible TM. Let x be a binary string ending in 1. Let $l(x)$ denote the length of the maximal prefix of x that is all 1's. The number of steps M_{BC} takes to reach q_f on input x is 1 if $l(x) = 0$ and is $2l(x) + 3$ if $l(x) > 1$.

Proof. If $l(x) = 0$, then the leftmost bit of x is 0. In this case, M_{BC} writes a 1 and transitions to q_f in the first step.

If $l(x) > 1$, then M_{BC} writes a # to mark its return location and moves right into state q_1 . The head continues to move right until it reaches a 0 or # symbol. ($l(x)$ steps so far.) It writes a # as a placeholder for the 0 or # and moves right. (One more step.) The new state will be q_2 or q_3 depending on whether it reached a 0 or a #. At this point, q_2 should be pointing to a 0 or 1 (since the rightmost bit is 1) and q_3 should be pointing to a #. It re-writes the same symbol and moves left to state q_4 . (One more step.) The current symbol should be # because it holds the place holder for the 0 or #. It replaces the # with a 1 and continues to move left past all the 0's until the next # is reached. ($l(x)$ more steps.) This # symbol marks the location where it started. It replaces the # with a 0 and transitions to q_f (One more step). The total number of steps has been $2l(x) + 3$. \square

For every $a \in \Gamma$, we add the rule $\delta(q_f, a) = (q_0, a, N)$ which makes M_{BC} well formed. Then if M_{BC} starts with an input of 1, it will repeatedly increment the string as long as it is allowed to run. For example, suppose M_{BC} starts with string x :

$$\begin{array}{c} q_0 \\ \downarrow \\ \vdash \quad 1 \quad 1 \quad 0 \quad 1 \quad \# \quad \# \quad \# \quad \# \quad \# \quad \dashv \end{array}$$

After the increment operation, the state will be:

$$\begin{array}{c} q_f \\ \downarrow \\ \vdash \quad 0 \quad 0 \quad 1 \quad 1 \quad \# \quad \# \quad \# \quad \# \quad \# \quad \dashv \end{array}$$

Then M_{BC} transitions to q_0 in place and the increment operation begins again:

$$\begin{array}{c} q_0 \\ \downarrow \\ \vdash \quad 0 \quad 0 \quad 1 \quad 1 \quad \# \quad \# \quad \# \quad \# \quad \# \quad \dashv \end{array}$$

For a particular chain length N , the starting configuration for M_{BC} will have the string 1, followed by $N - 3$ blank (#) symbols written on the work track and a binary witness string w of length $N - 2$ written on the witness track. We will call this input $(1, w)_N$.

- (1) Start in state q_0 at the left end of the string.
- (2) **if** the current bit is 0
- (3) Write a 1 and transition to q_f , stay in place
- (4) **else**
- (5) Write # (to mark the return location) move right into state q_1
- (6) **while** the current bit is 1,
- (7) Write a 0 and move right. Stay in state q_1
- (8) **if** current symbol is 0
- (9) Write a #, transition to q_2 and move right.
- (10) **else** (current symbol should be #)
- (11) Write a #, transition to q_3 and move right.
- (12) **if** current state is q_2 , the current symbol should be a bit b .
- (13) Write b , transition to q_4 and move left.
- (14) **else** (current state is q_3 , the current symbol should be #)
- (15) Write a #, transition to q_4 and move left.
- (16) Current symbol should be #. Write 1, transition to q_5 and move left.
- (17) **while** the current symbol is 0,
- (18) Write a 0 and move left. Stay in state q_5
- (19) **if** the current symbol is # (back at starting location),
- (20) Write a 0, transition to q_f , stay in place.

Figure 10: Pseudo-code for M_{BC} .

Definition 2.28. [Formula for $N(x)$]

$$N(x) = 5n(x^R) - 2w(x) - 4[n(x^R) \bmod 2],$$

where x is a binary string, ending in 1, x^R is the reverse of binary string x , $n(x)$ is the numerical value of the binary number represented by string x , and $w(x)$ is the number of 1's in x .

Lemma 2.29. [$N(x) - 2$ Steps of M_{BC} Produces String x] Let $N(x) = N \geq 5$. Starting with input $(1, w)_N$. If M_{BC} is run for $N - 2$ steps, it will never leave the segment of tape cells from 1 through $N - 4$. Moreover, at the end of the $N - 2$ steps, the configuration will be (x, w) with the head pointing to the left-most bits of x and w in state q_f .

Proof. M_{BC} takes two steps to add a 1 to the leftmost position if a 0 is present, beginning and ending in state q_f :

$$(q_f/0)x1\#^* \rightarrow (q_0/0)x1\#^* \rightarrow (q_f/1)x1\#^*$$

Let $f(n)$ be the number of steps required to go from the state $(q_f/1)\#^*$ to $(q_f/0)0^{n-1}1\#^*$, which is effectively moving the 1 over n locations. Note that the cost is the same if the starting configuration is $(q_f/1)0^n x\#^*$. In order to end up in configuration $(q_f/0)0^{n-1}1\#^*$, the TM must first reach $(q_f/1)1^{n-1}\#^*$ and then perform an increment operation. In order to reach $(q_f/1)1^{n-1}\#^*$, the first 1 is moved over by $n - 1$ (cost of $f(n - 1)$), then a new 1 is added (cost of 2), then that 1 is moved over by $n - 2$ (cost of $f(n - 2)$), etc. Thus the number of steps to reach $(q_f/1)1^{n-1}\#^*$ from $(q_f/1)\#^*$ is $f(n - 1) + f(n - 2) + \dots + f(1) + 2(n - 1)$. After one more increment operation, the state will be $(q_f/0)0^{n-1}1\#^*$. It takes 1 step to get to $(q_0/1)1^{n-1}\#^*$, and then according to Lemma 2.27, an additional $2n + 3$ steps to complete the increment. Therefore the function f obeys the recurrence:

$$f(n) = \sum_{j=1}^{n-1} f(j) + 2(n - 1) + 1 + (2n + 3) = \sum_{j=1}^{n-1} f(j) + (4n + 2).$$

The solution to this recurrence relation is $f(n) = 5 \cdot 2^n - 4$. The initial condition is $f(1) = 5$, and it requires 5 steps to go from $(q_f/1)\#\#^*$ to $(q_f/0)1\#\#^*$.

If the bits of x are numbered from left to right $x_1x_2 \cdots x_n$, then the number of steps to reach $(q_f/x_1)x_2 \cdots x_n\#\#^*$ from $(q_f/1)\#\#^*$ is

$$\sum_{j=2}^n x_j f(j-1) + 2(w(x) - 1) = \sum_{j=2}^n x_j (5 \cdot 2^{j-1} - 4) + 2(w(x) - 1)$$

If x^R is even ($x_1 = 0$), then this value is $5n(x^R) - 2w(x) - 2$. If x^R is odd then this value is $5n(x^R) - 2w(x) - 6$. Note also that M_{BC} starts in state q_0 instead of state q_f , so we can subtract 1 step to get:

$$N(x) - 2 = 5n(x^R) - 2w(x) - 2 - 4(n(x^R) \bmod 2).$$

Finally, we address whether the head tries to move out of the segment of tape symbols from 1 through $N(x) - 3$ in the first $N(x) - 2$ steps. If $N(x) \geq 5$, then there are 3 tape cells and the first increment operation can be completed. The first time the head reaches tape cell $n \geq 4$ is in incrementing 1^{n-2} . It takes $5(2^{n-2} - 1) - 2(n-2) - 4$ steps to reach 1^{n-2} and end in state q_f . It takes another n steps to reach tape cell n . We need that the total number of steps $5(2^{n-2} - 1) - n \geq n + 2$, which holds for every $n \geq 4$.

On the left end of the tape, M_{BC} starts with a binary string ending in 1. In each iteration in which it starts with a string ending in 1, it behaves properly. When it reaches q_f , it will again have a string ending in 1. It then transitions to q_0 and behaves properly on the next iteration. \square

It will be useful in the analysis to have a lower bound on $N(x)$ as a function of $|x|$.

Lemma 2.30. For $|x| \geq 2$, $N(x) \geq 2^{|x|}$.

Proof. Consider a string x of length n . $N(x)$ is minimized for $x = 0^{n-1}1$ or $10^{n-2}1$. Any additional 1's in x add at least 10 to $N(x)$ in the first term and only subtract 2 from the second term. For $10^{n-2}1$, $N(x) = 5(2^{n-1} + 1) - 10$ which is at least 2^n for any $n \geq 2$. For $0^{n-1}1$, $N(x) = 5(2^{n-1}) - 4$ which is also at least 2^n for any $n \geq 2$. \square

2.4.3 The Turing Machine M_{TV} used in the Hamiltonian for Finite Chains

In this section we establish that there is a reversible normal-form Turing Machine M_{TV} that satisfies the conditions required in the construction. Recall that we are reducing from $f \in \text{FP}^{\text{NEXP}}$. The polynomial time Turing Machine that computes f is called M and the query language is L . L is contained in NEXP and the exponential time verifier for L is called V . We will assume that there are constants c_1 and c_2 such that on input x , the number of queries made by M is at most $c_1|x|$ and if M makes a query \bar{x} to the oracle, the size of the witness required is at most 2^{c_2n} and the running time of V on input (\bar{x}, w) is at most $2^{c_2|x|}$. This assumption justified by the following lemma:

Lemma 2.31. [Padding Lemma] $f \in \text{FP}^{\text{NEXP}}$, then for any constants, c_1 and c_2 , f is polynomial time reducible to a function $g \in \text{FP}^{\text{NEXP}}$ such that g can be computed by polynomial-time Turing Machine M with access to a NEXP oracle for language L . The verifier for L is a Turing Machine V . Moreover, on input x of length n , M runs in $O(n)$ time, makes at most c_1n queries to the oracle. Also, the length of the queries made to the oracle is at most c_1n and the running time of V as well as the size of the witness required for V on any query made by M is $O(2^{c_2n})$

Proof. Suppose that M runs in $r_1(n)$ time and the running time of V is $O(2^{r_2(n)})$. Therefore, on input x , the number of queries made by M as well as the length of the input to the oracle are at most $r_1(|x|)$. Also, the running time as well as the size of witness required by V is at most $O(2^{r_2(r_1(|x|))})$.

The reduction will pad an input x to f with $10^{t(n)}1$, for a polynomial t chosen below. We will refer to this substring as the *suffix*. The algorithm for g will verify that the length of the suffix is in fact $t(n)$, where n is the number of bits not included in the suffix. If not, then the value of g is 0. If the input to g does have a suffix with the correct length then it erases the suffix and simulates M on the rest of the string. $t(n)$ will be chosen to

be large enough so that this computation can be done in $O(t(|x|))$ time. Note that the input length to g is now $\bar{n} = t(|x|) + |x| + 2$.

$t(n)$ is chosen so that $r_1(|x|) \leq c_1 t(|x|) < c_1 \bar{n}$, so that the running time of M and hence the number of oracles queries made, as well as the length of the inputs to those oracle queries are all bounded by $c_1 \bar{n}$. The running time of V on any of the query inputs is at most $c 2^{r_2(r_1(|x|))}$ for some c . t will also be chosen to be large enough so that

$$c 2^{r_2(r_1(|x|))} \leq 2^{c_2 t(|x|)} < 2^{c_2 \bar{n}}.$$

□

The following lemma establishes that there is a reversible normal-form Turing Machine M_{TV} that satisfies the conditions required in the construction.

Lemma 2.32. [Existence of M_{TV}] *There is a reversible normal-form Turing Machine M_{TV} such that*

1. M_{TV} behaves properly on all (a, b) , where $a, b \in \{0, 1\}^*$.
2. M_{TV} is 1-compact.
3. For all but a finite number of binary string x , if $N = N(x)$ and $w \in \{0, 1\}^{N-4}$, then M_{TV} halts on input (x, w) in at most $N - 3$ steps.
4. M_{TV} has $\text{OUT}(x, w, M, V)$ on its work tape when it reaches its final state.

Proof. Let $n = |x|$. By Lemma 2.30, $N(x) \geq 2^{|x|} = 2^n$ for any $|x| \geq 2$.

We first consider the time to compute the function outlined in Figure 2 on a RAM and then argue about the overhead in converting the algorithm to a reversible Turing Machine. Simulating M on input x takes time $r(n)$ for some polynomial r . By Lemma 2.31, we can assume that the number of queries made to V is at most $m \leq c_1 n$ and the running time of each call to V takes at most time $2^{c_2 n}$. Thus, the total time for running the verifier is at most $c_1 n 2^{c_2 n}$. Finally the time to compute $T(x, y)$ and write the resulting value in unary is $O(4^m)$ which is $O(2^{2c_1 n})$. Thus, for any constant d , the constants c_1 and c_2 can be chosen so that the running time to compute the function computer by M_{TV} is $O(N^d)$.

The RAM algorithm can be converted to a TM computation with at most polynomial overhead. Finally, by Theorem B.8 from [8], the TM can be converted to a reversible TM that behaves properly on all inputs with quadratic overhead. Therefore the constant d can be chosen to be small enough so that the running time of the reversible TM to compute M_{TV} is $o(N)$ which will be at most $N - 3$ for all but a finite number of strings x .

Finally, to satisfy the second assumption, we can add one additional state which cause the reversible TM to stay in place for one step before beginning its computation. □

2.4.4 Adjustments to the Two Turing Machines

The computation embedded in the Hamiltonian will execute M_{BC} for exactly $N - 2$ steps at which point a binary string will be written on the work tape. That string will then be the input to a second Turing Machine. In the finite construction, we can choose a particular N so that after $N - 2$ steps, M_{BC} is at the end of an increment operation and the desired x is on the work tape. In the infinite case, we will have less control over the number of steps for which M_{BC} is run and we will want the second Turing Machine to finish the increment operation before starting on its own computation. Thus, the second Turing Machine will be M_{BC} dovetailed with M_{TV} .

The first step is to expand the tape alphabet of M_{BC} and M_{TV} so that they have exactly the same tape alphabet Γ . The first lemma shows that this can be done while maintaining the properties that the Turing Machines are reversible and in normal-form.

Lemma 2.33. [Adding Symbols] *Let $M = (Q, \Gamma, \delta, q_0, q_f)$ be a normal-form reversible TM that acts as a permutation on $C_N(M)$. Let a be a symbol that is not in Γ . Let $M' = (Q, \Gamma \cup \{a\}, \delta', q_0, q_f)$, where for every*

$b \in \Gamma$,

$$\begin{aligned} \delta'(q, b) &= \delta(q, b) && \text{for } q \in Q \\ \delta'(q, a) &= (a, q, D_q) && \text{for } q \in Q - \{q_0, q_f\} \\ \delta'(q_0, a) &= (a, q_f, D_{q_f}) \\ \delta'(q_f, a) &= (a, q_0, D_{q_0}) \end{aligned}$$

Then M and M' have the same behavior starting from any configuration that does not have the symbol a anywhere on the tape. If M is reversible and in normal-form, then M' is as well.

Proof. By induction on the number of steps. If the current tape contents do not contain a , then the current symbol will not some $b \in \Gamma$. M' will not write a in the next step because $\delta'(q, b) = \delta(q, b)$ and M does not have the symbol a in its tape alphabet.

The reduced transition rule is still one-to-one. Moreover, the TM remains unidirectional. If M is in normal form, then the new rule $\delta'(q_f, a) = (a, q_0, D_{q_0})$ ensures that M' will also be in normal form. \square

Once the tape alphabets from M_{BC} and M_{TV} are expanded so that they are the same, the TM resulting from dovetailing the two together is well defined.

Definition 2.34. [Dovetailing Two TMs] Let $M_1 = (Q_1, \Gamma, I, \delta_1, q_0, q_f)$ and $M_2 = (Q_2, \Gamma, I, \delta_2, p_0, p_f)$ be two normal-form reversible TMs. Suppose also that M_1 and M_2 use the same set of tape symbols Γ and that $Q_1 \cap Q_2 = \emptyset$. Define $M_1 + M_2$ to be the Turing Machine with state set $Q_{1+2} = Q_1 \cup Q_2$, and for every $a \in \Gamma$,

$$\begin{aligned} \delta_{1+2}(q, a) &= \delta_1(q, a) && \text{for } q \in Q_1 - \{q_f\} \\ \delta_{1+2}(p, a) &= \delta_2(p, a) && \text{for } p \in Q_2 - \{p_f\} \\ \delta_{1+2}(q_f, a) &= (p_0, a, N) \\ \delta_{1+2}(p_f, a) &= (q_0, a, N) \end{aligned}$$

The initial state for $M_1 + M_2$ is q_0 and the final state is p_f .

Lemma 2.35. If M_1 and M_2 are normal-form reversible TMs, then $M_1 + M_2$ is a normal-form reversible TM.

Proof. We will show that $M_1 + M_2$ is unidirectional and has a one-to-one reduced transition function, which by Theorem 2.22, will imply that $M_1 + M_2$ is reversible. Since M_1 and M_2 are themselves reversible they are unidirectional. Since $M_1 + M_2$ preserves the direction of each state, $M_1 + M_2$ is also unidirectional. Note also that for $q \in Q_1 - \{q_f\}$, $\delta_1(q, a)$ does not map to state q_0 , otherwise the reduced transition function M_1 would not be one-to-one, since $\delta_1(q_f, a) = (q_0, a, N)$ for every $a \in \Gamma$. Similarly for $p \in Q_2 - \{p_f\}$, $\delta_2(p, a)$ does not map to state p_0 . This means that there is no conflict between the rules in the first two lines of the Definition 2.34 and the new rules added in the second two lines. Since the reduced transition functions of M_1 and M_2 are one-to-one and $Q_1 \cap Q_2 = \emptyset$, there are no conflicts between any two rules specified in the first two lines.

The final state of $M_1 + M_2$ is p_f and the initial state is q_0 . Since δ_{1+2} maps (p_f, a) to (q_0, a, N) for every $a \in \Gamma$, $M_1 + M_2$ is in normal form. \square

The computational process that will be embedded into the Hamiltonian will execute $N - 2$ steps of M_{BC} followed by $N - 2$ steps of $M_{BC} + M_{TV}$. Lemma 2.32 guarantees that the second process will reach a final state p_f within $N - 2$ steps for most N . At this point, the correct output is written on the work tape. However, it will be important for the construction that this correct output also be written on the input tape after exactly $N - 2$ steps.

Let q_0 be the start state of $M_{BC} + M_{TV}$ (since it was the original start state of M_{BC}) and let p_f be the final state of $M_{BC} + M_{TV}$ (since it was the original final state of M_{TV}). Recall that $M_{BC} + M_{TV}$ is in normal-form, so $\delta(p_f, a) = (q_0, a, N)$ for every $a \in \Gamma$. Also there are two symbols σ_A and σ_R in Γ such that in a correct computation, the TM halts with the head in the start position. Furthermore, the start cell contains σ_A or σ_R and there are no other occurrences of σ_A or σ_R on the rest of the tape.

Definition 2.36. [Transformed TM $\mathcal{T}(M_{BC} + M_{TV})$] Let $M_{BC} + M_{TV} = (Q, \Gamma, I, \delta, p_f, q_0)$. Define $\mathcal{T}(M_{BC} + M_{TV}) = (Q \cup \{q_*\}, \Gamma, I, \delta', p_f, q_0)$

$$\begin{aligned} \delta'(q, a) &= \delta(q, a) && \text{except for } (q, a) \in \{(q_f, \sigma_A), (q_f, \sigma_R)\} \\ \delta'(p_f, a) &= (q_*, a, R) && \text{for } a \in \{\sigma_A, \sigma_R\} \\ \delta'(q_*, b) &= (q_*, b, R) && \text{for } a \in \Gamma - \{\sigma_A, \sigma_R\} \\ \delta'(q_*, a) &= (q_0, a, N) && \text{for } a \in \{\sigma_A, \sigma_R\} \end{aligned}$$

Lemma 2.37. [Properties of $\mathcal{T}(M_{BC} + M_{TV})$] Let M_{TV} be a TM that satisfies the properties from Lemma 2.32. Then $\mathcal{T}(M_{BC} + M_{TV})$ is unidirectional and its reduced transition function is one-to-one. For all but a finite number of binary string x , and every $w \in \{0, 1\}^{N(x)-2}$, starting with input $(1, w)$, if $N(x) - 2$ steps of M_{BC} followed by $N(x) - 2$ steps of $\mathcal{T}(M_{BC} + M_{TV})$ are executed, then

1. the head of the Turing Machine never leaves the sequence of tape cells from 1 through $N(x) - 3$ in the course of executing the $2N(x) - 4$ steps.
2. the contents of the work tape are $\text{OUT}(x, w, M, V)$ at the end of the $2N(x) - 4$ steps.

Proof. Since $M_{BC} + M_{TV}$ is a normal-form TM, the direction associated with q_0 is N . All of the new rules added are therefore consistent with $D_{q_0} = N$ and $D_{q_*} = R$ and therefore $\mathcal{T}(M_{BC} + M_{TV})$ is uni-directional.

The rules $\delta(p_f, \sigma_A) = (q_0, \sigma_A, N)$ and $\delta(p_f, \sigma_R) = (q_0, \sigma_R, N)$ are removed and the rules $\delta(q_*, \sigma_A) = (q_0, \sigma_A, N)$ and $\delta(q_*, \sigma_R) = (q_0, \sigma_R, N)$ are added, so there is exactly one rule that maps on to each pair (q_0, σ_A) and (q_0, σ_R) . Finally the new rules $\delta(p_f, \sigma_A) = (q_*, \sigma_A, R)$, $\delta(p_f, \sigma_R) = (q_*, \sigma_R, R)$, and $\delta(q_*, a) = (q_*, a, R)$ are one-to-one. Since q_* is a new state, these rules do not conflict with any of the previous rules from $M_{BC} + M_{TV}$. Therefore the new reduced transition function is one-to-one.

By Lemma 2.29 the head never leaves the sequence of tape cells from 1 through $N(x) - 3$ in $N(x) - 2$ steps of M_{BC} as long as $N(x) \geq 5$. At this point, the string x is written on the work tape, the head is back in the starting location and the state is q_f . According to the definition of dovetailing, $M_{BC} + M_{TV}$ transitions from q_f to p_0 , which initiates M_{TV} . In the next $N - 3$ steps, M_{TV} will not move past tape cell $N(x) - 3$ due to the fact that it is 1-compact. Since M_{TV} behaves properly on input (x, w) , it will not move to the left of tape cell 1 on input (x, w) . According to Lemma 2.32, for all but a finite number of x 's, M_{TV} will reach p_f within $N - 3$ steps. Since M_{TV} behaves properly on (x, w) , when it halts, the head will be back at tape cell 1. The content of the work tape at this point is $\text{OUT}(x, w, M, V)$. Note that this output will have an σ_A or σ_R in cell 1 and no other occurrences of σ_A or σ_R on the rest of the tape. Therefore, the current state/tape symbol pair is (q_f, σ_A) or (q_f, R) . According to the rules of $\mathcal{T}(M_{BC} + M_{TV})$, the current symbol will be re-written and the head will move right into state q_* . As long as no σ_A or σ_R symbols are encountered, the head will continue to move to the right, leaving the tape contents intact. Therefore, the end of the $N(x) - 3$ steps will be reached before the head reaches tape cell $N(x) - 2$. At the end of the $N(x) - 2$ steps of $\mathcal{T}(M_{BC} + M_{TV})$, the tape contents will still be $\text{OUT}(x, w, M, V)$. \square

At this point M_{BC} and $\mathcal{T}(M_{BC} + M_{TV})$ have the same tape alphabet, but the state set for M_{BC} is a subset of the state set for $\mathcal{T}(M_{BC} + M_{TV})$. When we translate the transition functions for each TM into a Hamiltonian, they will have to be well-defined on the same state space. Therefore, we would like to expand the state set for M_{BC} so that its state set is the same as $\mathcal{T}(M_{BC} + M_{TV})$. The following fact allows us to add states without effecting the behavior of M_{BC} on the original state set.

Fact 2.38. [Adding States to a TM] Let $M = (Q, \Gamma, \delta, q_0, q_f)$ be a reversible normal-form Turing Machine. Let M' be the Turing Machine with $Q' = Q \cup \{q_{new}\}$. δ' will be the same as δ for all $q \in Q$, and $\delta'(q_{new}, a) = (q_{new}, a, N)$ for all $a \in \Gamma$. Then M' is a reversible normal-form Turing Machine that behaves exactly as M on any configuration whose state is $q \in Q$.

2.5 The Hamiltonian

We are now ready to describe the terms in the Hamiltonian. Section 2.5.1 describes the set of constraints which ensure that the computation tracks are well-formed, corresponding to a valid configuration of the Turing

Machine. As the Track 1 pointer sweeps from right to left, it will trigger one TM step on the computation tracks. Section 2.5.2 gives a generic description of the Hamiltonian terms that execute a TM step. Then Section 2.5.3 describes more specifically how each i -pointer effects the computation tracks. The propagation terms are given explicitly in this section. We have already added in Section 2.3 a number of terms that operate only on the clock tracks. Many of those will remain unchanged since they operate as the identity on the computation tracks. Some of them, however, will be replaced with terms that advance the clock as well as change the computation tracks. The transition terms introduced in Section 2.3 are numbered TR-1 through TR-46. We will indicate when a new transition rule replaces one of these transition rules. Finally, Section 2.5.4 describes additional penalty terms used to ensure that the lowest energy state corresponds to a correct computation.

2.5.1 Local Constraints to Make the Computation Tracks Well-Formed

The computation that will be embedded in the Hamiltonian will consist of $N-2$ steps of M_{BC} followed by $N-2$ steps of $\mathcal{T}(M_{BC} + M_{TV})$. It will be convenient to refer to have a more succinct name for $\mathcal{T}(M_{BC} + M_{TV})$:

$$M_{check} = \mathcal{T}(M_{BC} + M_{TV})$$

As per Lemmas 2.38 and 2.33, states and tape symbols have been added to both M_{BC} and M_{check} to ensure that they have the same set of symbols and the same tape alphabet. The previous section assumed a single track Turing Machine when in fact both Tracks 5 and 6 are Turing Machine tapes. Thus, the tape symbols for the Turing Machine consists of the set $\Gamma = \Sigma \times \{0, 1\}$, where Σ is the set of symbols for Track 5. The Turing Machines will always have the property that the state of Track 6 is never changed, so if the current symbol is some $a \in \Gamma$ which represents states $[x, 1]$ on Tracks 5 and 6, then the symbol written will always be of the form $[y, 1]$. In the next section, we will need to add a duplicate copy of every $q_L \in Q_L$ in order to execute the left-moving TM steps. Let Q'_L denote the set of added states.

Here are the standard basis states for the part of the Hilbert space of each particle corresponding to Tracks 4, 5, and 6.

- The standard basis states for Track 4 are $\{\circ, \odot\} \cup Q \cup Q'_R$.
- The set of standard basis states for Track 5 is Σ .
- The standard basis states for Track 6 are $\{0, 1\}$.

We will add Type I terms that will give an energy penalty to any standard basis state for the computation tracks that do not correspond to a well-defined Turing Machine configuration. These constraints will enforce the condition that:

Definition 2.39. [Well-Formed Computation Configurations] Let C_N denote the set of standard basis states for the computation tracks in which the state of Track 4 has the form: $\langle \odot \odot^* (Q + Q'_R) \circ^* \odot \rangle$. These are the well-formed computation configurations.

Definition 2.40. [The Hamiltonian Term Enforcing Well-Formed Computations Configurations] Let h_{wf-co} denote the Hamiltonian terms with the constraints that give an energy penalty for any state for Tracks 4 that is not well-formed.

2.5.2 Implementing TM Steps in Propagation Terms

We show here how a single sweep of a pointer on Track 1 from right to left will cause the TM configuration on Tracks 4 through 6 to advance by one TM step. The details of this part of the construction, as well as the proof Claim 2.41 below follow [16] closely. Note that since we are reducing from FP^{NEXP} instead of $\text{FP}^{\text{QMA-EXP}}$, all of the Turing Machines in our construction, including the verifier V , are classical reversible Turing Machines instead of Quantum Turing Machines.

The sweep of the Track 1 pointer begins from state $\langle \ominus \ominus \rangle$. The Track 1 pointer \ominus then sweeps all the way to the left end of the chain until the state $\langle \odot \ominus \rangle$ is reached. Each transition $|\odot \ominus \rangle \rightarrow |\ominus \circ \rangle$ will cause a unitary operation to be applied to the computation tracks below. We will write the pointer \ominus generically without a number and later discuss how the i -pointers work for different i .

We will need to execute the TM steps in which the head moves right or stays in the same place separately than the moves in which the head moves left. In order to do this, we introduce a new state q'_L for every $q_L \in Q_L$. We will call this set Q'_L . In a correct computation, it will never be the case that the TM is in state q'_L without a \ominus directly above it on Track 1. It will also never be the case that there is a \ominus in the same location as the head if the state is some $q_R \in Q_R$.

Define S to be the set of standard basis states associated with the computation tracks of two neighboring particles. S is the set of standard basis states of the following form:

$$\begin{array}{|c|c|} \hline p & q \\ \hline a & b \\ \hline \end{array} \quad \text{where:} \quad \begin{array}{l} (p, q) \in (Q \times \{\ominus\}) \cup (\{\ominus\} \times Q) \cup \{\ominus\ominus, \ominus\ominus\} \\ (a, b) \in \Gamma \times \Gamma \end{array}$$

We will be interested in two particular subsets of S . S_A is the subset of states from S where $q \notin Q_R$ and $p \notin Q'_L$. We also define S_B to be the subset of states from S , where $q \notin Q'_L$ and $p \notin Q_R$.

We will show the transformation P that maps S_A to S_B . The transformation P works in two parts. At the moment that the Track 1 pointer moves left from the position just to the right of the head, we execute the move for that location. For every $\delta(q, a) = (q_R, b, R)$, we write a b into the old location and move the head right into state q_R . For every $\delta(q, a) = (q_N, b, N)$, we write a b into the old location and change the state to q_N without changing the location of the head. For every $\delta(q, a) = (q_L, b, L)$, we write a b into the old location and change the state to q'_L without changing the location of the head. We need to defer the action of moving the head left until the Track 1 pointer has access to the new location for the head. In the next step of the clock when the head is aligned with the q'_L , we move the head left and convert it to q_L . In the rules shown below, the top row shows the state of Track 1, the middle row shows the state of Track 4 and the bottom row shows the combined state of Tracks 5 and 6. The first set of transitions are defined for every $q \notin Q'_L$:

$$\begin{array}{ccc} \delta(q, a) = (q_R, b, R) & \delta(q, a) = (q_N, b, N) & \delta(q, a) = (q_L, b, L) \\ \begin{array}{|c|c|} \hline \ominus \leftarrow \\ \hline q \\ \hline a \\ \hline \end{array} \leftarrow \begin{array}{|c|c|} \hline \ominus \leftarrow \\ \hline q_R \\ \hline b \\ \hline \end{array} & \begin{array}{|c|c|} \hline \ominus \leftarrow \\ \hline q \\ \hline a \\ \hline \end{array} \leftarrow \begin{array}{|c|c|} \hline \ominus \leftarrow \\ \hline q_N \\ \hline b \\ \hline \end{array} & \begin{array}{|c|c|} \hline \ominus \leftarrow \\ \hline q \\ \hline a \\ \hline \end{array} \leftarrow \begin{array}{|c|c|} \hline \ominus \leftarrow \\ \hline q'_L \\ \hline b \\ \hline \end{array} \end{array} \quad (9)$$

After this step, we are in a configuration in which the step has been performed, except that moving the head left has been deferred. If the TM is in a primed state that is aligned with the \ominus , that triggers the execution of the right-moving step.

$$\begin{array}{|c|c|} \hline \ominus \leftarrow \\ \hline q'_L \\ \hline \ominus \\ \hline \end{array} \leftarrow \begin{array}{|c|c|} \hline \ominus \leftarrow \\ \hline q_L \\ \hline \ominus \\ \hline \end{array} \quad (10)$$

Otherwise, the head just sweep right leaving the other tracks unchanged:

$$\begin{array}{|c|c|} \hline \ominus \leftarrow \\ \hline q_L \\ \hline \ominus \\ \hline \end{array} \leftarrow \begin{array}{|c|c|} \hline \ominus \leftarrow \\ \hline q_L \\ \hline \ominus \\ \hline \end{array} \quad \begin{array}{|c|c|} \hline \ominus \leftarrow \\ \hline q_N \\ \hline \ominus \\ \hline \end{array} \leftarrow \begin{array}{|c|c|} \hline \ominus \leftarrow \\ \hline q_N \\ \hline \ominus \\ \hline \end{array} \quad (11)$$

$$\begin{array}{|c|c|} \hline \ominus \leftarrow \\ \hline \ominus \\ \hline \ominus \\ \hline \end{array} \leftarrow \begin{array}{|c|c|} \hline \ominus \leftarrow \\ \hline \ominus \\ \hline \ominus \\ \hline \end{array} \quad \begin{array}{|c|c|} \hline \ominus \leftarrow \\ \hline \ominus \\ \hline \ominus \\ \hline \end{array} \leftarrow \begin{array}{|c|c|} \hline \ominus \leftarrow \\ \hline \ominus \\ \hline \ominus \\ \hline \end{array} \quad (12)$$

The criteria for S_A is that the Track 4 state of the left particle is not in Q'_L and the Track 4 state of the right particle is not in Q_R . Therefore, P is well-defined for every state in S_A . The criteria for S_B is that the Track 4 state of the right particle is not in Q'_L and the Track 4 state of the left particle is not in Q_R . Therefore, the range of $P|_{S_A}$ is in S_B . Since the computation state for a pair is in S_B after P is applied to that pair, the next pair over is in state S_A and P can then be applied to this new pair. Note that in a correct computation, if the Track 1 state is $|\ominus \leftarrow \ominus\rangle$, then the computational state for those two particles will be in S_A and if the Track 1 state is $|\ominus \ominus\rangle$, then the computational state for those two particles will be in S_B . P is one-to-one from S_A to S_B . This is formalized in Claim 2.41 below. Since S_A and S_B are both subsets of S , P can be extended to be a permutation on S . The Hamiltonian term will then be:

$$I_S \otimes |\ominus \ominus\rangle \langle \ominus \ominus| + I_S \otimes |\ominus \leftarrow \ominus\rangle \langle \ominus \leftarrow \ominus| + P \otimes |\ominus \leftarrow \ominus\rangle \langle \ominus \leftarrow \ominus| + P^\dagger \otimes |\ominus \leftarrow \ominus\rangle \langle \ominus \leftarrow \ominus|$$

Claim 2.41. *If the reduced transition rule δ is one-to-one, then Rules (9) through (12) define a one-to-one function from S_A to S_B .*

Proof. Each rule defines P on a disjoint subset of S_A . Moreover the images of all the rules are mutually disjoint, so we only need to show that each rule individually is one-to-one.

The rules in (11) and (12) act as the identity on the computational space of the two particles. The rule in (10) is one-to-one. Finally, we need to consider the rules given in (9). Since the reduced δ function is one-to-one, then this transformation is also one-to-one. \square

The two transition functions δ_{BC} and δ_{check} give rise to permutations P_{BC} and P_{check} defined on S .

Lemma 2.42. [**Left sweep of the 1-pointer executes on step of the TM**] *Consider a Turing Machine M with transition function δ that gives rise to permutation P according to Rules (9) through (12). Suppose that the state of the computation tracks corresponds to a valid configuration of M with the head in state q and current symbol a . Suppose further that the following two conditions are satisfied:*

1. *The head is not at the right-most location of the chain.*
2. *The head is not at the left-most location of the chain or $\delta(q, a)$ does not cause the head to move left.*

Then one sweep of \ominus from the right end of the chain to the left end of the chain results in the configuration corresponding to one step of M .

Proof. If the computation tracks are in a valid TM configuration, then the configuration of Track 4 has the form: $\odot \cdots \odot q \odot \cdots \odot$. Since the head is not in the right-most location, there must be at least one \odot to the right of the q . As the 1-pointer \ominus sweeps from right to left, the operation P is applied to each pair of particles from right to left. P will act as the identity as long as the Track 4 is $\odot \odot$. Eventually, a configuration is reached in which Track 1 is $\odot \ominus$ and Track 4 is $q \odot$. In the next move, as \ominus moves one location to the left, P applies a rule from (9) which executes one move of the TM. If the head moves right into state q_R , the TM move is complete. If the head stays in place and transitions to a state q_N , the move is also complete, but the 1-pointer is now co-located with q_N . Rule (11) is applied and the 1-pointer moves left without changing the computation tracks. If the head stays in place and transitions into a state q'_L , then according to the conditions of the lemma, the head is not in the left-most location and the move can be completed with Rule (10). The 1-pointer is now co-located with q'_L . Rule (11) is applied and the 1-pointer moves left without changing the computation tracks. P acts as the identity for the remainder of the left-sweep since the remaining pairs have $\odot \odot$ on Track 4. \square

2.5.3 Propagation Terms for Each of the 8 Segments

We will use the different i -pointers on Track 1 to trigger different δ transition functions on Tracks 4 through 6. Recall from the clock construction that the i -segments vary according to whether they begin or end at the left or right end of the chain and according to the number of back and forth iterations performed by the i -pointer before advancing to the next segment. The list below shows the segments for an entire cycle for Tracks 1 and 2 and how many steps of each δ function are triggered on the computation tracks during the segment. Segments 1 through 3 trigger a step of one of the two TMs as the 1-pointer moves from right to left. A sweep of the \ominus triggers the application of the corresponding P operation to each pair of particles from right to left. Segments 5 through 7 trigger the inverse operation of the TMs. A sweep of the \oplus triggers the application of the corresponding P^{-1} operation to each pair of particles from left to right. This will cause the state of the computation tracks to return to their original state after each cycle for Tracks 1 and 2. Segments 4 and 8 are used for checking purposes only. The 4 and 8-pointers act as the identity on the computation tracks. We will add Type I terms that cause a penalty in the presence of a 4 or 8-pointer to penalize certain conditions on the computation tracks.

Figure 12 shows a graphical representation of a cycle for Tracks 1 and 2, indicating the path of the i -pointer for each i -segment. Note that since the Track 1 pointer for Segment 1 begins at the left end of the chain and ends at the right end of the chain, it only triggers $N - 3$ steps of M_{BC} . The single iteration made by the 2-pointer causes one more step of M_{check} to be executed so that each Turing Machine always runs for $N - 2$ steps. The same holds for Segments 6 and 7 with the inverse of M_{BC} .

We now define enhanced propagation terms for the clock states that act non-trivially on the computation space. We will be replacing some of the transition rules defined in Section 2.3 with enhanced terms that apply

- | | |
|--------------------------------------|---|
| 1) $N - 3$ steps of δ_{BC} | 5) $N - 2$ steps of $(\delta_{check})^{-1}$ |
| 2) One step of δ_{BC} | 6) One step of $(\delta_{BC})^{-1}$ |
| 3) $N - 2$ steps of δ_{check} | 7) $N - 3$ steps of $(\delta_{BC})^{-1}$ |
| 4) Identity | 8) Identity |

Figure 11: The Turing Machine steps executed in each i -segment.

an operation on the computation tracks of the two particles to which the term applies. In each case, we will name the rule that is removed and give the new term that will be added in its place. The clock rules in Section 2.3 are expressed using arrows (such as $\circlearrowleft \circlearrowright \rightarrow \circlearrowright \circlearrowleft$) which implicitly represents the term:

$$\frac{1}{2} [|\circlearrowleft \circlearrowleft\rangle \langle \circlearrowleft \circlearrowleft| + |\circlearrowright \circlearrowright\rangle \langle \circlearrowright \circlearrowright| + |\circlearrowleft \circlearrowright\rangle \langle \circlearrowright \circlearrowleft| + |\circlearrowright \circlearrowleft\rangle \langle \circlearrowleft \circlearrowright|]$$

These terms will be replaced by a term of the form:

$$\frac{1}{2} [I_S \otimes |\circlearrowleft \circlearrowleft\rangle \langle \circlearrowleft \circlearrowleft| + I_S \otimes |\circlearrowright \circlearrowright\rangle \langle \circlearrowright \circlearrowright| + P \otimes |\circlearrowleft \circlearrowright\rangle \langle \circlearrowright \circlearrowleft| + P^\dagger \otimes |\circlearrowright \circlearrowleft\rangle \langle \circlearrowleft \circlearrowright|]$$

\mathcal{S} denotes the Hilbert spaces spanned by S , the set of standard basis states for the computation tracks of two neighboring particles in a well-formed configuration. In order to reduce notation, we will omit the factor of $1/2$ which should be applied to all the terms described in this subsection.

Segment 1: In the first segment, the 1-pointers perform $N - 3$ right-to-left sweeps in which we would like to execute one step of M_{BC} . Transition Rules TR-1 and TR-2 are placed by the following two terms:

$$\begin{aligned}
& I_S \otimes \left| \begin{array}{cc} \circlearrowleft & \circlearrowright \\ \rightarrow & \rightarrow \end{array} \right\rangle \left\langle \begin{array}{cc} \circlearrowleft & \circlearrowright \\ \rightarrow & \rightarrow \end{array} \right| + I_S \otimes \left| \begin{array}{cc} \circlearrowright & \circlearrowleft \\ \rightarrow & \rightarrow \end{array} \right\rangle \left\langle \begin{array}{cc} \circlearrowright & \circlearrowleft \\ \rightarrow & \rightarrow \end{array} \right| \\
& + P_{BC} \otimes \left| \begin{array}{cc} \circlearrowright & \circlearrowleft \\ \rightarrow & \rightarrow \end{array} \right\rangle \left\langle \begin{array}{cc} \circlearrowleft & \circlearrowright \\ \rightarrow & \rightarrow \end{array} \right| + (P_{BC})^\dagger \otimes \left| \begin{array}{cc} \circlearrowleft & \circlearrowright \\ \rightarrow & \rightarrow \end{array} \right\rangle \left\langle \begin{array}{cc} \circlearrowright & \circlearrowleft \\ \rightarrow & \rightarrow \end{array} \right| \\
& I_S \otimes \left| \begin{array}{cc} \circlearrowleft & \circlearrowright \\ \rightarrow & \uparrow \end{array} \right\rangle \left\langle \begin{array}{cc} \circlearrowleft & \circlearrowright \\ \rightarrow & \uparrow \end{array} \right| + I_S \otimes \left| \begin{array}{cc} \circlearrowright & \circlearrowleft \\ \rightarrow & \uparrow \end{array} \right\rangle \left\langle \begin{array}{cc} \circlearrowright & \circlearrowleft \\ \rightarrow & \uparrow \end{array} \right| + P_{BC} \otimes \left| \begin{array}{cc} \circlearrowright & \circlearrowleft \\ \rightarrow & \uparrow \end{array} \right\rangle \left\langle \begin{array}{cc} \circlearrowleft & \circlearrowright \\ \rightarrow & \uparrow \end{array} \right| + (P_{BC})^\dagger \otimes \left| \begin{array}{cc} \circlearrowleft & \circlearrowright \\ \rightarrow & \uparrow \end{array} \right\rangle \left\langle \begin{array}{cc} \circlearrowright & \circlearrowleft \\ \rightarrow & \uparrow \end{array} \right|
\end{aligned}$$

Segment 2: The next segment is the 2-segment in which the 2-pointer makes a single round trip, starting at the right end of the chain. As the 2 pointer moves, right to left, we would like to trigger one step of δ_{BC} . Transition Rule TR-7 is replaced by:

$$I_S \otimes |\circlearrowright \circlearrowright\rangle \langle \circlearrowright \circlearrowright| + I_S \otimes |\circlearrowleft \circlearrowleft\rangle \langle \circlearrowleft \circlearrowleft| + P_{BC} \otimes |\circlearrowright \circlearrowleft\rangle \langle \circlearrowleft \circlearrowright| + (P_{BC})^\dagger \otimes |\circlearrowleft \circlearrowright\rangle \langle \circlearrowright \circlearrowleft| \quad (13)$$

Segment 3: The next segment is the 3-segment in which the 3-pointer makes $N - 3$ plus one half iterations between the two ends of the chain. Because the 3-pointer starts on the right end of the chain, there are $N - 2$ right-to-left sweeps. In each of these, we would like to execute one step of M_{check} . The Rule TR-13 is replaced by:

$$I_S \otimes \left| \begin{array}{cc} \circlearrowright & \circlearrowleft \\ \bullet & \rightarrow \end{array} \right\rangle \left\langle \begin{array}{cc} \circlearrowright & \circlearrowleft \\ \bullet & \rightarrow \end{array} \right| + I_S \otimes \left| \begin{array}{cc} \circlearrowleft & \circlearrowright \\ \bullet & \rightarrow \end{array} \right\rangle \left\langle \begin{array}{cc} \circlearrowleft & \circlearrowright \\ \bullet & \rightarrow \end{array} \right| \quad (14)$$

$$+ P_{check} \otimes \left| \begin{array}{cc} \circlearrowleft & \circlearrowright \\ \bullet & \rightarrow \end{array} \right\rangle \left\langle \begin{array}{cc} \circlearrowright & \circlearrowleft \\ \bullet & \rightarrow \end{array} \right| + (P_{check})^\dagger \otimes \left| \begin{array}{cc} \circlearrowright & \circlearrowleft \\ \bullet & \rightarrow \end{array} \right\rangle \left\langle \begin{array}{cc} \circlearrowleft & \circlearrowright \\ \bullet & \rightarrow \end{array} \right| \quad (15)$$

Segment 5: In the 5-segment the 5-pointer on Track 1 makes $N - 3$ plus one half iterations starting at the left end of the chain, which results in $N - 2$ left-to-right sweeps. We use this segment to execute $N - 2$ steps of M_{check} . Transition Rule TR-23 is replaced with the rule shown below. Note that the rule of P_{check} and

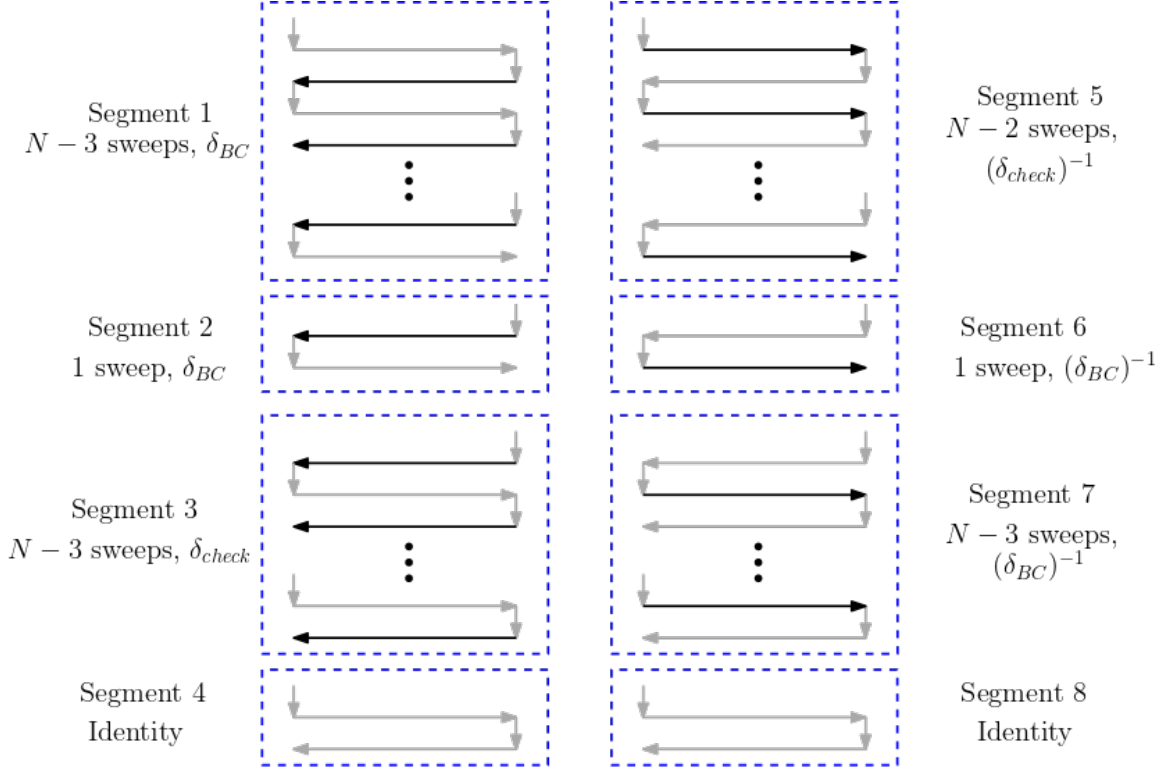


Figure 12: The segments in a cycle for Tracks 1 and 2, along with the transition function that is triggered with each sweep. The dark arrows show the steps of the Track 1 pointer that interact with the computation tracks. For Segments 1 through 3, the left-moving 1-pointer applies an operation to each pair of particles from right to left. For Segments 5 through 7, the right-moving 1-pointer applies an operation to each pair of particles from left to right. The light arrows show the steps of the Track 1 pointer which act as the identity on the computation tracks. The downward pointers correspond to a move at the end of the chain in which the Track 1 pointer changes direction. The horizontal pointers correspond to moves in the middle of the chain in which the Track 1 pointer moves right or left.

$(P_{check})^\dagger$ are switched so that $(P_{check})^\dagger$ is applied in the forward direction and P_{check} is applied in the reverse direction.

$$I_S \otimes \left| \begin{array}{cc} \leftarrow & \rightarrow \\ \leftarrow & \rightarrow \end{array} \right\rangle \left\langle \begin{array}{cc} \leftarrow & \rightarrow \\ \leftarrow & \rightarrow \end{array} \right| + I_S \otimes \left| \begin{array}{cc} \rightarrow & \leftarrow \\ \rightarrow & \leftarrow \end{array} \right\rangle \left\langle \begin{array}{cc} \rightarrow & \leftarrow \\ \rightarrow & \leftarrow \end{array} \right| \quad (16)$$

$$+(P_{check})^\dagger \otimes \left| \begin{array}{cc} \rightarrow & \leftarrow \\ \rightarrow & \leftarrow \end{array} \right\rangle \left\langle \begin{array}{cc} \rightarrow & \leftarrow \\ \rightarrow & \leftarrow \end{array} \right| + P_{check} \left| \begin{array}{cc} \leftarrow & \rightarrow \\ \leftarrow & \rightarrow \end{array} \right\rangle \left\langle \begin{array}{cc} \leftarrow & \rightarrow \\ \leftarrow & \rightarrow \end{array} \right| \quad (17)$$

Segment 6: Segment 6 is a single iterations with the Track 1 pointer beginning and ending at the right end of the track. The operation $(P_{BC})^\dagger$ is applied to each pair as the 1-pointer sweeps from left to right:

$$I_S \otimes \left| \begin{array}{cc} \rightarrow & \leftarrow \\ \rightarrow & \leftarrow \end{array} \right\rangle \left\langle \begin{array}{cc} \rightarrow & \leftarrow \\ \rightarrow & \leftarrow \end{array} \right| + I_S \otimes \left| \begin{array}{cc} \leftarrow & \rightarrow \\ \leftarrow & \rightarrow \end{array} \right\rangle \left\langle \begin{array}{cc} \leftarrow & \rightarrow \\ \leftarrow & \rightarrow \end{array} \right| + (P_{BC})^\dagger \otimes \left| \begin{array}{cc} \rightarrow & \leftarrow \\ \rightarrow & \leftarrow \end{array} \right\rangle \left\langle \begin{array}{cc} \rightarrow & \leftarrow \\ \rightarrow & \leftarrow \end{array} \right| + P_{BC} \otimes \left| \begin{array}{cc} \leftarrow & \rightarrow \\ \leftarrow & \rightarrow \end{array} \right\rangle \left\langle \begin{array}{cc} \leftarrow & \rightarrow \\ \leftarrow & \rightarrow \end{array} \right| \quad (18)$$

Segment 7: The next segment is the 7-segment in which the 7-pointer makes $N - 3$ plus one half iterations between the two ends of the chain. Because the 7-pointer starts on the right end of the chain, there are only $N - 3$ left-to-right sweeps. Because the right-moving 1-pointer also advances the pointer on Track 2, there are

two different transition rules that need to be augmented. The rule TR-31 is replaced by:

$$I_S \otimes \left| \begin{array}{cc} \rightarrow & \rightarrow \\ \leftarrow & \leftarrow \end{array} \right\rangle \left\langle \begin{array}{cc} \rightarrow & \rightarrow \\ \leftarrow & \leftarrow \end{array} \right| + I_S \otimes \left| \begin{array}{cc} \rightarrow & \rightarrow \\ \leftarrow & \leftarrow \end{array} \right\rangle \left\langle \begin{array}{cc} \rightarrow & \rightarrow \\ \leftarrow & \leftarrow \end{array} \right| \quad (19)$$

$$+(P_{check})^\dagger \otimes \left| \begin{array}{cc} \rightarrow & \rightarrow \\ \leftarrow & \leftarrow \end{array} \right\rangle \left\langle \begin{array}{cc} \rightarrow & \rightarrow \\ \leftarrow & \leftarrow \end{array} \right| + P_{check} \left| \begin{array}{cc} \rightarrow & \rightarrow \\ \leftarrow & \leftarrow \end{array} \right\rangle \left\langle \begin{array}{cc} \rightarrow & \rightarrow \\ \leftarrow & \leftarrow \end{array} \right| \quad (20)$$

The rule TR-32 is replaced by:

$$I_S \otimes \left| \begin{array}{cc} \rightarrow & \rightarrow \\ \leftarrow & \leftarrow \end{array} \right\rangle \left\langle \begin{array}{cc} \rightarrow & \rightarrow \\ \leftarrow & \leftarrow \end{array} \right| + I_S \otimes \left| \begin{array}{cc} \rightarrow & \rightarrow \\ \leftarrow & \leftarrow \end{array} \right\rangle \left\langle \begin{array}{cc} \rightarrow & \rightarrow \\ \leftarrow & \leftarrow \end{array} \right| + (P_{check})^\dagger \otimes \left| \begin{array}{cc} \rightarrow & \rightarrow \\ \leftarrow & \leftarrow \end{array} \right\rangle \left\langle \begin{array}{cc} \rightarrow & \rightarrow \\ \leftarrow & \leftarrow \end{array} \right| + P_{check} \left| \begin{array}{cc} \rightarrow & \rightarrow \\ \leftarrow & \leftarrow \end{array} \right\rangle \left\langle \begin{array}{cc} \rightarrow & \rightarrow \\ \leftarrow & \leftarrow \end{array} \right| \quad (21)$$

Definition 2.43. [h_{prop} **Sum of all the Propagation Terms**] Let h_{prop} denote the sum of all of the transition terms specified here and in Section 2.3 on the clock transition rules.

2.5.4 Additional Penalty Terms for the Finite Construction

Finally, we give some additional penalty terms that enforce the condition that for the lowest energy state, the computation state at the start of a Track 1-2 cycle is the initial configuration. The condition is checked as the \leftarrow pointer moves from right to left. In the correct initial configuration, the contents of Track 5 are $\leftarrow 1 \# * \rightarrow$, where $\#$ is the blank symbol. The state should be q_0 and the head should be pointing to the cell with the 1.

Throughout most of the discussion of the Turing Machine steps, we have combined the work tape (Track 5) and the witness tape (Track 6). However, the first of the two rules given below pertains to Tracks 1 and 5 only and implicitly acts as the identity on all other tracks. The third rule pertains to Tracks 1, 4, and 5:

$$h_{init} = \sum_{a \in \Gamma, x \in \Gamma - \{\#\}} \left| \begin{array}{cc} \leftarrow & \leftarrow \\ a & x \end{array} \right\rangle \left\langle \begin{array}{cc} \leftarrow & \leftarrow \\ a & x \end{array} \right| + \sum_{x \in \Gamma - \{1\}} \left| \begin{array}{cc} \leftarrow & \leftarrow \\ \leftarrow & x \end{array} \right\rangle \left\langle \begin{array}{cc} \leftarrow & \leftarrow \\ \leftarrow & x \end{array} \right| + \left| \begin{array}{cc} \leftarrow & \leftarrow \\ \leftarrow & 1 \end{array} \right\rangle \left\langle \begin{array}{cc} \leftarrow & \leftarrow \\ \leftarrow & 1 \end{array} \right|$$

After the 3 segment, the work tape will have the following form assuming that it started from a correct initial configuration at time 0:

$$\leftarrow (\sigma_A + \sigma_R)(\sigma_X)^T (\Gamma - \{\sigma_X, \sigma_A, \sigma_R\})^* \rightarrow$$

where $T = T(x, y)$. Recall that a well-formed Track 3 has the form $\leftarrow \oplus^* \rightarrow \oplus^* \otimes^* \rightarrow$ or $\leftarrow \oplus^* \leftarrow \oplus^* \otimes^* \rightarrow$ and the length is the number of \oplus or \otimes symbols. We add a penalty if there is any location in which Track 5 has a symbol from $\{\sigma_A, \sigma_R, \sigma_X\}$ and Track 3 does not have a symbol from $\{\oplus, \oplus, \rightarrow, \leftarrow\}$. Similarly, we add a penalty if there is any location in which Track 5 has a symbol that is not from $\{\sigma_A, \sigma_R, \sigma_X\}$ and Track 3 has a symbol from $\{\oplus, \oplus, \rightarrow, \leftarrow\}$. This effectively gives a penalty if the length of the Track 3 timer is anything other than $T(x, y)$. This condition will be checked by the 4-pointer as it moves from right to left. The rules apply to Tracks 1, 3, and 5:

$$h_{length} = \sum_{\substack{s \in \{\oplus, \oplus, \rightarrow, \leftarrow\} \\ a \notin \{\sigma_A, \sigma_R, \sigma_X\}}} \left| \begin{array}{cc} \leftarrow & \leftarrow \\ s & a \end{array} \right\rangle \left\langle \begin{array}{cc} \leftarrow & \leftarrow \\ s & a \end{array} \right| + \sum_{b \in \{\sigma_A, \sigma_R, \sigma_X\}} \left| \begin{array}{cc} \leftarrow & \leftarrow \\ \otimes & b \end{array} \right\rangle \left\langle \begin{array}{cc} \leftarrow & \leftarrow \\ \otimes & b \end{array} \right|$$

There is also a penalty if the Verifier V rejects on any of its computations. The left-most particle encodes the result of the verifier computations. The symbol will be σ_R if any of the verifier computations ended in a reject state. We wish to penalize rejecting computations.

$$h_V = \left| \begin{array}{cc} \leftarrow & \leftarrow \\ \leftarrow & \sigma_R \end{array} \right\rangle \left\langle \begin{array}{cc} \leftarrow & \leftarrow \\ \leftarrow & \sigma_R \end{array} \right|.$$

Finally, there is a penalty even for correct computations and clock configurations for every cycle for Tracks 1, 2, and 3. This cost is incurred whenever the left-moving 4-pointer reaches the left end of the chain and the

Lemma 2.44. [The Computation is Cyclic] Consider a sequence of clock steps from $|c_{T,s,p(N)-1}\rangle$ to $|c_{T,s+1,p(N)-1}\rangle$. If the computation tracks start out in a state $|\phi\rangle$, then the state of the computation tracks is unchanged at the end of the sequence of clock steps. That is, $p(N)$ clock steps applied to $|c_{T,s,p(N)-1}\rangle|\phi\rangle$ will result in the state $|c_{T,s+1,p(N)-1}\rangle|\phi\rangle$

Proof. Let P be a permutation applied to the computation tracks of two neighboring particles. The particles will be numbered from left to right 0 through $N - 1$, so the non-bracketed particles are 1 through $N - 2$. Applying P to particles i and $i + 1$ will be denoted $P^{(i,i+1)}$. In segments 1 and 2, each right-to-left sweep of the 1-pointer applies P_{BC} to every pair of particles: $P_{BC}^{(1,2)} P_{BC}^{(2,3)} \dots P_{BC}^{(N-3,N-2)}$. There are $N - 3$ sweeps in Segment 1 and one sweep in Segment 2, so the state of the computation tracks after Segment 2 will be:

$$(P_{BC}^{(1,2)} P_{BC}^{(2,3)} \dots P_{BC}^{(N-3,N-2)})^{N-2} |\phi\rangle$$

Segment 3 has $N - 2$ right-to-left in which P_{check} is applied to every pair of particles:

$$(P_{check}^{(1,2)} P_{check}^{(2,3)} \dots P_{check}^{(N-3,N-2)})^{N-2} (P_{BC}^{(1,2)} P_{BC}^{(2,3)} \dots P_{BC}^{(N-3,N-2)})^{N-2} |\phi\rangle$$

Then in Segment 5, there are $N - 2$ right-to-left sweeps in which $(P_{check})^\dagger$ is applied to every pair of particles, starting with $(1, 2)$ and ending with $(N - 3, N - 2)$, which results in the overall operation:

$$((P_{check}^{(N-3,N-2)})^\dagger \dots (P_{check}^{(2,3)})^\dagger (P_{check}^{(1,2)})^\dagger)^{N-2}$$

Finally, Segments 6 and 7 apply a total of $N - 2$ right-to-left sweeps in which $(P_{BC})^\dagger$ is applied to every pair of particles, resulting in:

$$((P_{BC}^{(N-3,N-2)})^\dagger \dots (P_{BC}^{(2,3)})^\dagger (P_{BC}^{(1,2)})^\dagger)^{N-2}$$

The net effect on the computation tracks is that they return to their original state $|\phi\rangle$. \square

Corollary 2.45. For any $0 \leq s < 2T + 1$ and any $0 \leq t < p(N)$, and $\phi \in C_N$, $p(N)$ transition steps applied to $|c_{T,s,t}\rangle|\phi\rangle$ will result in the state $|c_{T,s+1,t}\rangle|\phi\rangle$

2.6.2 Analysis of the Ground Energy

Let \mathcal{H}_{wf} denote the span of the bracketed well-formed clock configurations tensored with the C_N , the set of well-formed computation configurations on a chain of length N . It will be useful at this point to separate the state, head location, and work tape (Tracks 4 and 5) from the witness track (Track 6). We will denote a standard basis state in C_N as $|v\rangle|w\rangle$, where $|v\rangle$ is a standard basis state for Tracks 4 and 5, and $|w\rangle$ is a standard basis state for Track 6.

According to Lemmas 2.14 and 2.15, the configuration graph defined on the set of well-formed clock configurations consists of paths of relatively short length ($\leq p(N)$) and cycles of the correct clock states. We will first handle the the part of the Hilbert space in which the clock configuration is in one of these short paths. Let \mathcal{H}_{path} be the Hilbert space spanned by the states whose clock configuration is in a path in the configuration graph. $H_{N,prop}$ is the only term in the Hamiltonian that is not diagonal in the standard basis and $H_{N,prop}$ is closed on \mathcal{H}_{path} . Therefore, we can lower bound the the eigenvalues of H restricted to \mathcal{H}_{path} separately from the rest of the space.

Lemma 2.46. [Eliminating Incorrect Clock States] The lowest eigenvalue of H_N restricted to \mathcal{H}_{path} is at least $(1 - \cos(\pi/(2p(N) + 1)))$.

Proof. Let $|c_0\rangle, \dots, |c_l\rangle$ be the clock states in a path in the clock configuration graph. According to Lemma 2.15, $l \leq p(N) - 1$. Consider a state $|v\rangle|w\rangle$ for the computation tracks from C_N . Starting in state $|c_0\rangle|v\rangle|w\rangle$, after t applications of the transition function, the state of the system will be $|c_t\rangle|v'\rangle|w\rangle$, where $|v'\rangle$ is determined by (c_0, v, w, t) . We will call this state $|\phi(c_0, v, w, t)\rangle$, where $\phi(c_0, v, w, t) \in C_N$. Since the operations performed on the computation tracks are always permutations, the following set of states is orthonormal:

$$S(c_0) = \{|c_t\rangle|\phi(c_0, v, w, t)\rangle : \text{for } |v\rangle|w\rangle \in C_N, 0 \leq t \leq l\}.$$

The propagation term $H_{N,prop}$ is block diagonal on the space spanned by this set. Each block is specified by a choice of $|v\rangle|w\rangle$. If we express $H_{N,prop}$ in the standard basis, then each block is $l \times l$ and is the Laplacian of a path of length l .

The set $S(c_0)$ is the only set of states in the basis of \mathcal{H}_{wf} that has clock states $|c_0\rangle, \dots, |c_l\rangle$. Since the terms $H_{N,init} + H_{N,length} + H_{N,V}$ are diagonal in the standard basis, they are all closed on the span of $S(c_0)$. Since these terms are also positive semi-definite, we need only lower bound the smallest eigenvalue of $H_{N,prop} + H_{N,cl}$ on this space. According to Lemma 2.15, the final clock configuration in the path is illegal, which means that the upper-left element of the matrix will have an additional $+1$ from $H_{N,cl}$. According to Lemma 2.53, the smallest eigenvalue in this space is at least $(1 - \cos(\pi/(2p(N) + 1)))$. \square

We can now focus on the space of correct clock states: $|c_{T,s,t}\rangle$. According to Corollary 2.45, if the system starts out in state $|c_{T,s,0}\rangle|\phi\rangle$, where $\phi \in C_N$, then $p(N)$ steps later, the clock configuration will be $|c_{T,s+1,0}\rangle$ and the computation tracks will have returned to state $|\phi\rangle$. Therefore, if we fix the computation state to be some $|v\rangle|w\rangle$ at time $(0, 0)$, the state of the computation tracks at some time (s, t) , depends only on t and not on s or T . We will call this state $|\phi(v, w, t)\rangle$. Since the operations performed on the computation tracks are always permutations, the following set of states is orthonormal:

$$S_{cyc} = \{|c_{T,s,t}\rangle|\phi(p, w, t)\rangle : \text{for } |v\rangle|w\rangle \in C_N, \\ T \in \{0, \dots, N-3\}, s \in \{0, \dots, 2T\}, t \in \{0, \dots, p(N)-1\}\}.$$

Note that since the verifier V is classical, $|\phi(v, w, t)\rangle$ is also a classical standard basis state. The matrix for $H_{N,prop}$ expressed in the basis S is block diagonal. Each block is specified by a value for T and starting configuration $|v\rangle|w\rangle$ for the computation tracks. The block has dimension $(2T+1)p(N)$ and is $1/2$ times the Laplacian of a cycle of length $(2T+1)p(N)$. All other terms are diagonal in this basis.

We will refer to the correct starting configuration for Tracks 4 and 5 as $|v\text{-init}\rangle$. In this correct starting configuration, the contents of Track 5 are $\odot 1 \#^* \ominus$, the state on Track 4 is q_0 , and the head is at the same location as the 1 on Track 5.

There is a correct x for the length N of the chain. This is the string that is written on the computation track after M_{BC} runs for $N-2$ steps starting in $|v\text{-init}\rangle$. Once x is determined, the number m of queries to the oracle is also determined. The first m bits of the state of the witness track $|w\rangle$ is a string y which is used as the guesses for the responses to the oracle calls. Thus, once x and y are fixed (which are in turn determined by N and $|w\rangle$), the inputs to the oracles x_1, \dots, x_m are determined. In addition, the function $T(x, y)$ is also determined. Since the state of the witness track $|w\rangle$ does not change over time, the values of x_1, \dots, x_m and $T(x, y)$ are well-defined for a block. The verifier V will be run on the oracle queries for the casis in which the string y guesses that the query string is in L . Define the set

$$Y_{rej} = \{y \mid \text{for some } i \in [m], y_i = 1 \text{ and } x_i \notin L\}.$$

In order words, Y_{rej} is the set of oracle guesses for which there is at least one oracle call in which the guess is *yes* but the correct answer is *no*.

We will now partition S_{cyc} into four different sets and consider the subspace spanned by each set separately. The states from S_{cyc} will be put into one of the four sets in blocks. That is, each block is completely contained in one of the four sets.

S_1 consists of the states of the form $|c_{T,s,t}\rangle|\phi(v, w, t)\rangle$ in which $|v\rangle \neq |v\text{-init}\rangle$. These are the states from the blocks that do not start in the correct initial configuration.

S_2 consists of the states of the form $|c_{T,s,t}\rangle|\phi(p, w, t)\rangle$, where y is the string from the witness $|w\rangle$, such that $|v\rangle = |v\text{-init}\rangle$, but $T(x, y)$ is not equal to the length of Track 3 timer.

S_3 consists of the states of the form $|c_{T,s,t}\rangle|\phi(v, w, t)\rangle$ where y is the string from the witness $|w\rangle$, such that $|v\rangle = |v\text{-init}\rangle$, $T(x, y)$ is equal to the length of the Track 3 timer, and $y \in Y_{rej}$.

S_4 consists of the states of the form $|c_{T,s,t}\rangle|\phi(v, w, t)\rangle$ where y is the string from the witness $|w\rangle$, such that $|v\rangle = |v\text{-init}\rangle$, $T(x, y)$ is equal to the length of the Track 3 timer, and $y \notin Y_{rej}$.

$H_{N,prop}$ is closed on each S_i because the states from each block are completely contained in S_i or are disjoint from S_i . All of the other Hamiltonian terms besides $H_{N,prop}$ are all diagonal in the standard basis and are therefore diagonal on the basis S_{cyc} .

If $N = N(x)$ for some x , then starting with the correct input configuration $|v\text{-init}\rangle|w\rangle$, if we run the process M_{BC} for $N - 2$ steps followed by M_{check} for $N - 2$ steps, the contents of the work track should be $\text{OUT}(x, w, M, V)$, the same tape contents as M_{TV} on input (x, w) when it halts (See Figure 2). In order for the correct output to be produced, M_{check} needs to hit a final state within $N - 2$ steps and the computation needs to stay within the finite bounds of C_N . Lemmas 2.32 and 2.37 establish that there is an M_{TV} (used to form M_{check}) so that the correct output is in fact produced for most x . Throughout this section, the lemmas will assume that we the input x is *good* in this sense.

Lemma 2.47. [Eliminating States from $S_1, S_2,$ and S_3] *Suppose that the process $(M_{BC})^{N-2}$ followed by $(M_{check})^{N-2}$ starting in configuration $|v\text{-init}\rangle|w\rangle$ produces $\text{OUT}(x, w, M, V)$ on the work track. Then the smallest eigenvalue of H in the span of $S_1 \cup S_2 \cup S_3$, is at least $(1/8)(1 - \cos(\pi/(2p(N) + 1)))$.*

Proof. Since the terms are all closed on the spans of $S_1, S_2,$ and S_3 , we can lower bound each space separately. For a fixed $T, |v\rangle,$ and $|w\rangle$, consider the block defined by states of the form $|c_{T,s,t}\rangle|\phi(v, w, t)\rangle$. If $|v\rangle \neq |v\text{-init}\rangle$, then the configuration of Tracks 4 and 5 is not equal to $|v\text{-init}\rangle$ at time $(0, 0)$. Since the $\textcircled{5}$ does not alter Tracks 4 and 5 as it sweeps left, the state of Tracks 4 and 5 will not be equal to $|v\text{-init}\rangle$ for the preceding $N - 2$ time steps. There will be at least one point in time when the $\textcircled{8}$ is sweeping left that an illegal configuration from $H_{N,init}$ is hit. Call this time t' . Then for all s :

$$H_{N,init}|c_{T,s,t'}\rangle|\phi(v, w, t')\rangle = |c_{T,s,t'}\rangle|\phi(p, w, t')\rangle$$

Note that there may be more locations where an illegal configuration is reached but we need only consider one as the others can only increase the energy of a state. The diagonal matrix resulting from the 1's from those particular states at times (s, t') is 0 everywhere, except with a 1 at each location of the form $t' + s \cdot p(N)$, where $s \in \{0, \dots, 2T\}$. If we add this matrix to $H_{N,prop}$ which is $1/2$ times the Laplacian of a cycle graph of length $(2T + 1) \cdot p(N)$, then according to Lemma 2.55, the smallest eigenvalue of the sum of the matrices is at least $(1/8)(1 - \cos(\pi/(2p(N) + 1)))$. This reasoning can be applied to each block in the span of S_1 which gives a lower bound of $(1/8)(1 - \cos(\pi/(2p(N) + 1)))$ for any eigenvalue in this space.

A similar reasoning can be applied to the span of S_2 using the operator $H_{N,length}$. If a block is inside S_2 , then it is using the correct initial configuration $|v\text{-init}\rangle$ which produces the correct input x . Therefore the string y from the witness track and x determine the correct value $T(x, y)$ for the length of the clock on Track 3. This correct value is written in unary on the computation track at the end of the computation M_{TV} , which by assumption of the lemma corresponds to the contents of the work track after $(M_{BC})^{N-2}$ followed by $(M_{check})^{N-2}$ applied to $|v\text{-init}\rangle|w\rangle$. The contents of the track are $(\sigma_A + \sigma_R)(\sigma_X)^{T(x,y)}$. Since the first σ_A or σ_R symbol counts as a unary digit, the value encoded is $T(x, y) + 1$. The Track 1 pointer $\textcircled{4}$ will reach an illegal configuration if and only if the Track 3 clock does not have the correct length $T(x, y)$. As with the reasoning for S_1 , there may be more than one such violation, but we need only consider one that occurs regularly at times (s, t') for some fixed t' and $s \in \{0, \dots, 2T\}$. Since S_2 consists of those blocks in which the Track 3 timer has the incorrect length, the smallest eigenvalue of $H_{N,prop} + H_{N,length}$ in the span of S_2 will be at least $(1/8)(1 - \cos(\pi/(2p(N) + 1)))$.

A similar reasoning can be applied to the span of S_3 using the operator $H_{N,V}$. If a block is inside S_3 , then it is using the correct initial configuration $|v\text{-init}\rangle$ which produces the correct input x . Therefore the string y from the witness track and x determine the oracle queries x_1, \dots, x_m . If for any $i \in \{1, \dots, m\}$, $y_i = 1$ and $x_i \notin L$, the verifier will be run on input x_i and will reject, regardless of the string used as witness. By assumption of the lemma, the contents of the work track after the process $(M_{BC})^{N-2}$ followed by $(M_{check})^{N-2}$ starting in configuration $|v\text{-init}\rangle|w\rangle$ will be the correct output of M_{TV} on input (x, w) . This means that there will be an σ_R symbol written in the first location of the work tape after Segment 4. In this case, Track 1 pointer $\textcircled{4}$ will reach an illegal configuration:



Since S_3 consists of those blocks in which $y \in Y_{rej}$, the smallest eigenvalue of $H_{N,prop} + H_{N,V}$ in the span of S_3 will be at least $(1/8)(1 - \cos(\pi/(2p(N) + 1)))$. \square

Finally, we arrive at the space spanned by S_4 . It will be convenient to break up the witness $|w\rangle$ into a y , consisting of the first m bits and u consisting of the remaining $N - 4 - m$ bits. Define

$$S_{y,u} = \{|c_{T(x,y),s,t}\rangle|\phi(v\text{-init}, y, u, t)\rangle : 0 \leq s \leq 2T(x, y), 0 \leq t < p(N)\}$$

$S_{y,u}$ is the set of standard basis states for a single block, where the initial state is $|v\text{-init}\rangle|y\rangle|u\rangle$ and the Track 3 timer is the correct $T(x, y)$. Define S_y to be the union of $S_{y,u}$ over all possible u . Note that S_4 is the union of all S_y , where $y \notin Y_{rej}$. All of the terms in H are closed on the span of each $S_{y,u}$.

Lemma 2.48. [Smallest Eigenvalues for Blocks in S_4] *Suppose that the process $(M_{BC})^{N-2}$ followed by $(M_{check})^{N-2}$ starting in configuration $|v\text{-init}\rangle|w\rangle$ produces $\text{OUT}(x, w, M, V)$ on the work track. Let y be the first m bits of w , where m is the number of oracle queries made by M on input x . If $y \notin Y_{rej}$, then the minimum eigenvalue of the space spanned by S_y is exactly*

$$E(x, y) = \left(1 - \cos\left(\frac{\pi}{L+1}\right)\right),$$

where $L = (2T(x, y) + 1) \cdot p(N)$.

Proof. All of the terms in H except for $H_{N,prop}$, $H_{N,V}$, and $H_{N,final}$ are 0 on the entire space spanned by S_4 and are therefore 0 on any S_y such that $y \notin Y_{rej}$. Consider $H_{N,prop}$ restricted to the span of a particular $S_{y,u}$ and expressed in the $S_{y,u}$ basis. This matrix is $1/2$ times the Laplacian of a cycle of length $(2T(x, y) + 3) \cdot p(N)$. The term $H_{N,final}$ adds a $+1/2$ to two consecutive locations along the diagonal. Since $H_{N,V}$ is semi-positive definite, by Lemma 2.54, the smallest eigenvalue for this block is at least $E(x, y)$.

V is only run on those i such that $y_i = 1$. If $y \notin Y_{rej}$, we know that each such x_i is in L which means that there is a witness which will cause V to accept. Therefore, there is a u such that $H_{N,V}$ applied to every state in $S_{y,u}$ is 0. The lowest eigenvalue of H restricted to the space spanned by this $S_{y,u}$ is exactly the lowest eigenvalue of $H_{N,prop} + H_{N,final}$ restricted to this space, which by Lemma 2.54, is $E(x, y)$. \square

We are finally ready to establish that the smallest eigenvalue occurs within blocks S_y , where y is the set of correct oracle responses, which we refer to as \tilde{y} .

Lemma 2.49. [The Ground Energy Corresponds to Blocks with Correct Oracle Guesses] *Suppose that the process $(M_{BC})^{N-2}$ followed by $(M_{check})^{N-2}$ starting in configuration $|v\text{-init}\rangle|w\rangle$ produces $\text{OUT}(x, w, M, V)$ on the work track. The smallest eigenvalue for $H_N|_{\mathcal{H}_{br}}$ is $E(x, \tilde{y})$, where \tilde{y} are the correct oracle responses for input x .*

Proof. Recall that throughout the construction, we analyzed the smallest eigenvalue for H_N restricted to the space spanned by all bracketed states.

Note that since $\tilde{y} \notin Y_{rej}$, according to Lemma 2.48, there is an eigenvector whose eigenvalue is $E(x, \tilde{y})$, so we only need to show that every other eigenvalue is at least $E(x, \tilde{y})$.

The smallest eigenvalue of any state that is perpendicular to \mathcal{H}_{wf} is at least 1 from $H_{N,wf-cl}$ and $H_{N,wf-co}$. From Lemma 2.53, the smallest eigenvalue of any state in \mathcal{H}_{path} is at least $1 - \cos(\pi/(2p(N) + 1))$ which according to Claim 2.58 will always be larger than $E(x, y)$ for any y . By Lemma 2.47, the smallest eigenvalue of any state in the span of $S_1 \cup S_2 \cup S_3$ is at least $(1/8)(1 - \cos(\pi/(2p(N) + 1)))$ which according to Claim 2.58 will always be larger than $E(x, y)$ for any y . Therefore, the smallest eigenvalue for H will correspond to an eigenvector in the span of S_4 .

We will prove that if $y \neq \tilde{y}$, then the smallest eigenvalue of H restricted to the span of S_y is greater than $E(x, \tilde{y})$. Suppose that the first k bits of y are the same as the first k bits of \tilde{y} , but $y_{k+1} \neq \tilde{y}_{k+1}$. Note that the next oracle query x_{k+1} will be the same for y and \tilde{y} .

If $x_{k+1} \notin L$, then $\tilde{y}_{k+1} = 0$. If y matches \tilde{y} in the first k bits and has $y_{k+1} = 1$, then $y \in Y_{rej}$ which means that S_y is contained in S_3 and the smallest eigenvalue of H restricted to this space is larger than $E(x, y)$ for any y .

Now suppose that $x_{k+1} \in L$. Then $\tilde{y}_{k+1} = 1$. Consider a string y that matches \tilde{y} in the first k bits and has $y_{k+1} = 0$. The value of $T(x, y)$ for any such y must be at most:

$$T(x, y) = 2^m + 2^m \left[4^{m+1} + \sum_{j=k+2}^m 4^{m-j+1} + \sum_{j=1}^k \tilde{y}_j \cdot 4^{m-j+1} \right]$$

Meanwhile, the value of $T(x, \tilde{y})$ will be at least

$$T(x, \tilde{y}) = 2^m \left[4^{m+1} + 4^{m-k} + \sum_{j=1}^k \tilde{y}_j \cdot 4^{m-j+1} \right]$$

The lower bound for $T(x, \tilde{y})$ is larger than any $T(x, y)$, where y matches \tilde{y} in the first k bits and does not match \tilde{y} on bit $k+1$. Therefore $E(x, y) > E(x, \tilde{y})$ and the smallest eigenvalue for H restricted to S_y is greater than $E(x, \tilde{y})$. \square

2.6.3 Bracketed States and the Final Reduction

Throughout the construction, we have analyzed the Hamiltonian restricted to the space spanned by all bracketed states (\mathcal{H}_{br}). These states have the leftmost particle in state \ominus , right rightmost particle in state \oplus and none of the particles in between in state \ominus or \oplus . We now add an additional term to h to ensure that the ground state is in \mathcal{H}_{br} . We will denote a basis of the d -dimensional particles by $|\ominus\rangle, |\oplus\rangle$, and $|1\rangle, \dots, |d-2\rangle$. Let

$$\bar{h} = h + \sum_{j=1}^{d-2} \frac{1}{4} (|j\rangle\langle j| \otimes I + I \otimes |j\rangle\langle j|) + I \otimes |\ominus\rangle\langle \ominus| + |\oplus\rangle\langle \oplus| \otimes I$$

Let \bar{H}_N denote the Hamiltonian resulting from applying \bar{h} to each pair of neighboring particles in a chain of length N .

Lemma 2.50. $\lambda_0(\bar{H}_N) = \lambda_0(H_N|_{\mathcal{H}_{br}}) + \frac{N-2}{2}$

Proof. The first two terms in \bar{h} give a $1/4$ penalty to each end particle if it is not in a bracket states and $1/2$ penalty to each middle particle if it is not in a bracket state. The next two terms cause a penalty of $+1$ for any pair with a \ominus on the right and a $+1$ for any pair with a \oplus on the left.

Since \bar{H}_N is closed on \mathcal{H}_{br} and \mathcal{H}_{br}^\perp , we can consider each space separately. We will first consider the energy penalty from the additional terms in \bar{h} . The bracketed states will have an additional energy of exactly $(N-2)/2$ from the additional terms, since they add $1/2$ for every particle, except the two at the ends. Therefore, the lowest energy of any state in \mathcal{H}_{br} will be $(N-2)/2 + \lambda_0(H_N|_{\mathcal{H}_{br}}) < (N-2)/2 + 1/4$. Note that the bound in Lemma 2.49, on $\lambda_0(H_N|_{\mathcal{H}_{br}})$ is less than $1/4$ for any $N \geq 4$.

Consider a state which is not bracketed. We will only consider the energy from the additional terms which will give a lower bound for the energy for the state. If the particle on the left is not in state \ominus , then replacing it with \ominus will cause the energy to go down by at least $1/4$. Similarly, If the particle on the right is not in state \oplus , then replacing it with \oplus will cause the energy to go down by at least $1/4$. If there is a particle in a bracketed state in the middle, replacing it with a non-bracketed state will cause the energy to go down by at least $1/2$. The process can be repeated until the state is bracketed at which point the energy from the additional terms will be exactly $(N-2)/2$. Therefore any non-bracketed configuration will have energy at least $(N-2)/2 + 1/4$. \square

We are finally ready to put the pieces together to prove that FUNCTION-TIH is hard for FP^{NEXP} .

Theorem 2.51. [FUNCTION-TIH is hard for FP^{NEXP}] *For any $f \in \text{FP}^{\text{NEXP}}$, there is a Hamiltonian h that operates on two d -dimensional particles. Let H_N denote the Hamiltonian on a chain of N d -dimensional particles resulting from applying h to each neighboring pair in the chain. There is a polynomial time computable function $N(x)$ and polynomial $q = 32N^4 p(N)^4 = O(N^{12})$ such that, the value of $f(x)$ can be computed in time polynomial in $|x|$, given a value E such $|E - \lambda_0(H_N)| \leq 1/q(N)$.*

Proof. We have shown a construction for h based on the Turing Machine M that computes $f(x)$ and the TM V that is the verifier for the oracle language L in NEXP. The function N is the function given in Definition 2.28. By Lemma 2.49, if $N = N(x)$ for some string x and for every $w \in \{0, 1\}^{N-4}$, the process $(M_{BC})^{N-2}$ followed by $(M_{check})^{N-2}$ starting in configuration $|v\text{-init}\rangle|w\rangle$ produces $\text{OUT}(x, w, M, V)$ on the work track, then the ground energy of $H_N|_{\mathcal{H}_{br}}$ is

$$E(x, \tilde{y}) = \left(1 - \cos \left(\frac{\pi}{L+1} \right) \right),$$

where $L = (2T(x, \tilde{y}) + 1) \cdot p(N)$ and \tilde{y} is the string denoting the correct oracle responses on input x . Lemma 2.50 establishes that the state corresponding to the ground energy is in \mathcal{H}_{br} .

Lemmas 2.32 and 2.37 together establish that there is a Turing Machine M_{TV} that results in Turing Machine M_{check} such that for all but a finite set of x 's, it is in fact the case that for $N = N(x)$ and for every $w \in \{0, 1\}^{N-4}$, the process $(M_{BC})^{N-2}$ followed by $(M_{check})^{N-2}$ starting in configuration $|v\text{-init}\rangle|w\rangle$ produces $\text{OUT}(x, w, M, V)$ on the work track. Lemma 2.42 establishes that each right-to-left sweep of the pointer for Segments 1, 2, and 3 executes one step of the TM corresponding to the operation P applied to the computation tracks. The conditions of the lemma are satisfied since Lemma 2.37 allows us to assume that the head of the Turing Machine stays within the sequence of locations from 1 through $N - 3$. Segment 1 and 2 together apply $N - 2$ steps of M_{BC} and Segment 3 applies $N - 2$ steps of M_{check} . For the finite set of x for which the construction does not work, a finite look-up table can be used to determine $f(x)$.

For the other x 's, suppose you are given a value E where $|E - E(x, \tilde{y})| < 1/2N^4p(N)^4$. We will show that the value of $f(x, \tilde{y}) = f(x)$ can be computed in polynomial time. According to Claim 3.13, if L and L' are distinct positive integers, then

$$\left| \cos\left(\frac{\pi}{L+1}\right) - \cos\left(\frac{\pi}{L'+1}\right) \right| \geq \frac{1}{L^4}.$$

Therefore, the value of L is uniquely determined, given a value E such that $|E - E(x, \tilde{y})| \leq 1/2L^4$, where $L = (2T(x, \tilde{y}) + 1) \cdot p(N)$. Note that in order for the construction to work, $T(x, y)$ must be written in unary on the work tape, which means that $T(x, y) \leq N - 2$. Therefore, $L \leq 2Np(N)$, and as long as the estimate is within $32N^4p(N)^4$ of the true ground energy, L can be uniquely recovered.

Given E , the value of integer L can be found by binary search in time $O(\log L)$. Since the value of N is known, then $T(x, \tilde{y})$ can be recovered. The low order bits in the binary representation of $T(x, \tilde{y})$ are exactly $f(x, \tilde{y})$. The value of all the numbers in the calculations are polynomial in N and therefore take time polynomial in $\log N$, which by Lemma 2.30 is polynomial in $|x|$. \square

2.6.4 Eigenvalue Bounds

This section contains proofs for the bounds on the smallest eigenvalues of various matrices used in the construction. The end of the section contains a discussion of how these bounds relate to each other for the values of the variables that arise in the construction.

Let C_L be the propagation matrix for a matrix for a cycle of length L . Note that C_L is $1/2$ times the Laplacian matrix for a cycle of length L . Let P_L denote the propagation matrix for a path of length L . We will number the rows and columns of an $L \times L$ matrix with indices 0 through $L - 1$.

Definition 2.52. [Periodic Diagonal Matrix] For positive integers r and s , and $l \in \{0, \dots, s-1\}$, let $D_{r,s,l}$ be a $rs \times rs$ diagonal matrix which is zero everywhere except that the diagonal entries are $+1$ at locations $l + ks$ for $k \in \{0, \dots, r-1\}$.

Note that the matrix $D_{1,L,l}$ is zero everywhere, except for $+1$ in location l on the diagonal.

Lemma 2.53. [Smallest Eigenvalue for the Path Graph Plus a $1/2$ Penalty] The smallest eigenvalue for $P_L + D_{1,L,0}$ is at least

$$\left(1 - \cos\left(\frac{\pi}{2L+1}\right)\right)$$

Proof. [12] show that the smallest eigenvalue of $P_L + \frac{1}{2}D_{1,L,0}$ is exactly

$$\left(1 - \cos\left(\frac{\pi}{2L+1}\right)\right).$$

Since the $D_{1,L,0}$ is positive semi-definite, the smallest eigenvalue of $P_L + \frac{1}{2}D_{1,L,0}$ is a lower bound for the smallest eigenvalue of $P_L + D_{1,L,0}$. The lemma follows. \square

Lemma 2.54. [Smallest Eigenvalue for the Cycle Graph Plus Two $1/2$ Penalties] The smallest eigenvalue of $C_L + \frac{1}{2}D_{1,L,l} + \frac{1}{2}D_{1,L,l+1} \bmod L$ is exactly

$$\left(1 - \cos\left(\frac{\pi}{L+1}\right)\right).$$

Proof. It is sufficient to prove the lemma for $l = L - 1$ due to the dihedral symmetry of the cycle. A vector $\langle u_0, \dots, u_{L-1} \rangle$ is an eigenvector of $C_L + \frac{1}{2}D_{1,L,l} + \frac{1}{2}D_{1,L,l+1} \bmod L$ with eigenvalue λ if the following constraints are satisfied:

$$\frac{1}{2}(u_{L-1} + u_1) = \left(\frac{3}{2} - \lambda\right) u_0 \quad (22)$$

$$\frac{1}{2}(u_{k-1} + u_{k+1}) = (1 - \lambda) u_k \quad \text{for } k = 1, \dots, L - 2 \quad (23)$$

$$\frac{1}{2}(u_{L-2} + u_0) = \left(\frac{3}{2} - \lambda\right) u_{L-1} \quad (24)$$

Any vector of the form $u_k = e^{i(k+1)\theta} - e^{-i(k+1)\theta}$ satisfies the constraints in (23) for $\lambda = 1 - \cos \theta$. Let $\omega = e^{\pi i/(L+1)}$. Define vector \vec{u}_j to have entries $u_{jk} = \omega^{(j+1)(k+1)} - \omega^{-(j+1)(k+1)}$. Using the identity that $\omega^L = -\omega^{-1}$, it can be verified that \vec{u}_j also satisfies (22) and (24) when $\lambda_j = 1 - \cos(\pi(j+1)/(L+1))$ for $j \in \{0, \dots, L-1\}$. This gives L distinct eigenvalues for $C_L + \frac{1}{2}D_{1,L,l} + \frac{1}{2}D_{1,L,l+1} \bmod L$, the smallest of which occurs when $j = 0$. \square

Lemma 2.55. [Smallest Eigenvalue Lower Bound for the Cycle Graph Plus a Periodic Penalty] *If $L = rs$, then the smallest eigenvalue of $C_L + D_{r,s,l}$ is at least*

$$\frac{1}{8} \left(1 - \cos \left(\frac{\pi}{2s+1} \right) \right)$$

We will need the following claim in the proof of Lemma 2.55. First we need to define the Fourier basis vectors:

$$|f_k\rangle = \frac{1}{\sqrt{L}} \sum_{j=0}^{L-1} \omega^{jk} |j\rangle,$$

where $\omega = e^{2\pi i/L}$ is the L^{th} root of unity.

Claim 2.56. *Let $L = rs$. Then $\langle f_k | D_{r,s,0} | f_j \rangle = 1/s$ if $k \bmod r = j \bmod r$, and $\langle f_k | D_{r,s,l} | f_j \rangle = 0$ otherwise.*

Proof of Claim 2.56. For the purposes of this proof, let $D = D_{r,s,0}$. The a^{th} entry along the diagonal is 1 if and only if $a = xs$ for $x \in \{0, \dots, r-1\}$. Therefore

$$D|f_j\rangle = \frac{1}{\sqrt{L}} \sum_{k=0}^{r-1} \omega^{jxs} |xs\rangle = \frac{1}{\sqrt{L}} \sum_{k=0}^{r-1} \omega^{jxs} |xs\rangle.$$

Suppose that $j = yr + m$, where $m = j \bmod r$. Since $L = rs$ and ω is the L^{th} root of unity,

$$\omega^{jxs} = \omega^{(yr+m)xs} = \omega^{yxr s} \cdot \omega^{xsm} = \omega^{xsm}.$$

Therefore $D|f_j\rangle = 1/\sqrt{L} \sum_{k=0}^{r-1} \omega^{mks} |xs\rangle$. Similarly $\langle f_k | D = 1/\sqrt{L} \sum_{k=0}^{r-1} \omega^{-nxs} \langle xs|$, where $n = k \bmod r$.

$$\langle f_k | D | f_j \rangle = \frac{1}{L} \sum_{k=0}^{r-1} \omega^{(m-n)xs}.$$

Since $L = rs$, ω^s is the r^{th} root of unity. Therefore, the above is 0 if $m \neq n$ and is equal to $r/L = 1/s$ if $m = n$. \square

Proof of Lemma 2.55. It is sufficient to prove the lemma for $l = 0$ due to the dihedral symmetry of the cycle. Let $D_{r,s,0} = D$. We will use L to denote the size of the matrix: $L = rs$.

Suppose we express a state $|\phi\rangle$ in the Fourier basis: $\sum_{j=0}^{L-1} \alpha_j |f_j\rangle$. By Claim 2.56,

$$\langle \phi | D | \phi \rangle = \frac{1}{s} \sum_{x=0}^{r-1} \sum_{j=0}^{s-1} \sum_{k=0}^{s-1} \alpha_{kr+x}^* \alpha_{j+r+x}.$$

This means that D is block-diagonal in the Fourier basis. Each block is an $s \times s$ matrix, corresponding to a particular value for x , and is $1/s$ times the all 1's matrix. Let O_s be the $s \times s$ matrices of all 1's. D expressed in the Fourier basis and restricted to the set $S_x = \{|f_x\rangle, |f_{r+x}\rangle, \dots, |f_{(s-1)r+x}\rangle\}$ is exactly $(1/s)O_s$. Meanwhile C_L is diagonal in the Fourier basis. When restricted to S_x , the k^{th} entry along the diagonal is $1 - \cos(2\pi(kr + x/L))$. Call this matrix F_x . We will first show that for all x , $F_x \succeq (1/4)F_0$, where \succeq means that every element along the diagonal of F_x is greater than or equal to the corresponding element in $(1/4)F_0$. Then it will be sufficient the lower bound $\lambda_0((1/s)O_s + (1/4)F_0)$.

To show $F_x \succeq (1/4)F_0$, we first consider the case that $x \leq r/2$. We will rotate each angle $2\pi(kr + x)/L$ by $-2\pi x/L$. That is, $1 - \cos(2\pi(kr + x)/L)$ is replaced by $1 - \cos(2\pi(kr)/L)$ in the k^{th} entry along the diagonal. The resulting matrix is F_0 . We will show for each entry, that the new value is at most 4 times the old value. For $0 \leq k < s/2$, $2\pi(kr + x)/L < \pi$ and the new value is less than the old value. For $s/2 \leq k < s$, then $1 - \cos(2\pi(kr + x/L)) = 1 - \cos(2\pi((s-k)r - x/L))$ is replaced by $1 - \cos(2\pi((s-k)r/L))$. Note that $s-k$ is positive and $x \leq r/2$, so the new angle $2\pi(s-k)r/L$ is at most twice the original angle $2\pi((s-k)r - x)/L$. Using the half angle formula for \cos , it can be verified that $1/4(1 - \cos \theta) \leq (1 - \cos(\theta/2))$.

A symmetric argument can be applied if $r > x > r/2$, except that $1 - \cos(2\pi(kr + x)/L)$ is replaced by $1 - \cos(2\pi((k+1)r)/L)$, which is a rotation by $2\pi(r-x)/L$. The resulting matrix is \tilde{F}_0 , which is the same as F_0 , except that the diagonal entries are rotated by one location so that the $(L-1)^{\text{st}}$ entry is $1 - \cos(2\pi sr/L) = 0$. Since O_s is invariant under permutations of the rows and columns, the entries of the new matrix can be rotated back to form F_0 . Thus the eigenvalues of $(1/s)O_s + (1/4)F_0$ are the same as the eigenvalues of $(1/s)O_s + (1/4)\tilde{F}_0$.

Our task now is to lower bound $\lambda_0((1/s)O_s + (1/4)F_0)$. Let U_s denote the unitary to change from the standard to the Fourier basis on a matrix of size $s \times s$. If we change F_0 back to the standard basis, we just get the cycle graph on s vertices: $(U_s)^{-1}F_0U_s = C_s$. Meanwhile if we apply the change of basis to $(1/s)O_s$, we get $D(1, s, 0)$, the all 0's matrix with one +1 entry in the upper left corner. Therefore, we can lower bound $\lambda_0(D(1, s, 0) + (1/4)C_s)$ instead. Suppose that there is a $|\phi\rangle$ such that $\langle \phi | D(1, s, 0) + C_s | \phi \rangle = c$. The vector $|\phi\rangle$ when expressed in the standard basis is $\sum_{j=0}^{s-1} \alpha_j |j\rangle$. Let $|\tilde{\phi}\rangle$ be the length $2s$ vector obtained by doubling each entry from $|\phi\rangle$:

$$|\tilde{\phi}\rangle = \sum_{j=0}^{s-1} \frac{\alpha_j}{\sqrt{2}} (|2j\rangle + |2j+1\rangle).$$

We claim that

$$\langle \tilde{\phi} | (1/2)D(1, 2s, 0) + (1/2)D(1, 2s, 1) + C_{2s} | \tilde{\phi} \rangle = \frac{c}{2}.$$

To see why this claim is true, consider partitioning the matrix $(1/2)D(1, 2s, 0) + (1/2)D(1, 2s, 1) + C_{2s}$ into $s^2 2 \times 2$ submatrices. Let M_{jk} be the submatrix at the intersection of rows $2j$ and $2j+1$ and columns $2k$ and $2k+1$. Let E_{jk} be the entry in row j and column k in $D_{1,s,0} + C_s$. The key observation is that the sum of the entries in M_{jk} is equal to E_{jk} . Then

$$\begin{aligned} \frac{1}{2} \langle \phi | D_{1,s,0} + C_s | \phi \rangle &= \frac{1}{2} \sum_{jk} \alpha_j^* \alpha_k E_{jk} \\ &= \sum_{jk} \begin{pmatrix} \alpha_j/\sqrt{2} \\ \alpha_j/\sqrt{2} \end{pmatrix} M_{jk} \begin{pmatrix} \alpha_k/\sqrt{2} & \alpha_k/\sqrt{2} \end{pmatrix} \\ &= \langle \tilde{\phi} | (1/2)D(1, 2s, 0) + (1/2)D(1, 2s, 1) + C_{2s} | \tilde{\phi} \rangle \end{aligned}$$

Putting all the bounds together, we get that

$$\begin{aligned}
\lambda_0(C_L + D(r, s, l)) &= \max_x \{\lambda_0((1/s)O_s + F_x)\} \\
&\geq \lambda_0((1/s)O_s + (1/4)F_0) \\
&\geq \frac{1}{4}\lambda_0((1/s)O_s + F_0) \\
&= \frac{1}{4}\lambda_0(D(1, s, 0) + C_s) \\
&\geq \frac{1}{8}\lambda_0((1/2)D(1, 2s, 0) + (1/2)D(1, 2s, 1) + C_{2s}) = \frac{1}{8} \left(1 - \cos\left(\frac{\pi}{2s+1}\right)\right)
\end{aligned}$$

The first equality follows from expressing $C_L + D(r, s, l)$ and observing the block diagonal structure. The second inequality follows from the argument that for all x , $F_x \geq (1/4)F_0$ by rotating the angles by $2\pi x/rs$. Line 3 to 4 above follows from rotating from the Fourier basis back to the standard basis. The last equality follows from Lemma 2.54. \square

Lemma 2.55 is used to give a lower bound for computations that have a periodic cost occurring every $p(N)$ time steps. Lemma 2.54 gives an exact expression for the smallest eigenvalue corresponding to correct computations. Thus, we need to establish that the bound given in Lemma 2.54, which is applied for $L = (2T(x, y) + 3)p(N)$ is always smaller than the lower bound from Lemma 2.55, which is applied for $s = p(N)$.

First, we will need the following fact:

Fact 2.57. For $0 \leq \theta < 1$ and $c \geq 1$,

$$\left(1 - \cos\left(\frac{\theta}{c}\right)\right) \leq \frac{2}{c^2}(1 - \cos \theta).$$

Proof. We will show that

$$\frac{c^2}{2} \leq \frac{1 - \cos \theta}{1 - \cos(\theta/c)}.$$

Using the Taylor expansion for \cos , we have that $1 - \cos \gamma = \sum_{j=1}^{\infty} (-1)^{j+1} \frac{\gamma^{2j}}{(2j)!}$. We will show that for each pair of consecutive terms, the ratio is at least $c^2/2$:

$$\frac{\theta^{2x}}{(2x)!} - \frac{\theta^{2x+2}}{(2x+2)!} \geq \frac{c^2}{2} \left[\frac{(\theta/c)^{2x}}{(2x)!} - \frac{(\theta/c)^{2x+2}}{(2x+2)!} \right],$$

for $x \geq 1$. This is equivalent to showing that

$$1 - a \geq \frac{1}{2c^{2x-2}} - \frac{a}{2c^{2x}},$$

where $a = \theta^2/(2x+2)(2x+1)$. Using the fact that $0 \leq a < 1/4$ and $c \geq 1$:

$$1 - a \geq \frac{3}{4} \geq \frac{1}{2} - \frac{a}{2c^{2x}} \geq \frac{1}{2c^{2x-2}} - \frac{a}{2c^{2x}}.$$

\square

Claim 2.58. For any x and y and $N \geq 4$,

$$\left(1 - \cos\left(\frac{\pi}{(2T(x, y) + 1)p(N) + 1}\right)\right) < \frac{1}{8} \left(1 - \cos\left(\frac{\pi}{2p(N) + 1}\right)\right).$$

Proof. Since $N \geq 4$, $p(N) = 4(N-2)(2N-3) \geq 40$. For any x and y , $T(x, y) \geq 4$. Note that m in the definition of $T(x, y)$ is the number of oracle calls made by Turing Machine M on input x and $T(x, y)$ is always at least 2^{3m+2} . Therefore, even when $m = 0$, $T(x, y) = 4$.

$$\left(1 - \cos\left(\frac{\pi}{(2T(x, y) + 1)p(N) + 1}\right)\right) \leq \left(1 - \cos\left(\frac{\pi}{9p(N) + 1}\right)\right)$$

Since $p(N) \geq 40$, we know that $\pi/(2p(N) + 1) < 1$ and $(9p(N) + 1)/(2p(N) + 1) > 4$. Applying Fact 2.57,

$$\left(1 - \cos\left(\frac{\pi}{9p(N) + 1}\right)\right) < \frac{2}{4^2} \left(1 - \cos\left(\frac{\pi}{2p(N) + 1}\right)\right) \leq \frac{1}{8} \left(1 - \cos\left(\frac{\pi}{2p(N) + 1}\right)\right).$$

The bound in the Lemma follows. \square

3 Computing the Ground Energy Density in the Thermodynamic Limit

The parameters of the problem in the thermodynamic limit (not the instance) include two $d^2 \times d^2$ Hermitian matrices h_a^{row} and h_a^{col} denoting the energy interaction between two neighboring particles in the horizontal and vertical directions on a 2-dimensional grid. The dimension of each individual particle is a constant d . Then $H_a(N)$ is defined to be the Hamiltonian of an $N \times N$ grid of d -dimensional particles in which h_{row} is applied to each neighboring pair in the horizontal direction and h^{col} is applied to each neighboring pair in the vertical direction. $\lambda_0(H_a(N))$ is the ground energy of $H_a(N)$. The ground energy density of (h_a^{row}, h_a^{col}) in the thermodynamic limit is defined to be:

$$\alpha_0(h_a^{row}, h_a^{col}) = \lim_{N \rightarrow \infty} \frac{\lambda_0(H_a(N))}{N^2}.$$

When it is clear from context, we will drop the subscript a denoting the particular Hamiltonian terms, in which case α_0 denotes the ground energy density of h^{row} and h^{col} in the thermodynamic limit. We can assume that the Hamiltonian terms are scaled so that $0 \leq \alpha_0 \leq 1$. The problem itself will be characterized by h^{row} and h^{col} . Here is the function version of the ground energy density (GED) problem:

FUNCTION-GED FOR (h^{row}, h^{col})

Input: An integer n expressed in binary.

Output: A number α such that $|\alpha - \alpha_0| \leq 1/2^n$.

The following theorem encapsulates our results for Function-GED in the thermodynamic limit:

Theorem 3.1. *Function-GED problem is contained in $FEXP^{QMA-EXP}$ and is hard for $FEXP^{NEXP}$.*

3.1 Existence of the Limit

Before proceeding to the complexity results, it is important to establish that the quantity α_0 that we are trying to approximate always exists.

Lemma 3.2. *The limit $\alpha_0(h^{row}, h^{col}) = \lim_{N \rightarrow \infty} \frac{\lambda_0(H_N)}{N^2}$ always exists.*

Proof. We can apply an additive offset to h^{row} and h^{col} , so that $h^{row} \geq 0$ and $h^{col} \geq 0$. Let e_{max} be a constant such that $\|h^{row}\| \leq e_{max}$ and $\|h^{col}\| \leq e_{max}$. We will show that for any $\epsilon > 0$, there is a positive integer N_0 and an interval of size ϵ that contains $\lambda_0(H_N)/N^2$ for every $N \geq N_0$.

Fix a positive integer \hat{N} . Let $N_0 = (\hat{N})^2$ and let α denote $\lambda_0(H_{\hat{N}})/(\hat{N})^2$. The value of \hat{N} will be chosen at the end to obtain the desired ϵ . For any $N \geq N_0$, let $q = \lfloor N/\hat{N} \rfloor$ and $r = N \bmod \hat{N}$. The three facts that we will need about these variables are that $N - r = q\hat{N}$, $q/\hat{N} \leq 1/\hat{N}$, and $r/\hat{N} \leq 1/\hat{N}$.

An $N \times N$ grid can be packed with q^2 disjoint $\hat{N} \times \hat{N}$ sub-grid. The energy of the adjacent pairs of particles of tiles within a single $\hat{N} \times \hat{N}$ sub-grid is at least $\alpha \cdot (\hat{N})^2$. Therefore the energy density across the entire $N \times N$ grid will be

$$\begin{aligned} \frac{\lambda_0(H_N)}{N^2} &\geq \frac{q^2 \cdot \alpha \cdot (\hat{N})^2}{N^2} = \frac{\alpha(N - r)^2}{N^2} \\ &\geq \frac{\alpha N^2 - 2rN}{N^2} = \alpha - \frac{2r}{N} \geq \alpha - \frac{c}{\hat{N}}. \end{aligned}$$

To get an upper bound on $\lambda_0(H_N)/N^2$, consider the state that is a $q \times q$ tensor product of the ground state for each $\hat{N} \times \hat{N}$ sub-grid. The particles that are not contained in an $\hat{N} \times \hat{N}$ sub-grid will be set to $|0\rangle$. The

cost due to adjacent pairs of particles where both particles are contained in a single $\hat{N} \times \hat{N}$ sub-grid is at most $\lambda_0(H_{\hat{N}})$. Therefore the total cost due to all pairs of adjacent tiles where both particles are contained in the same $\hat{N} \times \hat{N}$ sub-grid is at most $\alpha \cdot q^2(\hat{N})^2 \leq \alpha N^2$.

There are at most $4\hat{N}$ pairs of adjacent particles that span the boundary of a particular $\hat{N} \times \hat{N}$ sub-grid. The total cost due to pairs of adjacent particles that span the boundary of any of the $\hat{N} \times \hat{N}$ sub-grids is at most $e_{max} \cdot q^2 \cdot 4\hat{N} \leq 4qe_{max}N$.

The number of grid locations in the N^2 grid that are not contained in any of the $\hat{N} \times \hat{N}$ sub-grids is

$$N^2 - q^2(\hat{N})^2 = N^2 - (N - r)^2 \leq 2rN.$$

Each particle is adjacent to at most 4 other particles, so the total cost due to adjacent pairs of particles where both tiles are outside all of the $\hat{N} \times \hat{N}$ sub-grids is at most $8rNe_{max}$. Putting the three upper bounds together, we get that

$$\begin{aligned} \frac{\lambda_0(H_N)}{N^2} &\leq \frac{\alpha N^2 + 4qNe_{max} + 8rNe_{max}}{N^2} \\ &= \alpha + \frac{4qe_{max}}{N} + \frac{8re_{max}}{N} \leq \alpha + \frac{4e_{max} + 8e_{max}}{\hat{N}} \end{aligned}$$

We have shown that $\lambda_0(H(N))/N^2$ lies in the interval between $\alpha - 2/\hat{N}$ and $\alpha + 12e_{max}/\hat{N}$. Since e_{max} is a constant, \hat{N} can be chosen so that $(12e_{max} + 2)/\hat{N} \leq \epsilon$ \square

3.2 Containment

We will use binary search to show that Function-GED is contained in $\text{FEXP}^{\text{NEXP}}$ as we did in the finite case for the problem but we first need to define a decision version of the problem (which we will call Decision-GED) to use in the binary search.

DECISION-GED FOR (h^{row}, h^{col})

Input: A number $\alpha \in [0, 1]$, specified with n bits.

Output: Accept if $\alpha_0 \leq \alpha$ and Reject if $\alpha_0 \geq \alpha + 1/2^n$.

Claim 3.3. *Decision-GED is contained in QMA-EXP*

The claim follows from Theorem 2.7 from [16] which shows that Decision-GED is complete for QMA-EXP when the two Hamiltonian terms (h^{row}, h^{col}) are given as part of the input along with α . This implies that the version in which the Hamiltonian terms are fixed for the problem (and therefore of constant size) and the input consists only of α , is also contained in QMA-EXP.

The algorithm to compute the Function-GED in $\text{FEXP}^{\text{QMA-EXP}}$ uses the same binary search procedure used for the finite version of the problem given in Figure 1, except with Decision-GED instead of Decision-TIH. The number of rounds is chosen to be n so that the final precision is $1/2^n$.

3.3 Hardness: Overview of the Reduction

The construction from the finite case must be adapted in a few ways to work for the infinite grid. Those changes are described in Section 3.6. For now, we will call this modified Hamiltonian term h_C and show how h_C is used for the construction for the infinite grid. We will layer h_C on top of the constraints of a Robinson tiling. If the constraints of the Robinson tiling are satisfied, then the infinite grid will be tiled with an infinite sequence of squares of size 4^k for every k . The density of squares of size 4^k is $1/4 \cdot 4^{2k}$. Then h_C is applied to every pair of particles in the horizontal direction on the top edge of each square.

We will start with a function f computed by an exponential time Turing Machine M with access to an oracle in NEXP. The language computed by the oracle will be called L , and V will denote the exponential time verifier for L . The input to the function f is a string x , where $|x| = n$.

We assume without loss of generality that if the first bit of x is 0, then $f(x) = 0$. If f does not have this property, then we can define a new function f' such that $f'(0x) = 0$ and $f'(1x) = f(x)$. Any polynomial time

algorithm to compute f' can be used to compute f . This allows us to refer to the value of input string x which is just the number represented by x in binary. Here is a formal statement of the hardness result which we will prove:

Theorem 3.4. *For any $f \in FEXP^{NEXP}$, there is a polynomial q , constant d , and interaction terms h^{row} and h^{col} that operate on pairs of d -dimensional particles, such that if α_0 is the energy density of h^{row} and h^{col} in the thermodynamic limit, then for all but a finite number of x 's, it is possible in time polynomial in $2^{|x|}$, to compute $f(x)$ given a value α , where $|\alpha - \alpha_0| \leq 1/2^{q(x)}$. $q(x)$ is the value of the polynomial q on the binary number x .*

3.4 Robinson Tiling

The Hamiltonian for the infinite case will have two different layers. The lower layer uses constraints that impose a quasi-periodic tiling of the infinite plane. A tiling can be seen as a classical Hamiltonian in which there are a finite number of tile types corresponding to classical basis states for a particle. A tiling system also has rules governing the cost of placing two tiles next to each other in the horizontal or vertical direction. These correspond to Type 1 terms in the Hamiltonian that impose an energy penalty for two neighboring particles in a particular pair of standard basis states. The tiling rules devised by Robinson [21] impose a structure on the infinite plane as shown in Figure 13. The essential feature of the tiling is that it has an infinite sequence of

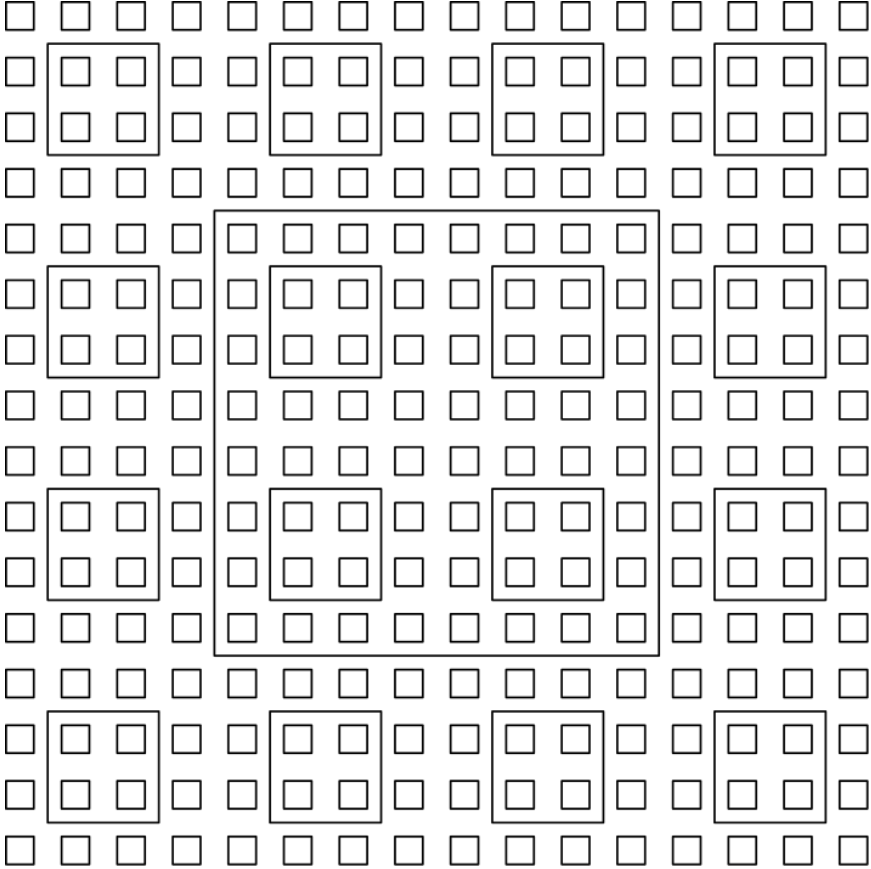


Figure 13: A low energy Robinson tiling of the plane.

interlocking squares of increasing size. The *size* of a square refers to the length of one of the sides. In the case of the Robinson tiles, the squares have size 4^k for $k \in \mathbb{Z}^+$. The density of squares of size 4^k is $1/4^{2k+1}$. A 4×4 square from a Robinson tiling is show in Figure 14.

Cubitt, Perez-Garcia, and Wolf were the first to make use of quasi-periodic tilings of the infinite plane in the context of Hamiltonian complexity [11]. We use this same idea to layer the 1D Hamiltonian used in the

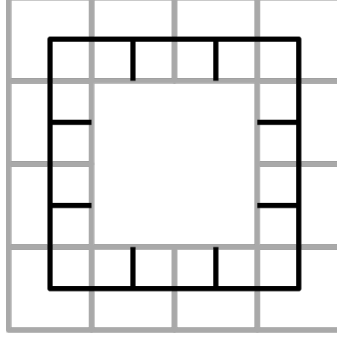


Figure 14: A 4×4 square in a Robinson tiling.

construction for finite chains on top of the tile type for the top of the perimeter of a square. The \square_{\leftarrow} and \square_{\rightarrow} states in the Robinson layer force the top layer to be in states \ominus and \otimes , which in turn forces the Hamiltonian to act on the top layer of the particles in between the \ominus and \otimes as the Hamiltonian used in our construction. The end result is that if the energy from the lower layer is 0, then the ground energy of the Hamiltonian will be the ground energy of the Hamiltonian from our construction on the top row of squares of size 4^k for every $k \geq 1$. The energy contribution is then weighted according to the density of the squares of each size. [11] establishes robustness criteria for the Robinson tiles so that it is more energetically favorable to have a correct tiling on the lower Robinson layer and pay the price of the energy contribution from the finite chains embedded in the squares. We are able to use the same robustness result which is summarized in Lemma 3.7. We introduce some modifications of the construction for finite chains (described below) to get a 2-particle term h_C . If $H_C(N)$ denotes the Hamiltonian resulting from applying h_C to each pair in a chain of length N , then the net results is that the ground energy density in the thermodynamic limit resulting from layering h_C on top of the Robinson rules will be:

$$\alpha_0 = \sum_{k=1}^{\infty} \frac{\lambda_0(H_C(4^k)|_{\mathcal{H}_{br}})}{4^{2k+1}}.$$

This is established more formally below. The reduction then must show that if α_0 can be approximated to a given level of precision, the value $\lambda_0(H_C(4^k))$ can be determined and then the value for the desired function of k can be extracted.

Let \mathcal{H}_R be the Hilbert space for each particle under the Robinson tiling. We will refer to this part of the space as the R -layer. The standard basis for \mathcal{H}_R is just $|t\rangle$, for each tile type t . Let \mathcal{H}_C be the Hilbert space for each particle given in our construction. We will refer to this part of the space as the C -layer. The Hilbert space for a particle will be $\mathcal{H}_R \otimes (|0\rangle \oplus \mathcal{H}_C)$. We will refer to $|0\rangle$ as the *blank* state for the C -layer. Let H_R be the Hamiltonian resulting from the Robinson tiling rules. Let H_C be the Hamiltonian resulting from our construction. The overall Hamiltonian acts as H_R on the R -layer. Then there are constraints that force the C -layer to be in state \ominus if and only if the R -layer is in state \square_{\leftarrow} . Similarly there are constraints that force the C -layer to be in state \otimes if and only if the R -layer is in state \square_{\rightarrow} . There are constraints between the layers that force low energy configurations to be in a blank state on the C -layer, except if the underlying tile type on the lower layer is \square_{\leftarrow} . The rules of the Robinson tiling will force particles in between the $\square_{\leftarrow}/\ominus$ on the left and $\square_{\rightarrow}/\otimes$ on the right to be in state \square_{\leftarrow} . The Hamiltonian on the top layer will act as H_C if the tile type below is \square_{\leftarrow} .

The details regarding the Robinson tiling are given in [11]. They also detail the specific requirements required of H_C to be layered in this manner. We call a Hamiltonian that satisfies these constraints a *Robinson-Embeddable* Hamiltonian. The term used in [11] is a *Gottesman-Irani* Hamiltonian, named after the construction from [16].

Definition 3.5. [Robinson-Embeddable Hamiltonian: Definition 50 from [11]] Let \mathcal{H} be a finite-dimensional Hilbert space with two distinguished orthogonal states $|\ominus\rangle$ and $|\otimes\rangle$. An Robinson-Embeddable Hamiltonian is a 1D, translationally-invariant nearest-neighbor Hamiltonian $H(N)$ on a chain of length $N \geq 4$ which acts on Hilbert space $(\mathcal{H})^{\otimes N}$ with local interaction h , which satisfies the following properties:

1. $h \geq 0$

2. $[h, |\langle\langle\rangle\rangle\rangle\langle\langle\rangle\rangle] = [h, |\langle\rangle\rangle\rangle\langle\rangle\rangle] = [h, |\langle\rangle\rangle\rangle\langle\rangle\rangle] = [h, |\langle\rangle\rangle\rangle\langle\rangle\rangle] = 0$
3. $\lambda_0(H(N)|_{\mathcal{H}_{br}}) < 1$, where \mathcal{H}_{br} is the subspace of states with fixed boundary conditions $|\langle\rangle\rangle$ and $|\langle\rangle\rangle$ at the left and right ends of the chain respectively.
4. For every positive integer k , $\lambda_0(H(4^k)|_{\mathcal{H}_{br}}) \geq 0$ and $\sum_{k=1}^{\infty} \lambda_0(H(4^k)|_{\mathcal{H}_{br}}) < 1/2$.
5. $\lambda_0(H(N)|_{\mathcal{H}_{<}}) = \lambda_0(H(N)|_{\mathcal{H}_{>}}) = 0$, where $\mathcal{H}_{<}$ and $\mathcal{H}_{>}$ are the subspaces of states with, respectively, a $|\langle\rangle\rangle$ at the left end of the chain or a $|\langle\rangle\rangle$ at the right end of the chain.

We first need to show that the Hamiltonian given in our constructions satisfies the constraints of being a Robinson-Embeddable Hamiltonian:

Lemma 3.6. *The Hamiltonian h_C in our construction is a Robinson-Embeddable Hamiltonian.*

Proof. Although the Hamiltonian term h_C used in the infinite case will be modified from the construction used in the finite case, it will not be different in any of the features used in this proof. We will go through each property in turn:

1. All terms are Type I or II terms as described in Section 2.2.2 which have no negative eigenvalues.
2. All of the transition rules that involve $\langle\rangle$ or $\rangle\rangle$ have the form: $\langle\rangle\bullet \rightarrow \langle\rangle\bullet$ or $\bullet\rangle\rangle \rightarrow \bullet\rangle\rangle$, where \bullet is not equal to $\langle\rangle$ or $\rangle\rangle$. These propagation terms resulting from those transition rules all commute with the operators described in item 2. All other terms are diagonal in the standard basis.
3. According to Lemma 2.49, The smallest eigenvalue of $H_N|_{\mathcal{H}_{br}}$ is

$$E(x, \tilde{y}) = \left(1 - \cos\left(\frac{\pi}{L+1}\right)\right),$$

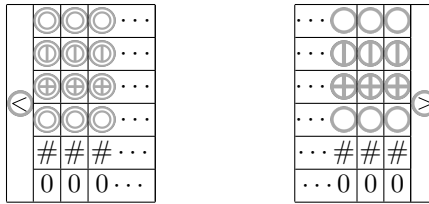
where $L = (2T(x, \tilde{y}) + 3) \cdot p(N)$. For $N \geq 4$, $L > 2$, and this value is always strictly less than 1.

4. The lower bound $\lambda_0(H_C(4^k)|_{\mathcal{H}_{br}}) \geq 0$ holds because $h_C \geq 0$. For the upper bound, we can plug in $p(N)$ to the expression above and use the fact that $T(x, y) \geq 0$ and the assumption that $N \geq 4$:

$$\lambda_0(H_C(N)|_{\mathcal{H}_{br}}) \leq \left(1 - \cos\left(\frac{\pi}{12(N-2)(2N-5)+1}\right)\right) \leq \frac{1}{N}.$$

The sum $\sum_{k=1}^{\infty} 1/4^k$ is strictly less than 1/2.

5. The standard basis states below are 0 energy states for $\mathcal{H}_{<}$ and $\mathcal{H}_{>}$. None of the transition rules apply since there is no pointer on Track 1.



□

$\lambda_0(N)$ is defined to be $\lambda_0(H_C(N)|_{\mathcal{H}_{br}})$, the ground energy of a bracketed finite chain of length N in which h_c is applied to every pair of neighboring particles in the chain. [11] prove a robustness bound for Robinson tiling which enables us to assume that the cost of H_C on the finite segments dominates in the ground energy density.

Lemma 3.7. (Lemma 52 from [11]) *Let h_R^{row} and h_R^{col} be the local interactions of the modified Robinson tiling acting on $\mathcal{H}_R \otimes \mathcal{H}_R$ as described in [11]. For a given ground state configuration (tiling) of H_R , let \mathcal{L} denote the set of all horizontal line segments of the lattice that lie between \square and \square tiles. Let h_C denote the local interaction of a Gottesman-Irani Hamiltonian $H_C(N)$ as in definition 3.5. Then there is a Hamiltonian H on a*

2D square lattice of width and height L with nearest neighbor interactions h^{row} and h^{col} such that for any L , the ground energy of H is in the interval $(\lambda_0(H(L)))$.

$$\left[\sum_{k=1}^{\lfloor \log_4(L/2) \rfloor} \left(\left\lfloor \frac{L}{2^{2n+1}} \right\rfloor \left(\left\lfloor \frac{L}{2^{2n+1}} \right\rfloor - 1 \right) \right) \lambda_0(4^k), \sum_{k=1}^{\lfloor \log_4(L/2) \rfloor} \left(\left\lfloor \frac{L}{2^{2n+1}} \right\rfloor \left(\left\lfloor \frac{L}{2^{2n+1}} \right\rfloor + 1 \right) \right) \lambda_0(4^k) \right] \quad (25)$$

The expression for the ground energy density in the thermodynamic limit which we will need in our construction follows from Lemma 3.7 and is encapsulated in the following Corollary.

Corollary 3.8. *The ground energy density of h^{row} and h^{col} in the thermodynamic limit is*

$$\alpha_0 = \sum_{k=1}^{\infty} \frac{\lambda_0(4^k)}{4^{2k+1}}.$$

Proof. Using the bounds in (25), the ground energy density of H on an $L \times L$ square is contained in:

$$\frac{\lambda_0(H(L))}{L^2} \in \sum_{k=1}^{\lfloor \log_4(L/2) \rfloor} \lambda_0(4^k) \left(\frac{1}{4^{2k+1}} \pm \frac{3}{2^{2k+1} \cdot L} \right)$$

Then

$$\begin{aligned} \alpha_0 &= \lim_{L \rightarrow \infty} \frac{\lambda_0(H(L))}{L^2} \\ &= \lim_{L \rightarrow \infty} \sum_{k=1}^{\lfloor \log_4(L/2) \rfloor} \lambda_0(4^k) \left(\frac{1}{4^{2k+1}} - \frac{3}{2^{2k+1} \cdot L} \right) = \lim_{L \rightarrow \infty} \sum_{k=1}^{\lfloor \log_4(L/2) \rfloor} \lambda_0(4^k) \left(\frac{1}{4^{2k+1}} + \frac{3}{2^{2k+1} \cdot L} \right) \\ &= \sum_{k=1}^{\infty} \frac{\lambda_0(4^k)}{4^{2k+1}} \end{aligned}$$

□

3.5 The Final Reduction: Mapping from the GED to $f(x)$

A few modifications for the finite construction are required for use in the infinite construction. We will describe those modifications in general terms here state Lemma 3.9 that encapsulate the key facts required of the construction. More specifics about the modifications as well as a proof of Lemma 3.9 is given in Section 3.6. In this section we will complete the proof of the hardness result for the thermodynamic limit using the claims from Lemma 3.9.

The first change is that in the infinite construction, we will not use squares of size 4^k for every k to encode the result of a computation. We will only use k 's that are a perfect square. Thus, we will use a chain of size 4^{x^2} to encode $f(x)$. This will allow us to use the bits from x^2 to $(x+1)^2$ in the energy density to encode $f(x)$. We need to add a way for $\lambda_0(H_{inf}(4^k))$ to be 0 if k is not a perfect square.

The second issue is the fact that the computation embedded in the Hamiltonian construction for the finite case may not finish in exactly $N - 2$ steps, where $N = 4^k$ is the length of the chain. Recall, that the clock in the construction ensures that the process is executed for exactly $N - 2$ steps. We can make sure that N steps is sufficient asymptotically, so that the construction will work on all but a finite number of k , but we need to control what happens for small $N = 4^k$ when the computation may not finish. We alter the construction so that in the cases where the computation does not finish, the ground energy is 0. We define the set \mathcal{K} to denote the set of k such that the computation does not finish in $N - 2$ steps if $N = 4^k$. We then prove that there is a Turing Machine that finishes the required computation in $o(N)$ steps, so that \mathcal{K} is finite. The analysis follows the finite case very closely and we establish the following lemma similar to the expression for the finite case.

Lemma 3.9. [Energy of the k^{th} square as a function of k] *For $N = 4^k$, where $k \in \mathcal{K}$ or k is not a perfect square, $\lambda_0(4^k) = 0$. If k is a perfect square, and $x = \sqrt{k}$, then*

$$\lambda_0(4^k) = \left(1 - \cos \left(\frac{\pi}{L+1} \right) \right),$$

where $L = (2T(x, \tilde{y}) + 3) \cdot p(4^k)$ and \tilde{y} is the string denoting the correct answers to the oracle queries made by M on input x .

Lemma 3.14 proven below uses Lemmas 3.9 and the results on Robinson tiling from Corollary 3.8 to complete the proof of Theorem 3.4. In particular, it shows that if the energies of the finite segments are as described in Lemma 3.9 and the ground energy density α is in fact the infinite sum given in Corollary 3.8, then there is a polynomial $q(x)$ such that if we are given α where $|\alpha - \alpha_0| \leq 1/2^{q(x)}$, it is possible to determine $\lambda_0(4^{x^2})$ to within a sufficient precision so that the integer L can be determined. From L , $T(x, \tilde{y})$ can be computed which in turn encodes the value of $f(x)$. Note that Lemma 3.14 makes the assumption that the Turing Machine M that computes f makes at most $2^{|x|/2}$ oracle calls on input x . This assumption is justified by the padding argument given in Lemma 3.17. We will start by setting up some notation and a few claims about the functions used in the proof.

Definition 3.10. For positive integer k ,

- $N_k = 4^{k^2}$
- $T_k = T(k^2, \tilde{y})$, where \tilde{y} is the set of correct responses to the oracle queries made by M on input k^2 .
-

$$l(k) = \frac{1}{4 \cdot (N_k)^2} \left(1 - \cos \left(\frac{\pi}{(2T_k + 1) \cdot p(N_k) + 1} \right) \right).$$

We will use the following three claims in the analysis:

Claim 3.11. Suppose that on input x , M makes at most $2^{|x|/2}$ oracle calls. Then $T_k \leq N_{k+1}/N_k$.

Proof. If m is the number of oracle calls made by M on input x , then the high order bit of $T(x, y)$ is in location $3m + 2$ for every y . Therefore $2^{3m+2} \leq T(x, y) \leq 2^{3m+3}$. By the assumption of the claim, on input k^2 , the number of oracle calls is at most k . Therefore $T(k^2, y) \leq 2^{3k+3}$. This is upper bounded by $N_{k+1}/N_k \leq 4^{(k+1)^2}/4^{k^2} = 4^{2k+1} = 2^{4k+2}$ for $k \geq 1$. \square

Claim 3.12.

$$l(k+1) < \frac{1}{2} \cdot l(k).$$

Proof. If m is the number of oracle calls made by M on input x , then the high order bit of $T(x, y)$ is in location $3m + 2$ for every y . Therefore $2^{3m+2} \leq T(x, y) \leq 2^{3m+3}$. As long as M makes as many queries on input $(k+1)^2$ as it does on input k^2 , $T_{k+1} \geq T_k/2$. Since $k \geq 1$, $N_{k+1} \geq 4^{2^2} = 64$, which implies that $p(N_{k+1})/p(N_k) \geq 4$. Therefore $(2T_k + 1)p(N_k) \leq (2T_{k+1} + 1)p(N_{k+1})$. Therefore,

$$\left(1 - \cos \left(\frac{\pi}{(2T_{k+1} + 1) \cdot p(N_{k+1}) + 1} \right) \right) \leq \left(1 - \cos \left(\frac{\pi}{(2T_k + 1) \cdot p(N_k) + 1} \right) \right)$$

Therefore $l(k+1)/l(k) \leq (N_k/N_{k+1}) = 4^{k^2}/4^{(k+1)^2} \leq 1/2$. \square

Claim 3.13. If x, x' , and y are positive integers greater than 5 and $x \neq x'$, then

$$\left| \cos \left(\frac{\pi}{yx + 1} \right) - \cos \left(\frac{\pi}{yx' + 1} \right) \right| \geq \frac{1}{y^2 x^4}.$$

Proof. The difference between the two cos terms is minimized for $x' = x + 1$, in which case, using the first

terms in the Taylor expansion for \cos , we have:

$$\begin{aligned}
& \left| \cos\left(\frac{\pi}{yx+1}\right) - \cos\left(\frac{\pi}{yx'+1}\right) \right| \\
& \geq \frac{\pi^2}{2(yx+1)^2} - \frac{\pi^2}{2(y(x+1)+1)^2} - \frac{\pi^4}{24(yx+1)^4} \\
& \geq \frac{\pi^2}{2} \left[\frac{y^2}{(yx+1)^2(y(x+1)+1)^2} - \frac{\pi^2}{12y^4x^4} \right] \\
& \geq \frac{\pi^2}{2} \left[\frac{1}{2y^2x^4} - \frac{(\pi^2/12y^2)}{y^2x^4} \right] \\
& \geq \frac{\pi^2}{2} \left[\frac{1}{2y^2x^4} - \frac{1}{4y^2x^4} \right] = \frac{\pi^2}{8} \left[\frac{1}{y^2x^4} \right] > \frac{1}{y^2x^4}
\end{aligned}$$

The inequality from the third to the fourth line uses the fact that for $x \geq 5$ and $y \geq 5$, $(yx+1)^2(y(x+1)+1)^2 \leq 2y^4x^4$. The inequality from the fourth to the fifth line uses the fact that for $y \geq 5$, $\pi^2/12y^2 \leq 1/4$. \square

Lemma 3.14. [Computing $f(x)$ from the GED] *Suppose that*

$$\alpha_0 = \sum_{k=1}^{\infty} \frac{\lambda_0(4^k)}{4^{2k+1}}$$

and $\lambda_0(4^k)$ satisfies the conditions in Lemma 3.9. Suppose also that on input x , the Turing Machine M that computes f makes at most $2^{\lceil x/2 \rceil}$ oracle calls. Then there is a polynomial q such that we can compute $f(x)$ in time that is polynomial in x , given α where $|\alpha - \alpha_0| \leq 1/2^{q(x)}$.

This lemma implies the proof of Theorem 3.4 in a straight-forward way.

Proof. The polynomial q is chosen so that $1/2^{q(x)} \leq l(x+1)$. Let $\mathcal{K}(k)$ be an indicator function which is equal to 1 if $k \in \mathcal{K}$ and is equal to 0 otherwise. Since $\lambda_0(4^k) = 0$ if k is not a perfect square or if $k \in \mathcal{K}$, we have that

$$\alpha_0 = \sum_{k=1}^{\infty} (1 - \mathcal{K}(k^2))l(k).$$

The inductive hypothesis is that for $s \leq x$, we have a α_s that satisfies:

$$\left| \alpha_s - \sum_{k=s}^{\infty} (1 - \mathcal{K}(k^2))l(k) \right| \leq \left(1 + \frac{s}{x}\right) l(x+1).$$

We will show that if $s^2 \notin \mathcal{K}$, then we can uniquely determine T_s in polynomial time. Moreover, if $s < x$, then we can find α_{s+1} such that

$$\left| \alpha_{s+1} - \sum_{k=s+1}^{\infty} (1 - \mathcal{K}(k^2))l(k) \right| \leq \left(1 + \frac{s+1}{x}\right) l(x+1).$$

Note that we start with $\alpha = \alpha_1$ that satisfies the inductive hypothesis for $s = 1$. Also, as long as $x^2 \notin \mathcal{K}$, from α_x , we can determine T_x from which $f(x)$ can be determined.

If $s^2 \in \mathcal{K}$, then

$$\sum_{k=s}^{\infty} (1 - \mathcal{K}(k^2))l(k) = \sum_{k=s+1}^{\infty} (1 - \mathcal{K}(k^2))l(k).$$

We can set $\alpha_{s+1} = \alpha_s$ and the inductive step is complete.

Now suppose that $s^2 \notin \mathcal{K}$. By Claim 3.12, $\sum_{k=s+1}^{\infty} l(k) \leq 2l(s+1)$. Therefore

$$|\alpha_s - l(s)| \leq 2 \cdot l(s+1) + \left(1 + \frac{s}{x}\right) l(x+1) \leq 4l(s+1)$$

The value $\lambda_0(N_s)$ is

$$\left(1 - \cos\left(\frac{\pi}{(2T_s + 1)p(N_s) + 1}\right)\right).$$

Plugging in the definition for $l(s)$ and multiplying by $4(N_s)^2$, we get that

$$|4(N_s)^2\alpha_s - \lambda_0(N_s)| \leq \frac{(N_s)^2}{(N_{s+1})^2} \cdot \left(1 - \cos\left(\frac{\pi}{(2T_{s+1} + 1) \cdot p(N_{s+1}) + 1}\right)\right) \quad (26)$$

$$\leq \frac{(N_s)^2}{(N_{s+1})^2} \cdot \left(\frac{(\pi/2)^2}{4(p(N_{s+1}))^2(T_{s+1})^2}\right) \quad (27)$$

$$\leq \frac{(N_s)^2}{(N_{s+1})^2(p(N_{s+1}))^2(T_{s+1})^2} \quad (28)$$

By Claim 3.11, for any $T \neq T_s$,

$$\left|\left(1 - \cos\left(\frac{\pi}{(2T_s + 1)p(N_s) + 1}\right)\right) - \left(1 - \cos\left(\frac{\pi}{(2T + 3)p(N_s) + 1}\right)\right)\right| \geq \frac{1}{(p(N_s))^2(T_s)^4}.$$

Therefore, if we can determine the value of $\lambda_0(N_s)$ to within $\pm 1/2(p(N_s))^2(T_s)^4$, the value of T_s is uniquely determined and can be computed by binary search in time that is poly-logarithmic in N_s , and therefore polynomial in x . If we can determine T_s , then we can use the Taylor approximation for the cos function to compute an approximation $\tilde{l}(s)$ of $l(s)$ to within $\pm l(x+1)/x$. We can then set $\alpha_{s+1} = \alpha_s - \tilde{l}(s)$.

$$\begin{aligned} \left|\alpha_{s+1} - \sum_{k=s+1}^{\infty} l(k)\right| &= \left|\alpha_s - \tilde{l}(s) - \sum_{k=s+1}^{\infty} l(k)\right| \\ &\leq |l(s) - \tilde{l}(s)| + \left|\alpha_s - \sum_{k=s}^{\infty} l(k)\right| \\ &\leq \frac{l(x+1)}{x} + \left(1 + \frac{s}{x}\right)l(x+1) = \left(1 + \frac{s+1}{x}\right)l(x+1) \end{aligned}$$

It remains to show that the bound from (28) is at most $1/2(p(N_s))^2(T_s)^4$. Thus, we need to show

$$\left[\frac{p(N_s)N_s}{p(N_{s+1})N_{s+1}}\right]^2 \leq \left[\frac{T_{s+1}}{2(T_s)^2}\right]^2 \quad (29)$$

Using the bounds from Claim 3.11, we get that $T_s \leq N_{s+1}/N_s$. Also, The polynomial $p(N) = 4(N-2)(2N-3)$. Since $N_{s+1} \geq N_s \geq N_2 \geq 64$, $p(N_s)/p(N_{s+1}) \leq 1/4$. Therefore

$$\left[\frac{p(N_s)N_s}{p(N_{s+1})N_{s+1}}\right]^2 \leq \left[\frac{p(N_s)}{p(N_{s+1})T_s}\right]^2 \leq \frac{1}{(4T_s)^2}$$

As long as M makes as many oracle queries on input $(s+1)^2$ as it does on s^2 , $2T_{s+1} \geq T_s$. The the bound required in (29) follows. \square

3.6 Modifications to the Hamiltonian from the Finite Case

The energy density in the thermodynamic limit will be

$$\sum_{k=1}^{\infty} \frac{\lambda_0(4^k)}{4^{2k+1}}.$$

With this expression in mind, we will describe required changes to the construction for the finite case. The first thing to notice is that the GED only encodes energies for chains of length $N = 4^k$, so the input to the function f from which we are reducing will be k which is logarithmic in N . The size of the input is $\log k$ which

means that N , the size of the chain, is doubly exponential in the input length. This is why we are reducing from $\text{FEXP}^{\text{NEXP}}$, instead of FP^{NEXP} as we did in the finite case.

Furthermore, we will not use all the k 's to encode the result of a computation. We will only use the k 's that are a perfect square. Thus, we will use a chain of size 4^{x^2} to encode $f(x)$. This will allow us to use the bits from x^2 to $(x+1)^2$ in the energy density to encode $f(x)$. We need to add a way for $\lambda_0(4^k)$ to be 0 if k is not a perfect square. We handle this case by encoding the fact that k is not a perfect square in the output of the verifier. Recall that M_{TV} writes a symbol σ_A or σ_R as the output of its verification process. If k is not a perfect square then we make sure that a different character σ_B is written in the first location when M_{TV} halts. The additional $+1$ in H_{final} is only triggered if the output of M_{TV} starts with an σ_A or an σ_R . If the initial symbol is neither σ_A nor σ_R , then there will be no additional terms along the diagonal besides H_{prop} . The equal superposition of all the states in the computation will be a 0 energy state.

Finally, we will need to alter the construction to ensure that no cost is incurred if M_{TV} does not finish its computation. Although $N - 2$ steps will be enough for $M_{BC} + M_{TV-inf}$ to complete its computation asymptotically, for small $N = 4^k$, this may not be the case. We will manage this by replacing the symbols $\{\sigma_A, \sigma_R, \sigma_B, \sigma_X\}$ with symbols from $\{\gamma_A, \gamma_R, \gamma_B, \gamma_X\}$ everywhere in the transition rules for M_{TV-inf} . The γ symbols do not trigger any penalty terms. Then there is a post-processing step in which $\{\gamma_A, \gamma_R, \gamma_B, \gamma_X\}$ are converted to $\{\sigma_A, \sigma_R, \sigma_B, \sigma_X\}$ in a controlled way so that if the computation halts before it finishes, there will be a 0 energy state.

After the binary counter Turing Machine runs for $N - 2$, we will run a process for $N - 2$ steps that consists of the following three Turing Machines dovetailed together:

1. M_{BC} is the same as in the finite case and is described in Section 2.4.2.
2. M_{TV-inf} will be an altered version of the M_{TV} used in the construction for the finite systems. The pseudo-code for M_{inf} is given in Figure 15.
3. M_{post} is a post-processing step which ensures that the symbols that trigger a periodic cost appear in a controlled way so that if the computation stops before completion, the ground energy will be 0. The pseudo-code for M_{post} is given in Figure 16. The transition rules are specified in Figure 17.

The rules for M_{post} are given in Figure 17.

Lemma 2.33 is used so that M_{BC} , M_{TV-inf} , and M_{post} all have the same tape alphabet Γ . Then the same transformation that was applied to $M_{BC} + M_{TV}$ in the finite case is applied here in the infinite case to $M_{BC} + M_{TV-inf} + M_{post}$, with the exception that the final state for $M_{BC} + M_{TV-inf} + M_{post}$ is r_f instead of p_f for $M_{BC} + M_{TV}$. Also the "time-wasting" subroutine is entered if the current character is in $\{\sigma_A, \sigma_R, \sigma_B\}$ when the final state r_f of M_{post} is reached. The finite case did not have a σ_B , so the time-wasting subroutine was entered only if the current character was σ_A or σ_R at the time that $M_{BC} + M_{TV}$ halts. More specifically, the rule $\delta(p_f, \sigma_B) \rightarrow (q_0, \sigma_B, N)$ is removed and the following two rules are added:

$$\begin{aligned}\delta(p_f, \sigma_B) &\rightarrow (q_*, \sigma_B, R) \\ \delta(q_*, \sigma_B) &\rightarrow (q_0, \sigma_B, N)\end{aligned}$$

These new rules preserve the properties of reversibility in exactly the same way as the original transformation did. We will call this altered transformation \mathcal{T}' and define:

$$M_{check-i} = \mathcal{T}'(M_{BC} + M_{TV-inf} + M_{post})$$

The process embedded in the Hamiltonian for the infinite case will be $N - 2$ steps of M_{BC} followed by $N - 2$ steps of $M_{check-i}$.

To summarize what happens with $M_{check-i}$. Suppose that $N = 4^k$. M_{BC} is run for $N - 2$ steps and ends in the middle of an increment operation. $M_{check-i}$ will pick up where M_{BC} left off and complete the increment operation, ending with some string z on the work tape. $N(z)$ will be 4^k plus the few steps required to complete the increment operation. Even though $N(z) \neq 4^k$, there is enough information to recover k from z since k will be $\lfloor \log_4 N(z) \rfloor$. If k is not a perfect square, then $M_{check-i}$ will end with the input (γ_B, z, w) on its work tape. In this case M_{post} will convert γ_B to σ_B and then halt. The time-wasting process is triggered which preserves the output of the tape until the clock runs out. If $k = x^2$, for some integer x , then M_{TV-inf} does exactly

```

INPUT:  $(z, w)$ 
(1)  Compute  $N = N(z)$ 
(2)  Compute  $k = \lfloor \log_4 N \rfloor$ 
(3)  Compute  $x = \lfloor \sqrt{k} \rfloor$ 
(4)  if  $x^2 = k$ 
(5)     $m$  is the number of oracle queries made by  $M$  on input  $x$ 
(6)     $r$  is the size of the witness used by  $V$  on any oracle query generated by  $M$  on input  $x$ 
(7)     $m$  and  $r$  are hard-coded functions of  $|x|$  determined by  $M$  and  $V$ .
(8)  Simulate Turing Machine  $M$  on input  $(x, y)$ 
(9)    Use  $y$  for the responses to the oracle queries,  $y$  denotes the first  $m$  bits of  $w$ 
(10)   Simulation generates  $x_1, \dots, x_m$ , inputs to oracle queries
(11)  REJECT = FALSE
(12)  for  $i = 1 \dots m$ 
(13)    if  $y_i = 1$ 
(14)      Simulate  $V$  on input  $(x_i, w_i)$ 
(15)         $w_i$  is the string formed by bits  $m + (i - 1)r + 1$  through  $m + ri$  of the witness track
(16)        If  $V$  rejects on input  $(x_i, w_i)$ 
(17)          REJECT = TRUE
(18)    if (REJECT)
(19)      Write " $\gamma_R$ " in the left-most position of the work tape
(20)    else
(21)      Write " $\gamma_A$ " in the left-most position of the work tape
(22)    Compute  $T(x, y)$ 
(23)    Write the value of  $T(x, y)$  in unary with " $\gamma_X$ " symbols starting in the second position of the work tape
(24)  if  $l^2 \neq k$ 
(25)    Write " $\gamma_B$ " in the left-most position of the work tape
(26)    Reverse the computation and finish with  $(\gamma_B, z, w)$  on the work tape
OUTPUT:
  if  $k$  is not a perfect square  $(\gamma_B, z, w)$ 
  if  $k$  is a perfect square  $(\{\gamma_A, \gamma_R\}(\gamma_X)^{T(x,y)}; z, w)$ 

```

Figure 15: Pseudo-code for the Turing Machine M_{TV-inf} .

what M_{TV} would do on input (x, w) , using the Turing Machines M and V for f . Note that lines (5) through (23) of M_{TV-inf} are exactly the same as lines (2) through (20) of M_{TV} . The functions for m , the number of oracle calls and r the size of the witnesses used for V are different but both are hard-coded into M and V . Therefore at the end of M_{TV-inf} 's computation, the output is exactly $\text{OUT}(x, w, M, V)$ as given in Definition 2.6 for the finite case, with the exception that M_{TV} has written its output with symbols $\{\gamma_A \gamma_R, \gamma_X\}$ instead of $\{\sigma_A \sigma_R, \sigma_X\}$. Then M_{post} changes the output $(\gamma_A + \gamma_R)(\gamma_X)^T$ to $(\sigma_A + \sigma_R)(\sigma_X)^T$. This is done in such a way that the σ_A/σ_R symbol is the very last symbol written.

Lemma 3.16 establishes that this process produces the correct output for the construction. It will be convenient to have a way to connect N , the size of the chain and the string z that will be one the work tape after $M_{check-i}$ finishes the last increment operation.

Definition 3.15. $\mathcal{N}(x)$ is the set of positive integers N such that $N \leq N(x)$ and there is no other $x' \neq x$ such that $N \leq N(x') < N(x)$.

Lemma 3.16. [$M_{check-i}$ Produces the Correct Output] Suppose that $N = 4^k$ for $k \geq 2$. Suppose also that $N \in \mathcal{N}(z)$ and M_{TV-inf} behaves properly on all binary input pairs (z, w) and is 1-compact. Then the process that starts with input $(1, w)$ for $w \in \{0, 1\}^{N-2}$, runs M_{BC} for $N - 2$ steps and runs $M_{check-i}$ for $N - 2$ steps

(1)	if current symbol is not in $\{\gamma_A, \gamma_R, \gamma_B\}$
(2)	Transition to s_f , stay in place.
(3)	else
(4)	move right into state s_R
(4)	while (current symbol is γ_X)
(5)	Change symbol to σ_X and move right in state s_R
(6)	if current symbol is not γ_X
(7)	Move left into s_L
(8)	Move left until a symbol from $\{\gamma_A, \gamma_R, \gamma_B\}$ is reached
(9)	Change $\gamma_A/\gamma_B/\gamma_R$ to $\sigma_A/\sigma_B/\sigma_R$, transition to q_f , stay in place

Figure 16: Pseudo-code for the Turing Machine M_{post} .

	γ_A	γ_R	γ_B	γ_X	σ_X	$a \neq \gamma_A, \gamma_R, \gamma_B, \gamma_X$
s_0	(s_R, γ_A, R)	(s_R, γ_R, R)	(s_R, γ_B, R)	(s_f, γ_X, N)	-	(s_f, a, N)
s_R	(s_L, γ_A, L)	(s_L, γ_R, L)	(s_L, γ_B, L)	(s_R, σ_X, R)	-	(s_L, a, L)
s_L	(s_f, σ_A, N)	(s_f, σ_R, N)	(s_f, σ_B, N)	*	(s_L, γ_X, L)	*

Figure 17: A summary of the transition rules for M_{post} . The transition rules are well-defined as long as the tape contents do not contain $\{\sigma_A, \sigma_R, \sigma_B, \sigma_X\}$ when M_{post} begins. The rules can be extended so that they are well defined on every $Q \times \Gamma$ pair, so that the reduced transition function remains one-to-one and the Turing Machine remains unidirectional. The rule $\delta(a, q_f) = (q_0, a, N)$ is included for every $a \in \Gamma$ so that the resulting Turing Machine is in normal-form.

will keep the head of the Turing Machine inside tape cells 1 through $N - 3$. Also

1. If $M_{BC} + M_{TV-inf} + M_{post}$ does not finish, then there will be no symbols from $\{\sigma_A, \sigma_R, \sigma_X\}$ on the work tape.
2. If $M_{BC} + M_{TV-inf} + M_{post}$ does finish and k is not a perfect square, then the process finishes with (σ_B, z, w) on its work tape.
3. If $M_{BC} + M_{TV-inf} + M_{post}$ does finish and $k = x^2$, then the process finishes with tape contents $\text{OUT}(x, w, M, V)$ as given in Definition 2.6 for the finite case.

Proof. According the Lemma 2.29, after $N - 2$ steps of M_{BC} , the head stays within tape cells 1 through $N - 4$. After $M_{check-i}$ takes over, the last unfinished increment operation is completed. The head can only reach one additional location past $N - 4$ in a single increment operation which means the head has stayed within locations 1 through $N - 3$. At this point the head is back in location 1 and M_{TV-inf} is launched. Since M_{TV-inf} behaves properly on all binary inputs, the head will not go to the left of tape cell 1. There are at most $N - 3$ steps remaining and since M_{TV-inf} is 1-compact, it will not go past location $N - 3$ on the right. When M_{TV-inf} finishes, the head is back at tape cell 1 at which point M_{post} is launched. At this point, at least 2 steps of $M_{check-i}$ have been run and there are at most $N - 4$ steps left to go. The head can not reach past location $N - 3$ in only $N - 4$ steps. Also, the rules M_{post} guarantee that the head will not move to the left of location 1. Furthermore, M_{post} will end in the location in which is began.

The only time a character from $\{\sigma_A, \sigma_R, \sigma_X\}$ is written, is in the last step of M_{post} , so if $M_{BC} + M_{TV-inf} + M_{post}$ does not finish, then there will be no occurrences of $\{\sigma_A, \sigma_R, \sigma_X\}$ on the tape.

If $M_{BC} + M_{TV-inf} + M_{post}$ does finish and k is not a perfect square, then the contents of the tape after M_{TV-inf} finishes is (γ_B, z, w) . M_{post} will convert the γ_B to a σ_B and then halt. The time-wasting process is launched and the tape contents will remain unchanged until the $N - 2$ steps of $M_{check-i}$ are complete.

If $M_{BC} + M_{TV-inf} + M_{post}$ does finish and $k = x^2$, then the contents of the tape after M_{TV-inf} finishes is $\text{OUT}(x, w, M, V)$, except that every σ_i is a γ_i . M_{post} will convert the γ 's to σ 's and the contents of the tape will be $\text{OUT}(x, w, M, V)$. When M_{post} finishes, the head will be pointing to the σ_A or σ_R which will launch the time-wasting process and the tape contents will remain unchanged until the $N - 2$ steps of $M_{check-i}$ are complete. \square

3.6.1 Existence of M_{TV-inf} that produces the correct output for most N

We now need to argue that there is a Turing Machine M_{TV-inf} that has the required properties so that the resulting $M_{check-i}$ produces the correct output for most values of N . As with the finite case, we need some assumptions about the running time of M and V which M_{TV-inf} simulates which can be proven using standard padding arguments.

Lemma 3.17. [Padding Lemma for $\text{FEXP}^{\text{NEXP}}$] *If $f \in \text{FEXP}^{\text{NEXP}}$, then for any constants, c_1 and c_2 , f is polynomial time reducible to a function $g \in \text{FEXP}^{\text{NEXP}}$ such that g can be computed by an exponential-time Turing Machine M with access to a NEXP oracle for language L . The verifier for L is a Turing Machine V . Moreover, on input x of length n , M runs in $O(2^{c_1 n})$ time, and makes at most $2^{c_1 n}$ queries to the oracle. Also, the length of the queries made to the oracle is at most $2^{c_1 n}$ and the running time of V as well as the size of the witness required for V on any query made by M is $O(2^{2^{c_2 n}})$*

Proof. Suppose that M runs in $O(2^{r_1(n)})$ time and the running time of V is $O(2^{r_2(n)})$. The reduction will pad an input x to f with $10^{t(n)}1$, for a polynomial t chosen below. We will refer to this substring as the *suffix*. The algorithm for g will verify that the length of the suffix is in fact $t(n)$, where n is the number of bits not included in the suffix. If not, then the value of g is 0. If the input to g does have a suffix with the correct length then it erases the suffix and simulates M on the rest of the string. Note that the input length to g is now $\bar{n} = t(n) + n + 2$. The polynomial t is chosen so that $2^{c_1 \bar{n}} \geq 2^{c_1 t(n)} \geq 2^{r_1(n)}$, so that the running time of M and hence the number of oracles made, as well as the length of the inputs to those oracles are all bounded by $2^{c_1 \bar{n}}$. The running time of V on any of the query inputs is at most $2^{r_2(2^{r_1(n)})}$. t will also be chosen to be large enough so that

$$2^{r_2(2^{r_1(n)})} < 2^{2^{c_2 t(n)}} < 2^{2^{c_2 \bar{n}}}.$$

\square

We need now to establish that M_{TV-inf} can be chosen so that for all but a finite set of k , $M_{BC} + M_{TV-inf} + M_{post}$ finishes in $4^k - 2$ steps for every witness w .

Definition 3.18. [Sufficient N for Completing $M_{BC} + M_{TV-inf} + M_{post}$'s Computation] *We say that N is sufficient for $M_{BC} + M_{TV-inf} + M_{post}$ if for every $w \in \{0, 1\}^{N-4}$, starting with input $(1, w)$, if M_{BC} is run for $N - 2$ steps, followed by $M_{BC} + M_{TV-inf} + M_{post}$ for $N - 2$ steps, the final state r_f for M_{post} is reached.*

Lemma 3.19. [Existence of M_{TV-inf} With Required Running Time] *There is a reversible normal-form Turing Machine M_{TV} such that*

1. M_{TV-inf} behaves properly on all (a, b) , where $a, b \in \{0, 1\}^*$.
2. M_{TV-inf} is 1-compact.
3. For all but a finite number of k , if $N = 4^k$ is sufficient for $M_{BC} + M_{TV-inf} + M_{post}$.
4. The behavior of M_{TV-inf} is as described in pseudo-code given in Figure 15.

Proof. If $N = 4^k$, the time to complete the increment operation after $N - 2$ steps of M_{BC} is $O(k)$.

Next we consider the time to compute the function outlined in Figure 15 on a RAM and then argue about the time to convert the algorithm to a reversible Turing Machine. The initial arithmetic computations can be done in time that is polylogarithmic in N . Now suppose that $k = x^2$. By Lemma 2.31, we can assume that the running time of M is on the order of $2^{c_1 |x|} \leq 2^{c_1 |k|} \leq k^{c_1}$. The number of queries made by M and the size of the input to those questions is also on the order of k^{c_1} . The running time of each call is on the order of $2^{2^{c_2 |x|}} \leq 2^{k^{c_2}}$. Thus, the total time for running the verifier is on the order of $k^{c_1} 2^{k^{c_2}}$. The time to compute $T(x, y)$ and write the resulting value in unary is $O(4^{k^{c_1}})$.

Finally, the time to run M_{post} after the final state of M_{TV-inf} is reached is $O(T(x, y))$ which is also $O(4^{c_1 k})$. Thus, for any constant d , the constants c_1 and c_2 can be chosen so that the running time to compute the function computer by M_{TV-inf} is $O(2^{dk})$.

The RAM algorithm can be converted to a TM computation with at most polynomial overhead. Finally, by Theorem B.8 from [8], the TM can be converted to a reversible TM that behaves properly on all inputs with quadratic overhead. Therefore the constant d can be chosen to be small enough so that the running time of the reversible TM to compute $M_{BC} + M_{TV-inf} + M_{post}$ is $o(4^k)$. Since $N = 4^k$, the total running time will be at most $N - 2$ for all but a finite number of values for k .

Finally, to satisfy the second assumption, we can add one additional state which causes the reversible TM to stay in place for one step before beginning its computation. \square

3.6.2 Additional Penalty Terms for the Infinite Construction

The clock and the propagation terms will be exactly the same as the finite case, except that $M_{check-i}$ is replaced by $M_{check-i}$ throughout. We need to adjust the penalty terms so that the ground energy is 0 for all N in which the process executed on the computation tracks does not have time to finish. Also, we only run the simulation on segments of size 4^k , where k is a perfect square. If k is not a perfect square then we want the Hamiltonian on that segment to have a ground energy of 0. We have set up the output of the Turing Machine so that these situations can be detected.

In the correct initial configuration, the contents of Track 5 are $\langle \ominus 1 \#^* \ominus \rangle$, where $\#$ is the blank symbol. The state should be q_0 and the head should be pointing to the cell with the 1. h_{init} is exactly as it was for the finite case. The first of the two rules given below pertains to Tracks 1 and 5 only and implicitly acts as the identity on all other tracks. The third rule pertains to Tracks 1, 4, and 5:

$$h_{init} = \sum_{a \in \Gamma, x \in \Gamma - \{\#\}} \left| \begin{array}{c} \text{5} \\ \text{a} \end{array} \right\rangle \left\langle \begin{array}{c} \text{5} \\ \text{x} \end{array} \right| + \sum_{x \in \Gamma - \{1\}} \left| \begin{array}{c} \text{5} \\ \text{x} \end{array} \right\rangle \left\langle \begin{array}{c} \text{5} \\ \text{x} \end{array} \right| + \left| \begin{array}{c} \text{5} \\ \neg q_0 \\ 1 \end{array} \right\rangle \left\langle \begin{array}{c} \text{5} \\ \neg q_0 \\ 1 \end{array} \right|$$

In order to understand the remaining changes, it will be useful to analyze what the contents of Track 5 (the work track) can be at various points in the computation. We will let $\bar{\Gamma}$ denote all the tape symbols Γ , except for $\{\gamma_A, \gamma_R, \gamma_B, \gamma_X, \sigma_A, \sigma_R, \sigma_B, \sigma_X\}$. At any point in the computation of M_{BC} the tape contents are always from $(\bar{\Gamma})^*$. At any point in the computation of $M_{TV-inf} + M_{post}$, the tape contents will be in one of the following forms:

$$(\bar{\Gamma})^* \quad M_{TV-inf} \text{ running} \quad (30)$$

$$(\gamma_A + \gamma_R + \gamma_B)(\bar{\Gamma} + \gamma_X)^* \quad M_{TV-inf} \text{ running} \quad (31)$$

$$(\gamma_A + \gamma_R + \gamma_B)(\sigma_X)^*(\gamma_X)^*(\bar{\Gamma})^* \quad M_{post} \text{ sweeping right} \quad (32)$$

$$(\gamma_A + \gamma_R + \gamma_B)(\sigma_X)^*(\bar{\Gamma})^* \quad M_{post} \text{ sweeping left} \quad (33)$$

$$(\sigma_A + \sigma_R + \sigma_B)(\sigma_X)^*(\bar{\Gamma})^* \quad \text{last step of } M_{post} \quad (34)$$

(30) through (33), show the possibilities for the tape contents up until the point where $M_{check-i}$ hits a final state. The fifth case (34), corresponds to a finished $M_{check-i}$ which keeps its tape contents for the remainder of the $N - 2$ steps. Therefore, we would like to have any symbol from the set $\Sigma = \{\gamma_A, \gamma_R, \gamma_B, \sigma_A, \sigma_R, \sigma_B, \sigma_X\}$ count as a symbol for checking the length of the Track 3 timer. Recall that the Track 3 timer always has the form $\oplus^*(\ominus + \ominus)\oplus^*\otimes^*$. Thus, as the Track 1 4-pointer sweeps left, it will check that the symbol on Track 5 is from the set Σ if and only if the Track 3 state is from the set $\{\oplus, \ominus, \ominus, \oplus\}$.

$$h_{length} = \sum_{\substack{s \in \{\oplus, \oplus, \ominus, \ominus\} \\ a \notin \Sigma}} \left| \begin{array}{c} \text{3} \\ \text{s} \\ \text{a} \end{array} \right\rangle \left\langle \begin{array}{c} \text{3} \\ \text{s} \\ \text{a} \end{array} \right| + \sum_{b \in \Sigma} \left| \begin{array}{c} \text{3} \\ \otimes \\ \text{b} \end{array} \right\rangle \left\langle \begin{array}{c} \text{3} \\ \otimes \\ \text{b} \end{array} \right|$$

If $M_{check-i}$ finishes and $N = 4^k$, where k is not a perfect square, then the number of σ_X 's will be $T(x, y)$ and the h_{length} term will check that the Track 3 timer has the correct length as in the finite case.

Track 3 will correspond to the symbols from the set $\{\gamma_A, \gamma_R, \gamma_B, \sigma_X\}$ on Track 5. Furthermore, $H_{N,V}$ and $H_{N,final}$ will be 0 because there will never be an σ_A or an σ_R on the work tape since those symbols are written in the last step of $M_{check-i}$ before it hits a final state. The overall energy for this state will be 0. \square

Lemma 3.21. [Ground Energy for $N = 4^k$ where k is not a Perfect Square] *Suppose that $N = 4^k$ is sufficient for $M_{BC} + M_{TV-inf} + M_{post}$ and k is not a perfect square. Then $\lambda_0(4^k)$.*

Proof. The ground state for this Hamiltonian will correspond to the cycle in which the clock has length 0 and the computation starts in state $(1, w)$ with the head in state q_0 at the left end of the chain. In this case $H_{N,init}$ will be 0 because the initial configuration is correct. $H_{N,length}$ will also be 0 because the tape contents at the end of the process (in Segment 4) will be (σ_B, z, w) , where $4^k \in \mathcal{N}(z)$. This will be consistent with a clock of length 0. Furthermore, $H_{N,V}$ and $H_{N,final}$ will be 0 because neither σ_A nor σ_R are on the work tape at the end of the process. The overall energy for this state will be 0. \square

Definition 3.22. [Set of k where 4^k is not Sufficient] *Let \mathcal{K} denote the set of k which are not sufficient for $M_{check-i}$. Lemma 3.19 shows that M_{TV-inf} can be chosen so that 4^k is sufficient for $M_{BC} + M_{TV-inf} + M_{post}$ for all but a finite set of k . We will fix a M_{TV-inf} that satisfies those properties and let \mathcal{K} denote the finite set of k such that 4^k is not sufficient for $M_{BC} + M_{TV-inf} + M_{post}$*

This final lemma characterizes $\lambda_0(4^k)$ for all k .

Proof. [Proof of Lemma 3.9] Lemmas 3.20 and 3.21 show that for $k \in \mathcal{K}$ or when k is not a perfect square, then $\lambda_0(4^k) = 0$. Finally, we have the case where $N = 4^k$, k is a perfect square ($k = x^2$) and 4^k is sufficient for $M_{BC} + M_{TV-inf} + M_{post}$. Then according to Lemma 3.16 after $N - 2$ steps of M_{count} and $N - 2$ steps of $M_{check-i}$ starting in configuration $(1, w)$, the contents of the tape will be $\text{OUT}(x, w, M, V)$, corresponding to the correct output of $M_{TV-inf} + M_{post}$. Note that this is the same as the output for M_{TV} (for the finite case) on input x and w , simulating TMs M and V . The functions for m , the number of query calls, and r the length of the witnesses for V are a different function of $|x|$ but those functions are assumed to be hard-coded into M and V . The analysis of the ground energy now is the same as the finite case. Lemmas 2.47, 2.48, and 2.49 all hold. In particular, Lemma 2.49 says that $\lambda_0(4^k) = E(x, \tilde{y})$, where \tilde{y} is the string denoting the correct answers to the oracle queries made by M on input x and

$$E(x, y) = \left(1 - \cos\left(\frac{\pi}{L+1}\right)\right),$$

where $L = (2T(x, \tilde{y}) + 3) \cdot p(4^k)$. \square

Note Added

After announcing these results we found that similar results were achieved independently by Watson and Cubitt; they are posted simultaneously on the arXiv.

4 Acknowledgements

We are grateful to the Simons Institute for the Theory of Computing, at whose program on the ‘‘The Quantum Wave in Computing’’ this collaboration began. We would also like to thank the following people for fruitful conversations regarding this work: Ignacio Cirac, Toby Cubitt, James Watson, Johannes Bausch, Sevag Gharibian, and David Perez-Garcia. We are especially grateful to Ignacio Cirac for suggesting the formulation of the problem studied in this paper.

References

- [1] Dorit Aharonov, Daniel Gottesman, Sandy Irani, and Julia Kempe. The power of quantum systems on a line. *Communications in Mathematical Physics*, 287(1):41–65, Jan 2009.

- [2] Dorit Aharonov and Leo Zhou. Hamiltonian sparsification and gap-simulation. In Avrim Blum, editor, *10th Innovations in Theoretical Computer Science Conference, ITCS 2019, January 10-12, 2019, San Diego, California, USA*, volume 124 of *LIPICs*, pages 2:1–2:21. Schloss Dagstuhl - Leibniz-Zentrum für Informatik, 2019.
- [3] A. Ambainis. On physical problems that are slightly more difficult than qma. In *2014 IEEE 29th Conference on Computational Complexity (CCC)*, pages 32–43, 2014.
- [4] Andris Ambainis. On physical problems that are slightly more difficult than qma. In *2014 IEEE 29th Conference on Computational Complexity (CCC)*, pages 32–43, 2014.
- [5] Johannes Bausch, Toby S. Cubitt, Angelo Lucia, and David Perez-Garcia. Undecidability of the spectral gap in one dimension. *Physical Review X*, 10(3), Aug 2020.
- [6] Johannes Bausch, Toby S. Cubitt, and James D. Watson. Uncomputability of phase diagrams. *Nature Communications*, 12(1), Jan 2021.
- [7] Johannes Bausch, Sevag Gharibian, and James Watson. Personal Communication.
- [8] Ethan Bernstein and Umesh V. Vazirani. Quantum complexity theory. *SIAM J. Comput.*, 26(5):1411–1473, 1997.
- [9] Sergey Bravyi and David Gosset. Gapped and gapless phases of frustration-free spin-1/2 chains. *Journal of Mathematical Physics*, 56, 03 2015.
- [10] Toby Cubitt and Ashley Montanaro. Complexity classification of local hamiltonian problems. *SIAM Journal on Computing*, 45(2):268–316, 2016.
- [11] Toby S. Cubitt, David Perez-Garcia, and Michael M. Wolf. Undecidability of the spectral gap. *Nature*, 528(7581):207–211, Dec 2015.
- [12] Percy Deift, Mary Beth Ruskai, and Wolfgang Spitzer. Improved gap estimates for simulating quantum circuits by adiabatic evolution. *Quantum Inf. Process.*, 6(2):121–125, 2007.
- [13] Sevag Gharibian, Yichen Huang, Zeph Landau, and Seung Woo Shin. Quantum hamiltonian complexity. *Foundations and Trends® in Theoretical Computer Science*, 10(3):159–282, 2015.
- [14] Sevag Gharibian, Stephen Piddock, and Justin Yirka. Oracle complexity classes and local measurements on physical hamiltonians, 2019.
- [15] Sevag Gharibian and Justin Yirka. The complexity of simulating local measurements on quantum systems. *Quantum*, 3:189, September 2019.
- [16] Daniel Gottesman and Sandy Irani. The quantum and classical complexity of translationally invariant tiling and hamiltonian problems. *Theory of Computing*, 9(2):31–116, 2013.
- [17] A. Yu. Kitaev, A. H. Shen, and M. N. Vyalyi. *Classical and Quantum Computation*. American Mathematical Society, USA, 2002.
- [18] Mark W. Krentel. The complexity of optimization problems. In Alan L. Selman, editor, *Structure in Complexity Theory*, pages 218–218, Berlin, Heidelberg, 1986. Springer Berlin Heidelberg.
- [19] R. Oliveira and B. Terhal. The complexity of quantum spin systems on a two-dimensional square lattice, 2005.
- [20] Christos H. Papadimitriou. *Computational complexity*. Addison-Wesley, 1994.
- [21] Raphael Robinson. Undecidability and nonperiodicity for the tilings of the plane. *Invent. Math.*, 12:177–209, 1971.
- [22] James D. Watson, Johannes Bausch, and Sevag Gharibian. The complexity of translationally invariant problems beyond ground state energies, 2020.